BIG DATA FOR SAFETY MONITORING, ASSESSMENT, AND IMPROVEMENT

FINAL REPORT

Southeastern Transportation Center

MOHAMED ABDEL-ATY

ESSAM RADWAN

JAEYOUNG LEE

LING WANG

QI SHI

SEPTEMBER 2016

US Department of Transportation grant DTRT13-G-UTC34

DISCLAIMER

1. Report No.	2. Government Accession No.	3. Recipient's Catalog No.
4. Title and Subtitle Big Data for Safety Monitoring, Assessment, and Improvement		5. Report Date September 2016
		6. Source Organization Code Budget
7. Author(s) Abdel-Aty, Dr. Mohamed; Radwan, Dr. Ahmed; Lee, Dr. JaeYoung; Wang, Dr. Ling; Shi, Dr. Qi		8. Source Organization Report No. STC-2015-##-XX
9. Performing Organization Name and Address Southeastern Transportation Center UT Center for Transportation Research 309 Conference Center Building Knoxville TN 37996-4133		10. Work Unit No. (TRAIS)
		11. Contract or Grant No. DTRT13-G-UTC34
12. Sponsoring Agency Name and Address US Department of Transportation Office of the Secretary of Transportation–Research 1200 New Jersey Avenue, SE Washington, DC 20590		13. Type of Report and Period Covered Final Report: May 2014 – October 2016
		14. Sponsoring Agency Code USDOT/OST-R/STC
15. Supplementary Notes:		

16. Abstract

This project implemented big data for traffic safety monitoring, assessment, and improvement. Data were collected from multiple sources and integrated to explore the traffic safety mechanisms of expressway mainlines, expressway ramps, expressway weaving segments, and intersections. Data visualization was first carried out for facilitating researchers' understanding of the traffic and crash patterns on the studied expressway system. Then, based on big traffic data, a well-calibrated and validated microscopic simulation VISSIM network was built to find the real-time conflict contributing factors for expressway weaving segments. Additionally, travel time reliability parameters were found to be significant traffic safety contributing factors for both crash frequency and real-time safety analysis studies. In addition to microscopic traffic data and roadway geometric characteristics, macroscopic data were also attempted in microscopic safety studies: real-time crash analysis for expressway ramps and safety performance functions for intersections. The results showed that macroscopic parameters had significant impacts and improved the model performance. In the real-time crash analysis for ramps, the integration of data mining method and traditional statistic model largely eliminated over fitting issue and improved model accuracy. In the intersection safety study, the optimal macro-level spatial unit was recommended for each crash type.

17. Key Words Big data; Traffic safety; Expressway; Intersections; Data visualization; Microscopic simulation VISSIM; Travel time reliability; Real-time safety analysis; Safety performance function	18. Distribution Statement Unrestricted; Document is available to the public through the National Technical Information Service; Springfield, VT.

19. Security Classif. (of this report) Unclassified	20. Security Classif. (of this page) Unclassified	21. No. of Pages 125	22. Price …

Form DOT F 1700.7 (8-72) Reproduction of completed page authorized

TABLE OF CONTENTS

LIST OF FIGURES iv

LIST OF TABLES v

LIST OF ABBREVIATIONS vii

EXECUTIVE SUMMARY 1

CHAPTER 1: INTRODUCTION 3

CHAPTER 2: DATA COLLECTION AND INTEGRATION 6

2.1 Crash Data 6

2.2 Traffic Data 7

2.3 Road Geometric Data 11

2.4 Macroscopic data 13

CHAPTER 3: PRELIMINARY SAFETY EVALUATION 15

3.1 Introduction 15

3.2 Visualization of Spatio-temporal Hourly Volume Distributions 15

3.3 Visualization of Congestion 18

3.4 Visualization of Crashes on Expressways 25

3.5 Summary 28

CHAPTER 4: REAL-TIME CONFLICT PRECURSORS FOR WEAVING SEGMENTS . 29

4.1 Introduction 29

4.2 Experiment Design 30

4.3 VISSIM Network Calibration and Validation 39

4.4 Model Estimation 41

4.5 Summary 44

CHAPTER 5: TRAVEL TIME RELIABILITY AND TRAFFIC SAFETY 46

5.1 Introduction 46

5.2 Background 46

5.3 Data Preparation 48

5.4 Descriptive Analysis 50

5.5 Methodology 51

5.6 Model Results 53

5.7 Summary 59

CHAPTER 6: REAL-TIME EVALUATION FOR RAMP CRASHES 60

6.1 Introduction 60

6.2 Methodology 61

6.3 Data Preparation 65

6.4 Model results 68

6.5 Summary 72

CHAPTER 7: INTERSECTION SAFETY PERFORMANCE FUNCTIONS 73

7.1 Introduction 73

7.2 Methodology 76

7.3 Macro-level Spatial Units 78

7.4 Data Preparation 82

7.5 Results and discussion 84

7.6 Summary 97

CHAPTER 8: CONCLUSIONS 100

REFERENCES 104

APPENDIX 112

Publications 112

Oral Presentations 112

Posters 113

LIST OF FIGURES

Figure 2-1 Deployment of AVI sensors on CFX expressway network 9

Figure 2-2 Deployment of MVDS detectors on expressway network 11

Figure 3-1 Weekday hourly volume along SR 408 16

Figure 3-2 Spatio-temporal hourly volume distribution on SR 408 17

Figure 3-3 Mainline weekday travel time index of SR 408 22

Figure 3-4 Mainline weekday occupancy of SR 408 23

Figure 3-5 Mainline weekday congestion index of SR 408 24

Figure 3-6 Spatial pattern of traffic crashes in 2011 27

Figure 3-7 Spatial pattern of traffic crashes in 2012 27

Figure 3-8 Spatial pattern of traffic crashes in 2013 27

Figure 3-9 Spatial pattern of traffic crashes in 2014 28

Figure 4-1 Two level calibration and validation procedure 32

Figure 4-2 Speed distribution for each group 35

Figure 4-3 Traffic data extraction 36

Figure 6-1 Variable importance 71

Figure 7-1 Hierarchical structure of intersection-level and macro-level data 77

Figure 7-2 Various geographic units in Orlando metropolitan area, Florida......................... 81

Figure 7-3 Intersection-level and macro-level variables 82

Figure 7-4 Comparison of adjusted ρ^2 values of the SPFs with macro-level random-effects and variables 88

LIST OF TABLES

Table 2-1 AVI segments on CFX expressway system 8

Table 2-2 MVDS segments on CFX expressway system 9

Table 2-3 RCI geometric data 12

Table 3-1 Travel time index and congestion levels 19

Table 3-2 MVDS-based congestion index and congestion levels 20

Table 4-1 Speed distribution for each location 34

Table 4-2 Variable definition 38

Table 4-3 Simulated conflict count and field crash count 41

Table 4-4 Real-time conflict prediction model for weaving segment 42

Table 5-1 Descriptive analysis for crash frequency analysis 50

Table 5-2 Descriptive analysis for real-time safety analysis 51

Table 5-3 Parameter estimation for MV crash frequency 54

Table 5-4 Parameter estimation for SV crash frequency 54

Table 5-5 Parameter estimation for real-time MV and SV crash risk 57

Table 6-1 Descriptive analysis for real-time ramp analysis 67

Table 6-2 Logistic regression model result for ramp 68

Table 6-3 Performance of SVM models 70

Table 7-1 Area and intersection counts by spatial unit 82

Table 7-2 Descriptive statistics of the prepared data 83

Table 7-3 Summary of model performances 86

Table 7-4 The estimated safety performance functions for total crashes at intersections with macro-level variables 93

Table 7-5 The safety performance functions for severe crashes at intersections with macro-level variables 94

Table 7-6 The safety performance functions for pedestrian crashes at intersections with macro-level variables 95

Table 7-7 The safety performance functions for bicycle crashes at intersections with macro-level variables 96

LIST OF ABBREVIATIONS

AADT	Annual Average Daily Traffic
ACS	American Community Survey
AIC	Akaike information criterion
ATM	Active Traffic Management
AUC	Area Under the Curve
AVI	Automatic Vehicle Identification
BG	Block group
BIC	Bayesian information criterion
CARS	Crash Analysis Reporting System
CC0	Stand still distance
CC1	Following headway time
CC2	Following variation
CCD	Census county division
CFX	Central Florida Expressway Authority
CI	Congestion index
CT	Census tract
DLCD	Desired lane change distance
ETC	Electronic Toll Collection
FAST Act	Fixing America's Surface Transportation Act
FDOT	Florida Department of Transportation
FHWA	Federal Highway Administration

HGV	Heavy Goods Vehicle
HSM	Highway Safety Manual
ITS	Intelligent Transportation System
LOS	Level of service
MAP-21 Act	Moving Ahead for Progress in the 21st Century
MAUP	Modifiable Areal Unit Problem
MP	Milepost
MPO	Metropolitan Planning Organization
MV	Multi-vehicle
MVDS	Microwave Vehicle Identification System
PC	Passenger car
PET	Post-encroachment-time
RCI	Road Characteristics Inventory
S4A	Signal Four Analytics
SPF	Safety performance function
SR 408	State Roads 408
SR 414	State Roads 414
SR 417	State Roads 417
SR 429	State Roads 429
SR 528	State Roads 528
SSAM	Surrogate Safety Assessment Model
SV	Single-vehicle

SVM	Support Vector Machine
SWTAZ	Statewide Traffic Analysis Zone
TAD	Traffic analysis district
TAZ	Traffic analysis zones
TSAZ	Traffic safety analysis zone
TTC	Time-to-collision
TTI	Travel time index
V/C	Volume-to-capacity ratio
ZCTA	ZIP-Code Tabulation Area

EXECUTIVE SUMMARY

With the development of data and communication technologies, huge information is being collected and processed with the aim of understanding human behavior, making better decisions, etc. The huge information is called "Big Data". Big data have brought about changes to human life, and transportation is one of the areas, which have been heavily impacted by big data. This study collected and integrated various data sources for safety monitoring, assessment, and improvement. The data included crash, traffic, road geometric design, and macroscopic data. For each type of data, different data sources were used, for example, traffic data were provided by Automatic Vehicle Identification sensors and Microwave Vehicle Detection System.

First, the big data visualization was conducted to facilitate researchers' understanding of the traffic and crash patterns on the expressway system in Central Florida. The spatiotemporal distribution of crashes along with traffic flow offer valued insights and can guide future statistical inference thus is a necessary step in Big Data analysis. Then, a microscopic simulation network for expressway weaving segments was built based on big traffic data. Its volume, speed, and safety were highly consistent with those of field traffic due to the high resolution of big traffic data input. Based on the well-calibrated and validated simulation network, real-time conflict estimations have been carried out to explore the crash mechanism of weaving segments. The result showed that the real-time safety analysis at smaller time intervals was able to provide better prediction accuracy.

The project verified the significant impact of travel time reliability on crash frequency and crash types in real-time for expressway mainlines. Additionally, it recommended

applying different travel time reliability indexes in different safety studies. The results also implied that the crash mechanisms for single- and multi-vehicle crashes were not the same. The safety of a roadway facility is not only determined by the facility's geometric design and traffic, but also it might be impacted by the macroscopic characteristics of the zone which a roadway facility lies in. Therefore, the macroscopic parameters were attempted in real-time safety analysis for ramps and in crash frequency prediction for intersections. The results indicated that the macroscopic parameters indeed had significant impact on safety.

Moreover, Support Vector Machine along with logistic regression model was used in real-time safety analysis for ramps. The integration of the two models largely eliminated overfitting issue and improved model accuracy. The intersection safety analyses were carried out for different crash types and different macro-level spatial units. The best spatial unit was recommended to crash frequency estimation for each crash type.

Finally, potential application of this project and future relevant research are also discussed.

CHAPTER 1: INTRODUCTION

With the development of technologies such as computer technology, Internet technology, and Intelligent Transportation System (ITS), huge information is collected and processed with the aim of understanding human behavior, making better decisions, increasing greater operational efficiency, reducing risk, etc. The huge information, characterized by variety, volume, velocity, variability, complexity, and value, is often referred to “Big Data” (Katal et al., 2013). Big data have already brought about promises and challenges to human life. Transportation is one of the fundamental elements of human life, it has also been heavily impacted by big data.

In the past few decades, ITS continuously collected traffic information from different sources over vast scale. Meanwhile, transportation related databases were built, for example, geometric characteristic for each road segment. The huge size and rich transportation related big data could significantly enhance understanding of the efficiency and safety of transportation system. Additionally, Active Traffic Management (ATM) for improving system performance becomes possible due to the real-time nature of the big data.

This project focuses on the safety monitoring, assessment, and improvement based on big data. Big data from different sources were collected and integrated. Automatic Vehicle Identification (AVI) and Microwave Vehicle Identification System (MVDS) are the two main sources for real-time traffic data. The utilization of these two traffic detection systems provided rich information regarding the expressway traffic conditions in real-time. Roadway geometric characteristics and crash data were acquired to find the relationship between geometric design and roadway safety. Additionally, macroscopic, which includes but not limited to trip generation and land-use data, were used to explore the impact macroscopic parameters on traffic safety. Different roadway facilities were studied: expressway mainline, expressway weaving segments, expressway ramps, and intersections.

The main objective of this study was to implement big data in traffic safety studies. Different data sources were analyzed and the safety of different roadway facilities were investigated. To be more specific, eight tasks were carried out.

• Task 1: Visualizing big data to facilitate the understanding of traffic and crash patterns;

• Task 2: Analyzing real-time conflict potential for weaving segments in microscopic simulation which was based on big traffic data;

• Task 3: Exploring the impact of travel time reliability on safety from both crash frequency prediction and real-time safety analysis aspects. It is based on integrated traffic data sources: AVI and MVDS;

• Task 4: Investigating crash mechanisms for single-vehicle (SV) and multi-vehicle (MV) crashes, separately;

• Task 5: Evaluating crash risk for expressway ramps with a focus of finding whether macroscopic data would contribute to better model performance;

• Task 6: Integrating data mining method and traditional statistical model to improve the prediction accuracy for real-time safety analyses;

• Task 7: Estimating crash frequencies for different types of intersection crashes based on microscopic and macroscopic data;

• Task 8: Recommending the optimal macro-level spatial unit for each type of intersection crashes.

Following this chapter, Chapter 2 describes the data that were collected, including crash, traffic, road geometric characteristics, and macroscopic data. Chapter 3 carries out data visualization with the aims to facilitate researchers' understanding of the traffic and crash patterns on the studied objects. Then, Chapter 4 takes traffic simulation as a cost-effective method to estimate traffic safety, and implements big traffic data in constructing a simulation network. The simulation network is used to conduct real-time conflict analysis. Chapter 5 analyzes the impact of travel time reliability on SV and MV crashes, and it models the real-time MV crash potential given a crash occurrence. Different travel time reliability indexes have been tried. Chapter 6 estimates real-time crash potential for expressway ramps using traffic, trip generation, and land-use parameters. Additionally, both data mining method and traditional statistical model are implemented in the real-time ramp crash analysis to provide a better model accuracy. Chapter 7 focuses on crash frequency analyses for intersections for different crash types and different macro-level spatial units. The potential safety contributing factors include microscopic intersection traffic data and macroscopic data. Conclusions are summarized in Chapter 8.

CHAPTER 2: DATA COLLECTION AND INTEGRATION

This project focuses on various aspects of safety evaluation and improvement of roadway system using big data. Hence, the data related to traffic safety need to be collected. In general, primary crash factors are environmental (e.g., geometric characteristics) and traffic (e.g., speed, volume). Additionally, the safety of a roadway facility might be impacted by the macroscopic characteristics of the zone, which the facility lies in. Hence, macroscopic parameters, which include but not limited to trip generation and land-use factors, are also collected.

2.1 Crash Data

The raw crash data were obtained from Signal Four Analytics (S4A) and Crash Analysis Reporting System (CARS). S4A provides time of crash, crash coordinate, number of vehicles involved, type and severity of the crash, the number of injuries and/or fatalities involved, weather, road surface and light condition, etc. CARS provides more crash information. In addition to the data recorded by S4A, CARS also offers drivers' information, e.g., age, gender, race.

In early years, S4A database mainly collected long form crashes, but short form crash data were not complete. The long form crash reports are designed to keep records of injury crashes, and short form crashes are mainly used to record property damage only crashes. Nevertheless, after June 2012, S4A has complete crash data from both report types for whole Florida. However, CARS is not as complete as S4A. For example, from 2012 to 2013, there were 6,741 crashes on Florida's Turnpike in S4A database. On the other hand, CARS only reported 5,109 crashes on Florida's Turnpike in the same period. Compared with S4A, CARS underreported 24.2% of crashes. Because S4A can provide more crash observations and CARS can provide more details for each crash observation, both of them were used in this study.

2.2 Traffic Data

Traffic flow data were provided by Florida Department of Transportation (FDOT) and the Central Florida Expressway Authority (CFX). The Annual Average Daily Traffic (AADT) was from FDOT's Road Characteristics Inventory (RCI) database. Microscopic traffic data, such as volume at 1-minute intervals, were obtained from CFX.

There are two types of microscopic traffic data provided by CFX: AVI and MVDS. The AVI system is used for Electronic Toll Collection (ETC). If a vehicle traveling on CFX's expressways is equipped with a SunPass transponder, AVI sensors will automatically record the vehicle's tag ID and the timestamps this vehicle passes the AVI detector. Then, the expressway system will charge the vehicle according to the distance that the vehicle traveled. By subtracting the timestamps between two AVI sensors, the travel time can be obtained. Since the distance between two sensors is known based on the milepost (MP) of AVI sensors, the space mean speed is obtained using Eq. 2-1.

$$Speed = \frac{\left| Milepost_{downstream} - Milepost_{upstream} \right|}{Timestamp_{downstream} - Timestamp_{upstream}} \tag{2-1}$$

Table 2-1 illustrates the number of AVI segments per direction and basic statistics on each of the five expressways in Central Florida for January 2016. The five expressways are State Road 408 (SR 408), State Road 414 (SR 414), State Road 417 (SR 417), State Road 429 (SR 429), and State Road 528 (SR 528).

Table 2-1 AVI segments on CFX expressway system

Route ID	Direction	No. of Segments	Segment Length Mean	Std.	Min	Max
SR 408	EB	26	0.87	0.47	0.17	1.85
	WB	23	0.97	0.53	0.33	2.29
SR 414	EB	5	1.06	0.73	0.29	2.02
	WB	4	1.32	0.81	0.35	2.31
SR 417	NB	18	1.84	0.84	0.63	3.98
	SB	23	1.42	0.78	0.38	3.10
SR 429	NB	14	1.41	1.08	0.30	4.27
	SB	15	2.00	1.20	0.61	4.54
SR 528	EB	8	2.74	2.25	0.33	7.06
	WB	8	2.74	2.22	0.86	7.60

Figure 2-1 illustrates the deployment of AVI sensors on the CFX expressway network. The AVI sensors on SR 408 is the densest, and SR 408 has the smallest mean AVI segment length of the five expressways in CFX system. The density of AVI sensors are mainly determined by two aspects: the need for collecting toll and for estimating travel time. The SR 408 carries the heaviest traffic and travel through the downtown area of Orlando. The on- and off-ramp density of SR 408 is much higher than other expressways, and AVI sensors need to put close to on- and off-ramps for toll collection. Additionally, the heavy traffic produces low travel time reliability and makes the travel time varies a lot for each segment. Hence, dense AVI sensors are required to more precisely predict travel time.

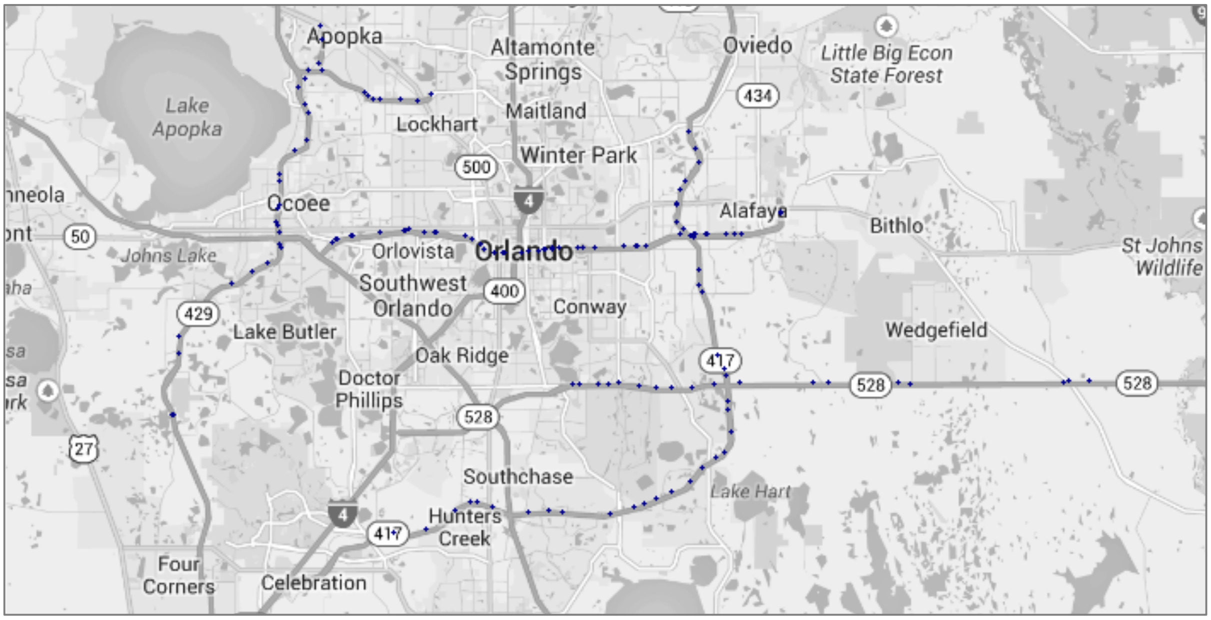

Figure 2-1 Deployment of AVI sensors on CFX expressway network

MVDS was introduced to CFX's expressway system since 2012, and the MVDS data have been available since July 2013. The system is specifically designed for traffic monitoring. MVDS detectors were installed at almost every merging and diverging points of expressway systems. They collect the traffic volume, occupancy, and average speed for each lane at 1-minute intervals. In addition to the traffic data above, MVDS detectors recognize the length of passing vehicles and classifies them under four groups:

- Type 1: vehicles 0 to 10 feet in length
- Type 2: vehicles 10 to 24 feet in length
- Type 3: vehicles 24 to 54 feet in length
- Type 4: vehicles over 54 feet in length

There are 364 MVDS detectors along the CFX expressways with an average spacing of 0.574 miles. Table 2-2 shows the MVDS detector information for each direction for the five expressways in January 2016.

Table 2-2 MVDS segments on CFX expressway system

Route ID	Direction	No. of Segments	Segment Length			
			Mean	Std.	Min	Max
SR 408	EB	56	0.38	0.18	0.10	1.00
	WB	53	0.41	0.20	0.10	1.00
SR 414	EB	13	0.44	0.17	0.20	0.70
	WB	12	0.46	0.23	0.10	0.90
SR 417	NB	54	0.59	0.29	0.20	1.50
	SB	54	0.59	0.29	0.20	1.30
SR 429	NB	28	0.68	0.54	0.20	2.80
	SB	28	0.68	0.59	0.10	3.10
SR 528	EB	28	0.84	0.79	0.10	3.00
	WB	28	0.84	0.82	0.10	3.10

Figure 2-2 illustrates the deployment of MVDS detectors on the CFX expressway network. Similar as AVI detectors, the density of MVDS detectors on SR 408 is the highest. The MVDS detectors are used to monitor traffic conditions for expressways, which change at locations where traffic enters or exits expressway network. SR 408 services the areas with high traffic demand and need provide more accesses to nearby areas. The high access density requires more MVDS detectors.

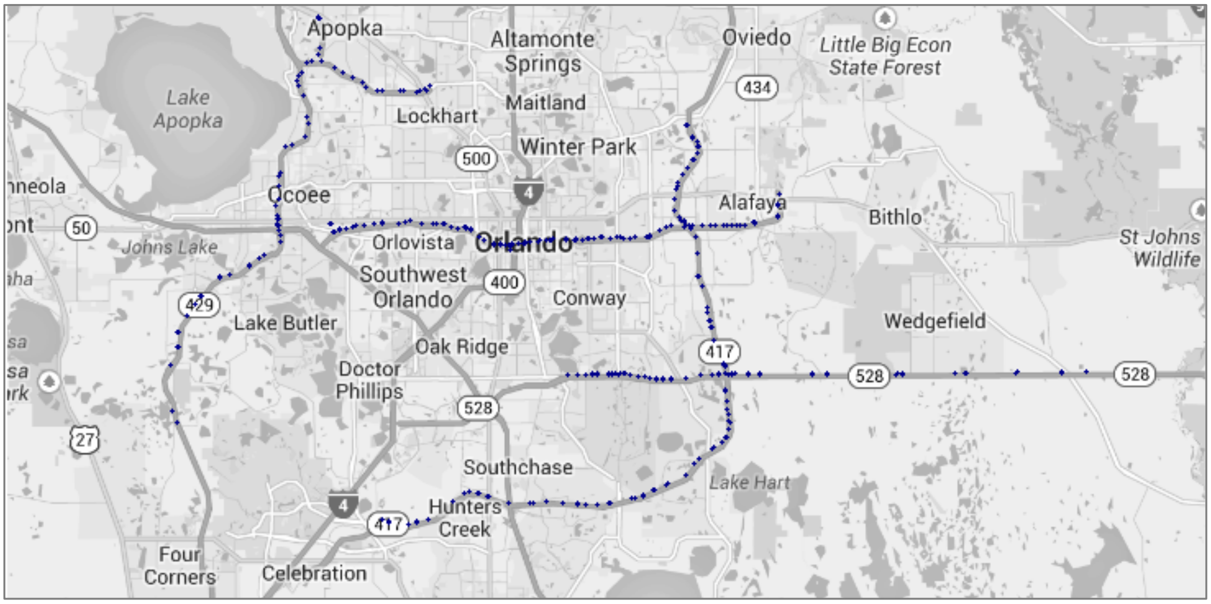

Figure 2-2 Deployment of MVDS detectors on expressway network

There are much more MVDS detectors than AVI detectors. Comparing Table 2-1 to Table 2-2, it can be found the number of MVDS detectors is more than twice of AVI sensors for the majority of directions. Additionally, only part of vehicles equipped SunPass, so AVI sensors cannot obtain all vehicles' information. Furthermore, AVI sensors do not distinguish the lane a vehicle uses and vehicle length, but MVDS detectors are able to provide traffic data for each lane and recognize vehicle length. Hence, this study more focuses on the implementation of MVDS traffic data.

2.3 Road Geometric Data

Geometric data were obtained from RCI, which is maintained by FDOT, or manually collected by using ArcGIS map. The RCI records 323 features and characteristics for the roadway system (FDOT, 2014). When multiple geometric variables are selected, homogeneous segments of the roadway were generated automatically. Segments of extreme short distance (less than 0.1 mile) were combined with adjacent segment, which shared higher similarity. The selected geometric characteristics in this study included the number of lanes, existence of auxiliary lanes, speed limit, horizontal degree of curvature, median width, and shoulder width. Vertical curves are seldom observed on the expressways because of the flat terrain in Central Florida and thus were not included. Table 2-3 gives an example on the RCI data.

Table 2-3 RCI geometric data

RDWYID	Begin milepost	Number of lanes	Auxiliary lanes type	Shoulder width	Median width	Horizontal curve	Speed limit	AADT
75008170	1.417	2		10.0	40	0	55	41000
75008170	1.581	2		10.0	40	0	65	41000
75008170	2.206	2		10.0	40	0	65	52500
75008170	2.455	2		10.0	40	0	65	52500
75008170	2.664	2		10.0	40	0	65	52500
75008170	2.903	2		10.0	40	0	65	52500
75008170	3.078	2		10.0	40	0	65	52500
75008170	3.264	2		10.0	40	0.75	65	52500
75008170	3.543	2		10.0	40	0.75	65	52500
75008170	3.717	2		10.0	40	0	65	52500
75008170	3.879	2		10.0	40	1	65	52500
75008170	3.980	3		10.0	40	1	65	52500
75008170	4.242	3		10.0	40	0	65	52500
75008170	4.789	3		10.0	40	2.75	65	52500
75008170	5.027	3		10.0	40	0	65	52500
75008000	0.382	3		10.0	20	1.5	65	46000
75008000	0.640	3	4	10.0	20	1.5	65	46000
75008000	0.725	3	4	10.0	20	0	65	46000
75008000	0.866	3		10.0	20	0	65	46000

Some geometric information was not provided by RCI, e.g., ramp type (on- or off-ramp), ramp configuration (loop, diamond, etc.), weaving segment length. Hence, there was a need to collect these data manually by using ArcGIS map.

2.4 Macroscopic data

The FDOT Central Office periodically develops statewide planning data, network, and model based on Statewide Traffic Analysis Zones (SWTAZs). The data includes trip generation variables. The trip generation data include diverse types of trip productions and trip attractions. A trip production refers to a trip end connected to a residential land-use in a zone whereas a trip attraction is defined as a trip end connected to a nonresidential land-use in a zone. For the SWTAZs that the studied ramps are in, total production trips and attractions trips per day were 5,601 and 5,666, respectively. Such trip production and attraction trips are provided by trip purposes (i.e., working, social or recreational, shopping, and total). The trip generation data were processed and converted to percentages by trip purposes. Among the total trip productions, 15.8% were home-based shopping productions, 14.8% were home-based-work productions, and 7.1% were home-based social or recreational productions. On the other hand, among the total trip attractions, 16.4% were home-based-work attractions, 9.3% were home-based shopping attractions, and 8.4% were home-based social or recreational attractions. Furthermore, the SWTAZ model also provided land-use variables including population density, employment density, school enrollment density, and the number of employees by industry. It was shown that there are averagely about 2,215 residents per square mile (i.e., population density), 1,577 employees per square mile, and 902 enrollments per square mile.

Regarding the percentage of employees by industry type, the percentage of service employment was the highest (50%), and then is the percentages of retail employment (19.3%).

The macroscopic data for the studied intersections were collected from the American Community Survey (ACS) of the U.S. Census Bureau. Because multiple spatial units (i.e., block group, traffic analysis zone, census tract, ZIP-code tabulation area, traffic analysis district, census county division, and county) were used in this study, the descriptive statistics were also provided by these geographic units. It is noteworthy that the basic statistics can be different by the level of aggregation. For instance, the average population based on block groups is 2,559; but it is only 631.9 based on counties. This issue is call the Modifiable Areal Unit Problem (MAUP), which is presented when artificial boundaries are imposed on continuous geographical surfaces and the aggregation of geographic data cause the variation in statistical results. The MAUP was observed in the datasets used in this study as there are more number of zones in the urban area whereas the number of zones is smaller in the rural area, especially in small zone systems such as block groups, traffic analysis zones, census tracts, etc. Thus, the average values are more affected by the urban zones in such small zone systems. The collected variables are as follows: demographic (i.e., population density, proportions of children, adolescent, middle-age, young elderly, and elderly), transportation mode (i.e., the proportions of commuters using car, public transit, tax, motorcycle, bicycle, walking, and other means), socio-economic variables (i.e., the proportion of people working at home, the school enrollment density, the proportion of people with bachelor's degree or higher, the proportion of households below poverty line, the proportion of households with no vehicle, and median household income). Lastly, the proportion of urbanized area was also attempted.

CHAPTER 3: PRELIMINARY SAFETY EVALUATION

3.1 Introduction

This chapter carries out visualization of traffic and crash data. Big data are well known for their huge size, thus, it is usually hard to interpret them without a series of detailed investigations. Data visualization facilitates researchers' understanding of the traffic and crash patterns on the studied subjects. As one of the major expressways in Central Florida area, SR 408 was chosen as a main study area in this chapter to show the preliminary analysis. SR 408 travels along east-west direction through Orlando and carries commuting traffic, especially in morning and evening peak-hours. Both AVI and MVDS data from July 2014 were selected for visualizing traffic-related big data, including spatio-temporal hourly volume and congestion. Meanwhile, traffic crashes from 2011 to 2014 on all five expressways were analyzed using crash density visualization.

3.2 Visualization of Spatio-temporal Hourly Volume Distributions

Figure 3-1 shows the spatio-temporal characteristics of weekday hourly traffic volume on mainline of SR 408. For SR 408, the eastbound experiences significant high travel demands during evening peak-hours, whereas, the traffic reaches its peak on the westbound during morning peak-hours.

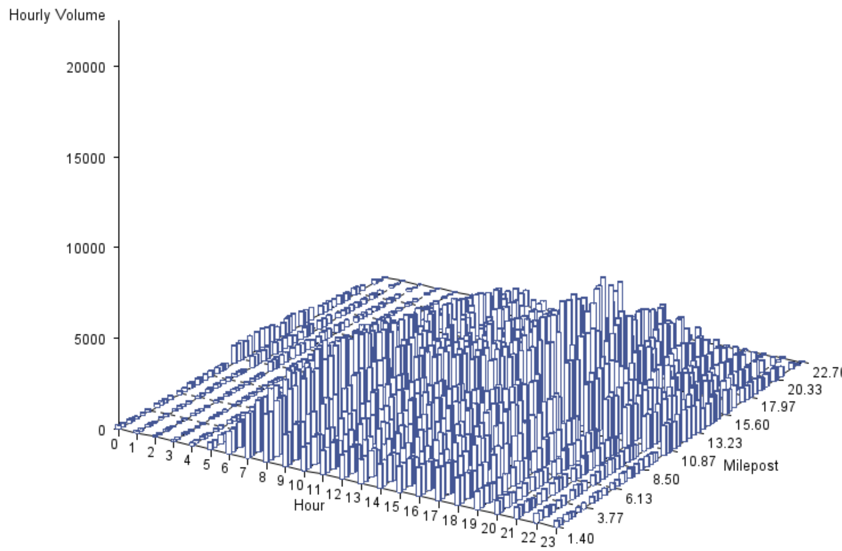

(a) Eastbound

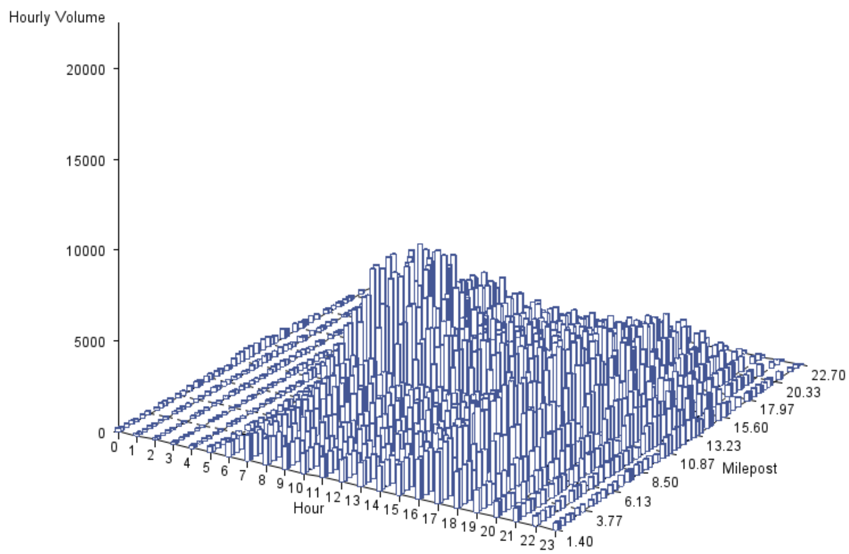

(b) Westbound

Figure 3-1 Weekday hourly volume along SR 408

Figure 3-2 depicts the contour plots of spatio-temporal hourly volume distribution on SR 408. With the contour plots, the pattern can be interpreted more clearly. Hourly traffic volume on SR 408 during peak-hours rises to about 7,000 vehicles. The highest demand exists around from 6:00 A.M. to 9:00 A.M. for westbound and from 4:00 P.M. to 7:00 P.M.

for eastbound. The segments that experience the highest volume extend from MP (milepost) 11 to MP 17 for both eastbound and westbound. For other segments during other time, the traffic volumes are relatively stable and mostly below 3,000 vehicles per hour. This preliminary review of SR 408 suggests when and where the congestion is likely to occur. Future studies on congestion evaluation should focus on these segments during peak hours.

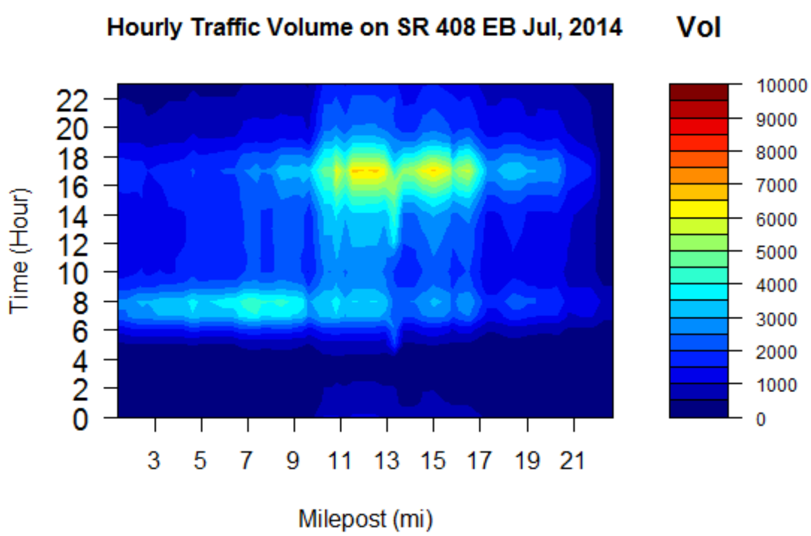

(a) Eastbound

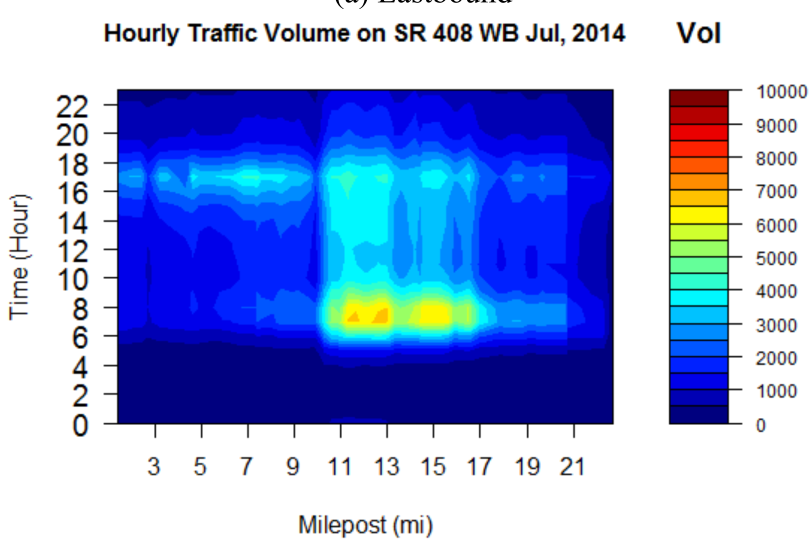

(b) Westbound

Figure 3-2 Spatio-temporal hourly volume distribution on SR 408

3.3 Visualization of Congestion

Traffic operation on expressways focuses on providing motorists with efficient movements to their destinations. To achieve this goal, improving congestion is one of the most important task. Accurate congestion measurement is a prerequisite in congestion management. Traditionally, volume-to-capacity (V/C) ratios and level of service (LOS) were implemented by transportation authorities as indicators of congestion intensity (Grant et al., 2011). Nevertheless, traffic demand can vary considerably in both temporal and spatial dimensions. Roadway capacity is not fixed, because it might be impacted by crashes, weather, etc. In such cases, V/C and LOS lack the capability to capture the variability of congestion. With the fast development of ITS technology, real-time congestion measurement is becoming an urgent call. On the expressway system, both AVI and MVDS traffic detection systems are employed. Both of these systems archive the traffic data in real-time manner. In this project, multiple congestion measures were introduced and compared based on these two traffic detection systems.

3.3.1 AVI-based Congestion Measurement

Congestion measurement is mainly based on three indexes, namely density, travel time, and travel speed. AVI system is able to calculate the travel time of vehicles on a segment. Therefore, congestion measured using travel-time was introduced for the AVI system. Travel time index (TTI) is a commonly accepted measure used to evaluate traffic congestion. It is defined as the ratio of actual travel time to an ideal (free-flow) travel time (Cambridge Systematics, Inc., 2005). The formulation is shown in Eq. 3-1:

$$\text{TTI} = (\text{Actual travel time}) \,/\, (\text{Free-flow travel time}) \tag{3-1}$$

It indicates the additional time spent on a trip compared to an ideal trip on the same corridor. On the Central Florida expressway system, free flow travel time for each segment is in the AVI traffic data. Free-flow travel time is calculated based on segment length and its speed limit. If a segment has more than one speed limit, then the average speed limit is used. According to a study by Griffin (2011), the levels of congestion and the corresponding travel time index are listed in Table 3-1.

Table 3-1 Travel time index and congestion levels

Functional Classification	Travel Time Index for Different Congestion Levels		
	No congestion	Moderate congestion	Heavy congestion
Freeway	less than 1.25	1.25 to 1.99	Higher than 2.00

3.3.2 MVDS-based Congestion Measurement

Different from the AVI system, MVDS detectors reflect the traffic conditions at the installed points rather than segments. Speed, volume, and lane occupancy are archived on one-minute interval basis by MVDS. Multiple congestion measures can be developed from the MVDS traffic data. Occupancy is defined as the percent of time a point on the road is occupied by vehicles (Hall. 1996). Gerlough and Huber (1975) referred to occupancy as a surrogate for density. Compared with traditional V/C Ratio or LOS, occupancy has the advantage that it could be monitored in real-time. Meanwhile, the rate of reduction in speed caused by congestion from the free flow speed condition is adopted as congestion index (Hamad and Kikuchi, 2002; Hossain and Muromachi, 2012). The congestion index (CI) is expressed as:

$$CI = \begin{cases} (free - flow\ speed - Actual\ speed) / (free - flow\ speed) & When\ CI > 0 \\ 0 & When\ CI \leq 0 \end{cases} \quad (3\text{-}2)$$

The CI is a continuous congestion indicator ranging from zero to one. The free flow speed is the 85^{th} percentile speed at the studied location for the whole study period. From Eq. 3-2 above, it can be seen that when the actual speed is above free flow speed, CI will be recorded as zero. When CI increases, the congestion becomes more severe.

Currently, for the congestion measures calculated from MVDS data, there is no specific relationship between occupancy or CI and level of congestion is available. However, the TTI value of 1.25 and 2 are approximately equivalent to CI value of 0.2 and 0.5. According to the congestion plots, when CI reaches 0.2 and 0.5, the corresponding occupancy (%) is about 15 and 25. Therefore, congestion levels defined by occupancy and CI as displayed in Table 3-2 (Shi, 2014). Nevertheless, further refinement of these thresholds might be possible.

Table 3-2 MVDS-based congestion index and congestion levels

Congestion measure	Travel Time Index for Different Congestion Levels		
	No congestion	Moderate congestion	Heavy congestion
Occupancy (%)	≤ 15	15 – 24.99	≥ 25
CI	≤ 0.2	0.2 – 0.499	≥ 0.5

3.3.3 Expressway Mainline Congestion

To measure expressway mainline congestion conditions, the traffic data were aggregated at five-minute interval and were averaged by the weekdays for July 2014. Contour plots were generated to illustrate the spatio-temporal property of the congestion. The TTI congestion plots shown in Figure 3-3 illustrate a proportion of AVI data near MP 20 were missing for both directions in July 2014, because those sensors in that month were under maintenance. Despite the incompleteness of AVI data, some patterns could be found from Figure 3-3, on SR 408 eastbound, congestion is found near MP 9.0 and MP 18.0 in the evening peak hours. On SR 408 westbound, morning congestion is observed from MP 11.0 to MP 15.0. These congestion patterns could also be found in Figure 3-4 and Figure 3-5, indicating that AVI data could reflect congestion to certain extent. However, it is still important to have complete data to evaluate the performance of AVI-based congestion measure.

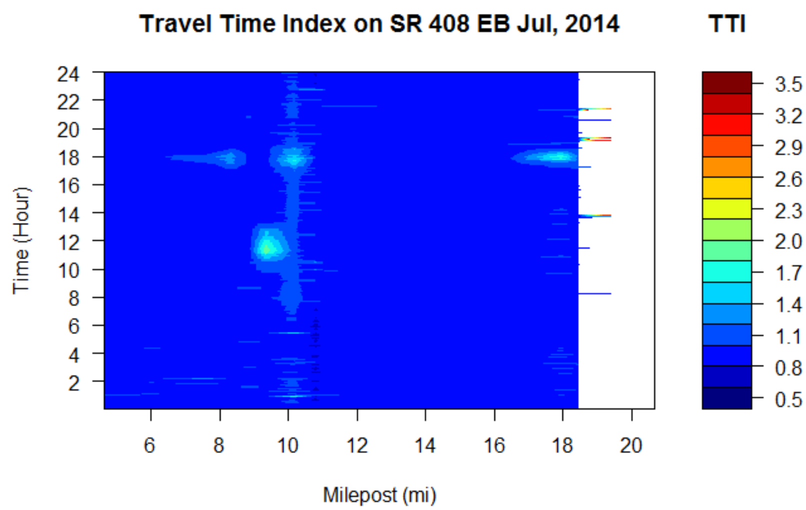

(a) Eastbound

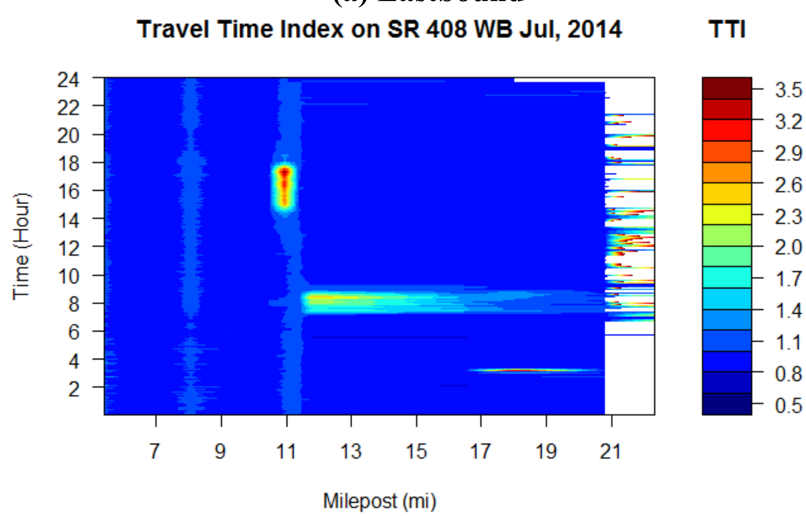

(b) Westbound

Figure 3-3 Mainline weekday travel time index of SR 408

The congestion plots derived from occupancy and CI (Figure 3-4 and Figure 3-5) exhibit comparable congestion patterns for the expressways. As mentioned above, the number of MVDS sensors installed along the expressways is significantly more than that of the AVI sensors. Additionally, the MVDS system is stable in terms of active sensors during the study time period. Therefore, the MVDS data is relatively complete and stable.

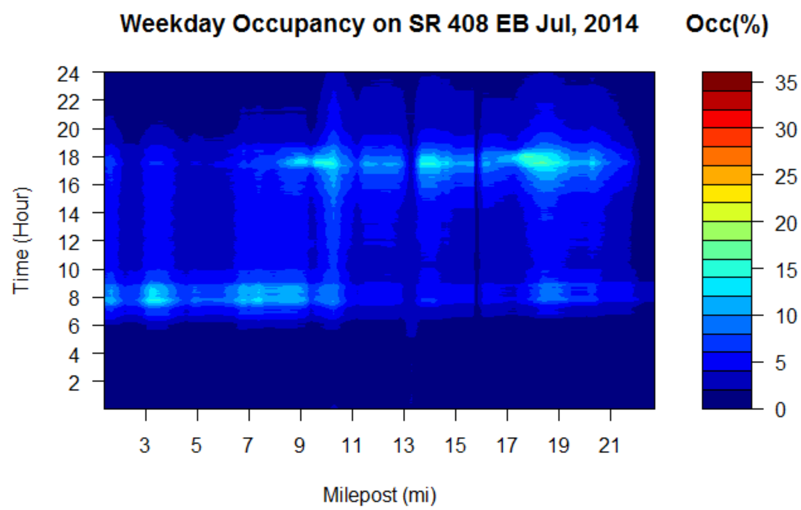

(a) Eastbound

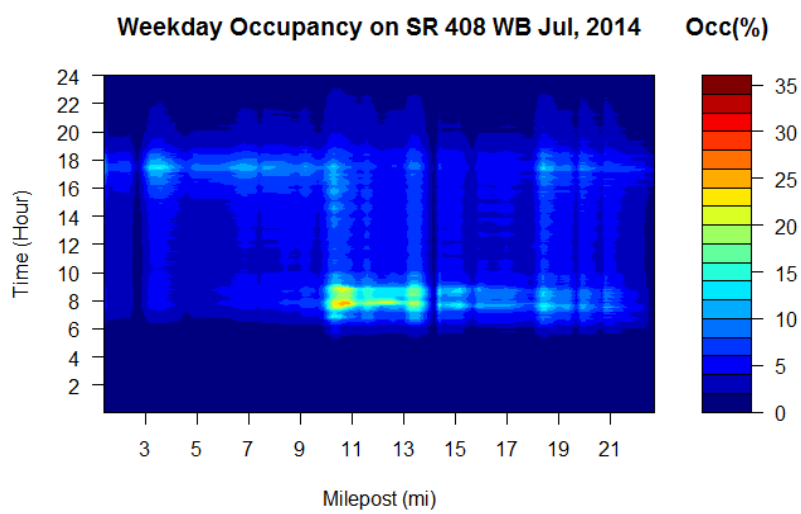

(b) Westbound

Figure 3-4 Mainline weekday occupancy of SR 408

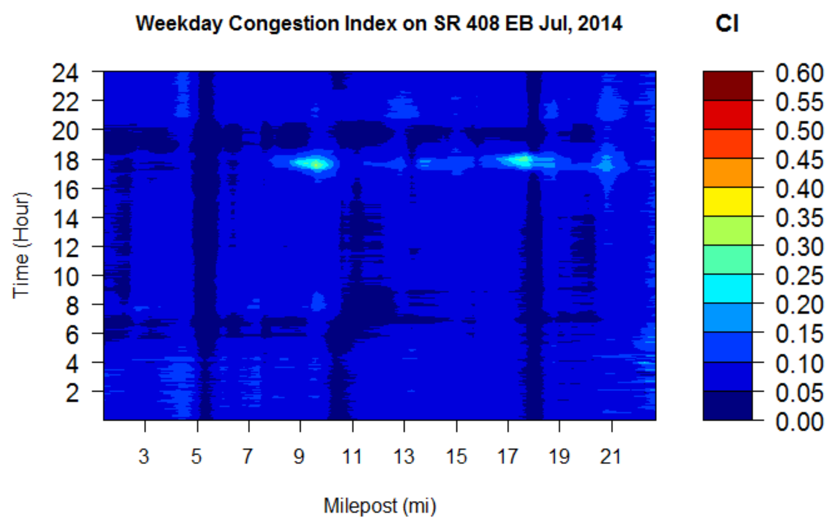

(a) Eastbound

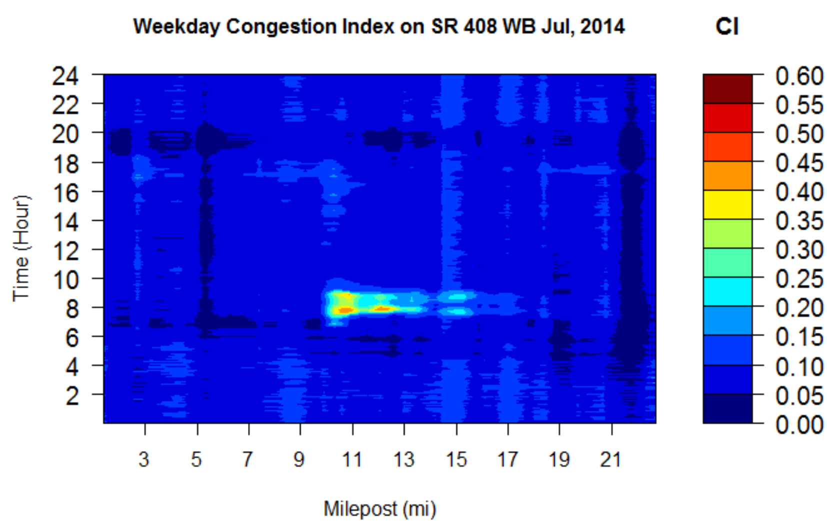

(b) Westbound

Figure 3-5 Mainline weekday congestion index of SR 408

Based on occupancy and CI, congestion conditions on SR 408 can be summarized. SR 408 experiences moderate congestion on eastbound in morning peak hours and heavy congestion on westbound in the evening peak hours. However, it should be noticed that the congestion intensity changes with time. When it is approaching peak hours, the congestion intensity gradually increases. Once the peak time is passed, the congestion becomes less severe. The congested area for SR 408 is approximately from MP 17.0 to MP 19.0 on eastbound and from MP 10.0 to MP 13.0 on westbound.

3.4 Visualization of Crashes on Expressways

For the total crashes on the expressway system, the spatial pattern of crashes is examined through crash density. The spatial distribution of crashes on mainlines and ramps can be found in Figures 3-6 to 3-9. Toll plazas in Central Florida expressway system have two types of lane: express lane and cash lane. Vehicles on expressway lanes use ETC to pay toll fee automatically, but those on cash lane need to stop at tollbooth to pay toll. Hence, the driver behaviors on toll plaza cash lane are different from other mainlines, and the crash pattern of cash lane was explored separately.

From the figures, the concentration of crashes and the changes from January 2011 to June 2014 can be found. For the mainline crashes, the segment on SR 408 between the interchange with Semoran Blvd and SR 417 is the most concentrated area of mainline crashes in 2011. After 2011, the mainline crashes began to shift to the interchange of SR 408 and I-4. In the first six months of 2014, the segment that has the most mainline crashes is near the interchange of SR 408 and I-4 while the interchange with SR 417 is no longer identified as the hot spot. This reduction of crashes at the segment near SR 417 might be caused by the interchange improvement project on this specific interchange. Also, in 2013 and 2014, the segment on SR 528 near the interchange with Semoran Blvd has become a crash hot post. This area is the same segment that experiences congestion on SR 528. Limited express lanes and lower speed limit on the lanes might contribute to the crash occurrence.

The number of crashes on mainline toll plaza cash lanes is relatively small compared with those of mainline and ramp crashes. The low number of cash lane crashes result in significant crash pattern change even though a small variation of crash counts. Hence, crash hot spots for toll plaza cash lanes were not fixed in these years. Nevertheless, Pine Hills Mainline Toll Plaza, Conway Road Mainline Toll Plaza on SR 408, John Young Parkway Mainline Toll Plaza, University Mainline Toll Plaza on SR 417, and Beachline Mainline Toll Plaza on SR 528 were found to be the toll plazas on the mainline that can have more crashes on their cash lanes.

For the ramp crashes, the similar pattern as mainline crashes on SR 408 were also detected. From 2011 to 2013, ramps at the interchange between SR 408 and SR 417 had the highest crash density. However, this pattern changed in 2014 as that the interchange between SR 408 and I-4 becomes the concentration area of ramp crashes on SR 408. The interchange between SR 417 and SR 528 is also a major area for ramp crashes. Also, the ramps on SR 417 at John Young Parkway and Orange Blossom Trail were found to be more likely to have ramp crashes. The findings of mainline crashes, mainline toll plaza cash lane crashes, and ramp crashes shows the concentrated locations of each type of these crashes. The changes in crash density on the expressway system are found. The results can be used for potential safety improvement projects in the future.

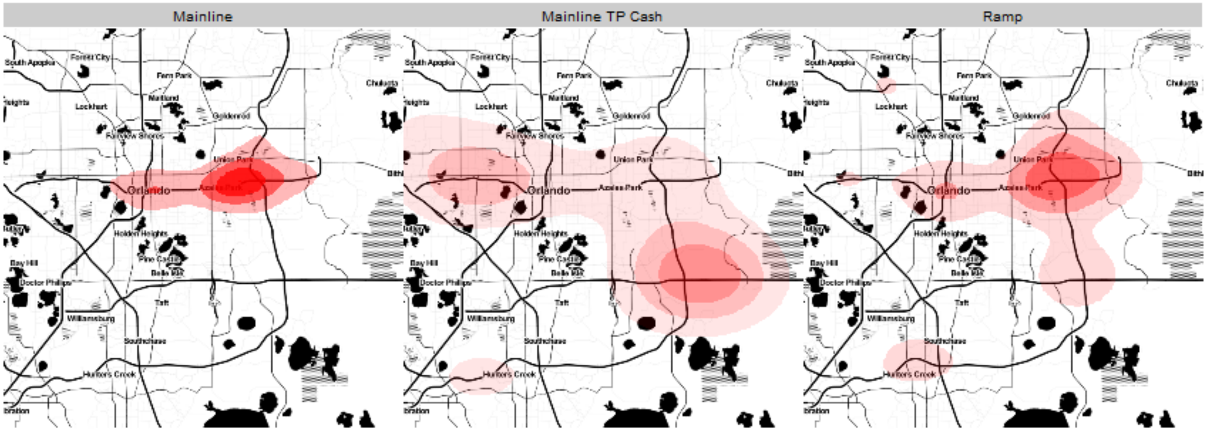

Figure 3-6 Spatial pattern of traffic crashes in 2011

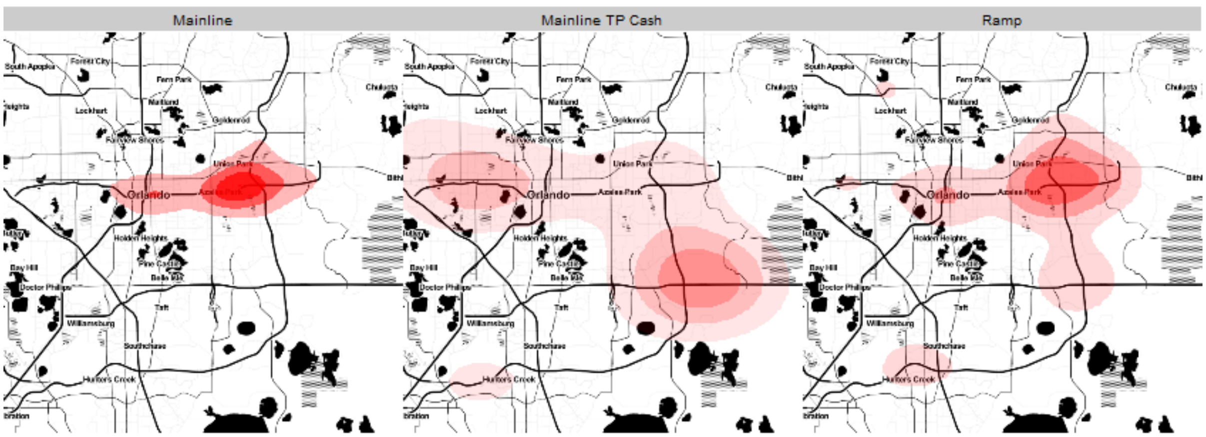

Figure 3-7 Spatial pattern of traffic crashes in 2012

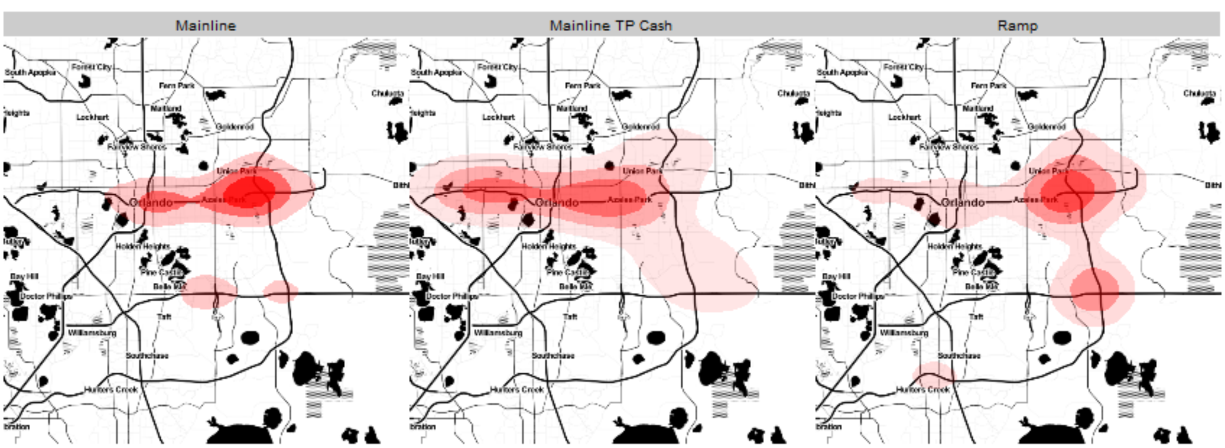

Figure 3-8 Spatial pattern of traffic crashes in 2013

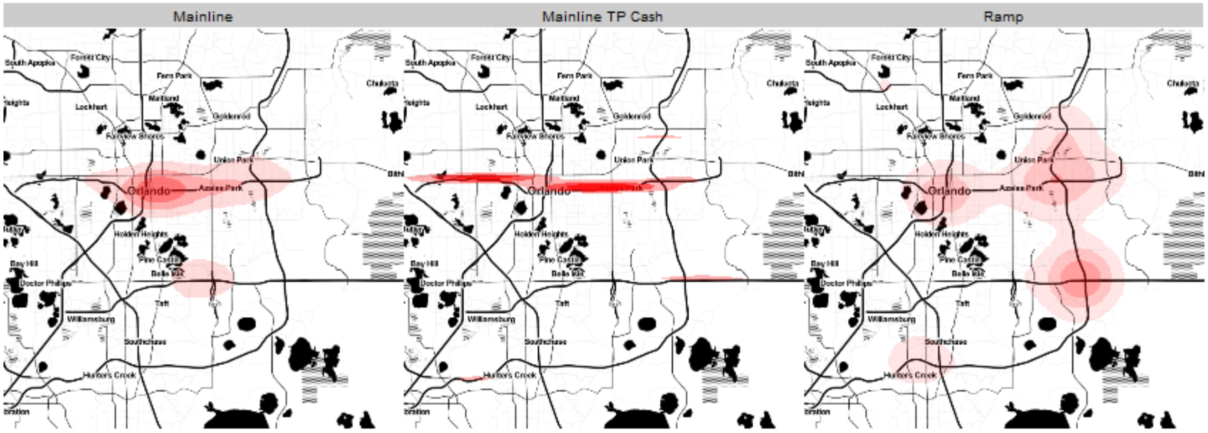

Figure 3-9 Spatial pattern of traffic crashes in 2014

3.5 Summary

In this chapter, visualization of traffic conditions on the most busiest expressway in Central Florida (SR 408) is conducted. Three-dimension spatio-temporal and contour plots were depicted to describe hourly volume distribution. Congestion levels on SR 408 were visualized by using TTI, occupancy, and CI. Subsequently, the spatial patterns of traffic crashes by facility types were visualized from 2011 to 2014. The visualization of crashes enables researchers to easily detect crash hotspots and to suggest appropriate engineering countermeasures. Data visualization facilitates researchers' understanding of the traffic and crash patterns on the studied objects. The spatiotemporal distribution of crashes along with corresponding traffic flow offer valued insights and can guide future statistical inference thus is a necessary step in big data analyses.

CHAPTER 4: REAL-TIME CONFLICT PRECURSORS FOR WEAVING SEGMENTS

4.1 Introduction

Traditional traffic safety studies are mainly based on historic traffic crash data. However, the usage of crash data is sometimes limited because of the unreliability of crash records and the long time needed to collect adequate crash samples (Glennon and Thorson, 1975; Essa and Sayed, 2015). Therefore, there has been plenty of traffic safety studies, which rely on surrogate safety measures.

One of the most commonly used surrogate measures is traffic conflicts. A traffic conflict was defined as a traffic event involving two or more road users, in which one user performs some unusual actions, such as a change in direction or speed, these unusual actions place another user in the danger of a collision unless an evasive maneuver is undertaken (Migletz et al., 1985). Previous studies have proven that conflict counts are positively related to crash counts, and the relationship is statistically significant (Meng and Qu, 2012; Sacchi and Sayed, 2016). Furthermore, researchers collected field conflict counts on roadway facilities to uncover potential safety hazard (Van Der Horst et al., 2014), and to verify the safety impacts of countermeasures, such as raised crosswalks (Cafiso et al., 2011; Autey et al., 2012). However, the majority of previous studies only focused on conflict count, but were not interested in the cause of each conflict and did not analyze conflicts from a microscopic aspect.

One of the studies that explore traffic safety from a microscopic aspect is real-time safety analysis. The real-time safety analysis intends to identify precursors that are relatively more “hazard prone” that other parameters. It is accomplished by comparing and analyzing traffic, weather, and other conditions right before the occurrence of hazard and non-hazard events, and furthermore by estimating the likelihood of hazard events. The hazard events include crash and conflict events. The real-time crash analysis research has been successfully done by plenty of previous studies (Zheng et al., 2010; Yu and Abdel-Aty, 2013a). However, there has not been enough real-time conflict analyses.

This chapter implements microscopic simulation and Surrogate Safety Assessment Model (SSAM) to conduct real-time conflict study. To build a well-calibrated and validated simulation network, this study first adopted high-resolution big traffic data from MVDS to serve as the traffic volume input and desired speed distribution input. Meanwhile, the microscopic simulation network were built based on a two level calibration and validation method. The method is able to enhance the consistency between simulated safety and filed safety, and between simulated traffic and field traffic. In simulation, conflicts are identified by SSAM, a software developed by Federal Highway Administration (FHWA). The SSAM automatically conducts conflict analysis by directly processing vehicle trajectory data from simulation output. The conflict analysis contains conflict location, time, type, etc. After obtaining time and location of a conflict or non-conflict event, the event is matched with the traffic data just before it. Then a logistic regression models are employed to distinguish conflict events from non-conflict events using traffic parameters.

4.2 Experiment Design

4.2.1 VISSIM Network Building

One of the most important parts of this chapter is building a calibrated and validated VISSIM network. Previous studies on weaving segments' microscopic simulation only compared simulated traffic with field traffic (Wu et al., 2005; Jolovic and Stevanovic, 2013). The results showed that the simulated traffic was consistent with field traffic if driver behavior parameters in the simulation were adjusted. However, this chapter focuses on real-time conflict analysis in microscopic simulation. Hence, not only traffic condition in simulation needs to be calibrated and validated, but also safety condition of the simulation network requires validation.

In order to ensure both traffic and safety of the simulation network are consistent with those of the field, a two level calibration and validation method was used. At the first level, the traffic conditions of weaving segments were calibrated and validated based on field MVDS data. At the second level, the simulated conflict count of each weaving segment was compared to its crash frequency. If the simulated speed or conflict is not consistent with its corresponding field value, driver behavior parameters need to be adjusted. The calibration and validation procedure is shown in Figure 4-1.

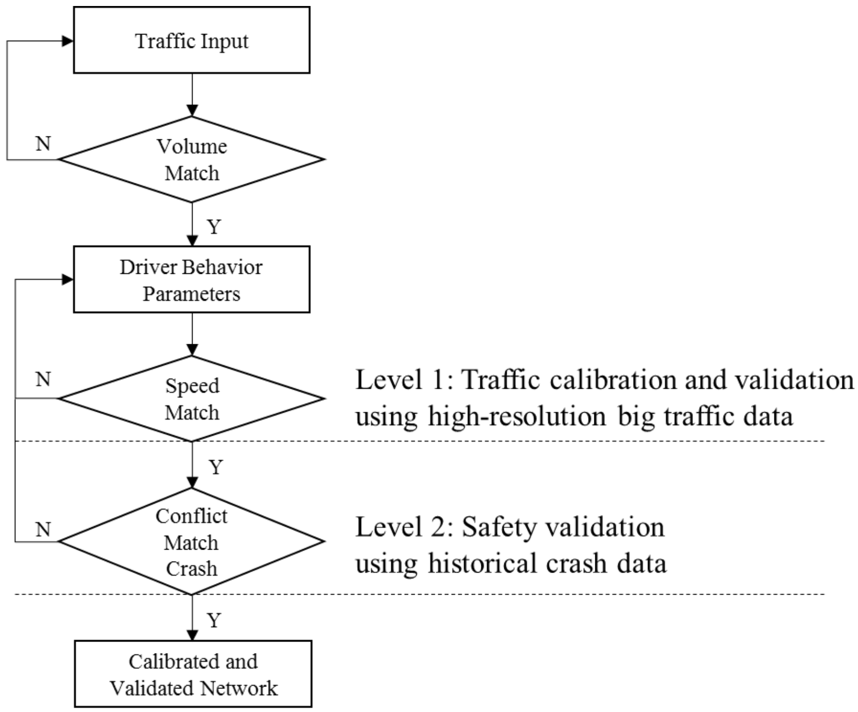

Figure 4-1 Two level calibration and validation procedure

4.2.2 Simulation Network Data Preparation

The study chose 16 weaving segments located on SR 408. Two datasets were collected for these 16 weaving segments: crash and traffic. Crash data were from S4A. Eighty-three crashes were identified on the 16 studied weaving segments from July 2013 to July 2014. The traffic data were obtained from MVDS.

It was assumed that the weekday daytime moderate traffic (from 1:00 P.M. to 3:00 P.M), which is neither the peak hour traffic nor the lowest traffic, can represent the average traffic condition. The peak hour of SR 408 for weekday is 6:00 A.M. to 9:00 A.M. in the morning and 4:00 P.M. to 7:00 P.M. in the afternoon. The traffic data from 1:00 P.M. to 3:00 P.M. on four Thursdays in August 2014 were aggregated into 15 minutes to provide the

VISSIM traffic input, including volume and Heavy Goods Vehicles (HGVs) percentage. The Type 3 and Type 4 vehicles in MVDS data were considered as HGVs in VISSIM.

Desired speed distribution is also an important input for the VISSIM network. If not hindered by other vehicles or network objects, e.g. signal controls, a driver will travel at his/her desired speed (PTV, 2013). The speed data during 11:00 A.M. to 1:00 P.M. on Thursdays in August 2014 were chosen. During this period, the traffic volume is the lowest in the daytime. Thus, the possibility of a vehicle constrained by other vehicles is low and vehicles are more likely to travel at their desired speed. Generally, the desired speed distribution is decided by geometric design, e.g., degree of curvature, speed limit. The desired speed distribution for each location might not be the same. Hence, this study divided the locations of SR 408 into seven groups according to the similarity of speed limit and field speed distribution of each location. The group information is in Table 4-1. In the table, for each location, the beginning two letters stand for direction, i.e., WB is westbound and EB is eastbound; the numbers stand for milepost.

Table 4-1 Speed distribution for each location

Speed Limit	Group	Locations
55	1	WB 22.7, EB 21.8, WB 10.3, EB 22.7, EB 9.2
	2	EB 9.4, EB 9.6, WB 9.9,WB 20.8, EB 10.8,WB 10.6, WB 8.1, WB 14.5, WB 8.4, WB 9.7, WB 12.1, WB 20.7, EB 10.3
	3	WB 7.4, WB 9.2, WB 11.3, EB 11.5, EB 8, EB 12.5, WB 10.9, EB 8.4, WB 8.9, WB 15.2, EB 22.3, EB 7.6, WB 13, EB 10.6, EB 7, WB 11.6, WB 14.4
	4	EB 12.9, EB 8.9, WB 7.3, WB 14.2, EB 11.2, EB 7.4, EB 12.1, EB 14.5, WB 22.3, EB 6.8, EB 14.7, WB 12.6, EB 16.1, WB 6.8, WB 15.7, WB 21.8, WB 7.6, EB 15.7
65	5	EB 20.8, WB 19.7, WB 1.4, WB 1.6,WB 5.3, EB 5.3, WB 2.4, EB 20.3
	6	WB 15.9, EB 18.4, EB 16.5, WB 18.4, WB 4.6, EB 2.4, WB 19.9, EB 1.4, EB 4.6, WB 16.5, WB 3.6, WB 18.8, EB 3.6, EB 4.3, EB 18, EB 18.8, EB 20.1, WB 17, WB 2, WB 4.9, WB 17.8, WB 18, EB 19.5, EB 2.2, EB 17.7, WB 16.1, EB 17.3, EB 1.7, WB 4.3
	7	EB 4.9

Figure 4-2 shows the cumulative percentage of desired speed distribution for each group.

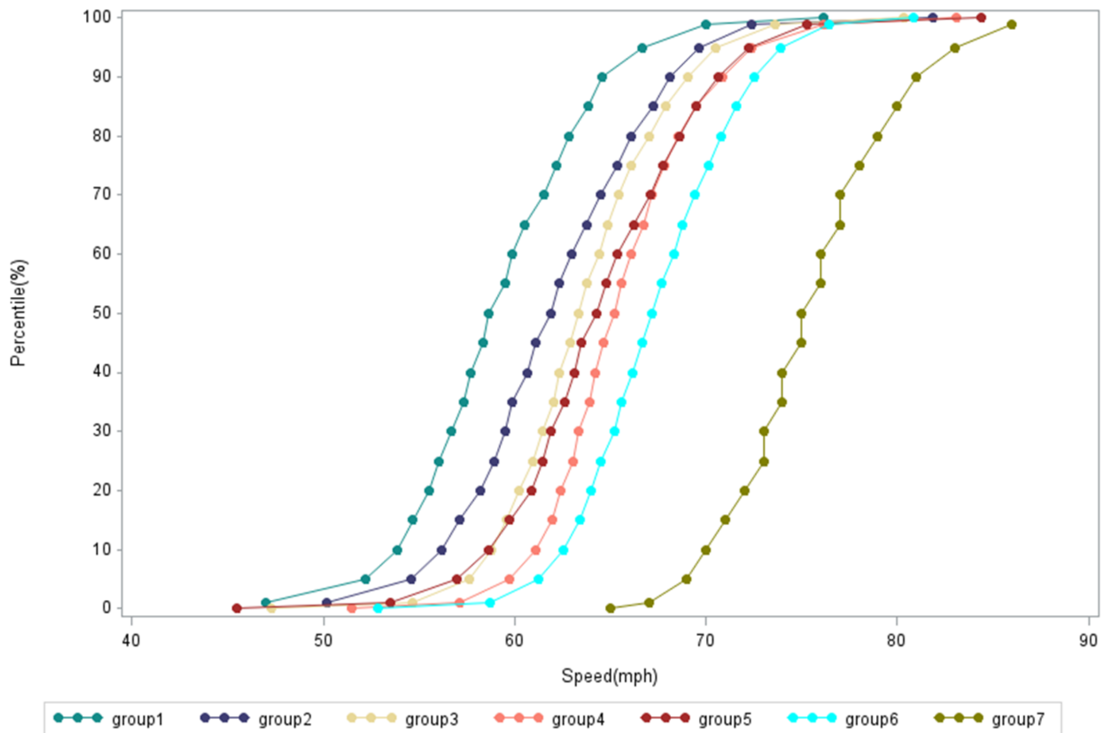

Figure 4-2 Speed distribution for each group

The desired speed distribution in the figure is the average speed of all vehicles, including passenger cars (PCs) and HGV. However, PC and HGV are at different speeds. Johnson and Murray (2010) concluded that the average speed difference between cars and trucks was 8.1 miles per hour. The HGVs might be considered as trucks. The HGV percentage of these 16 weaving sections is about 13%. Suppose *x* is the speed of passenger cars, then the speed for HGV is equal to (*x*-8.1), the average speed is *y*, then,

$$87\%x + 13\%(x - 0.81) = y \qquad (4\text{-}1)$$

From Eq. 4-1, PC speed is about *y*+1, and the truck speed is about *y*-7. By shifting the curve in Figure 4-2 to the right by 1 mph, speed distributions of PC for each group can be obtained. Similarly, by shifting the curve by 7 mph to the left, HGV speed distributions can be gained. Finally, there are 14 desired speed distributions, among which seven are for PCs and seven for HGVs.

4.2.3 Data Extraction

Once driver behavior parameters were obtained after the calibration and validation procedure, they were put into the VISSIM network. Then, 15 simulation runs were carried out. The trajectory files from simulation output were analyzed in SSAM to provide conflict information. For each conflict, its corresponding traffic data were from data collection points in VISSIM. The layout of data collection points in VISSIM is illustrated in Figure 4-3. When vehicles pass the data collection points, the points collected every vehicle's data, including entry time, exit time, vehicle classification, speed, occupancy, etc.

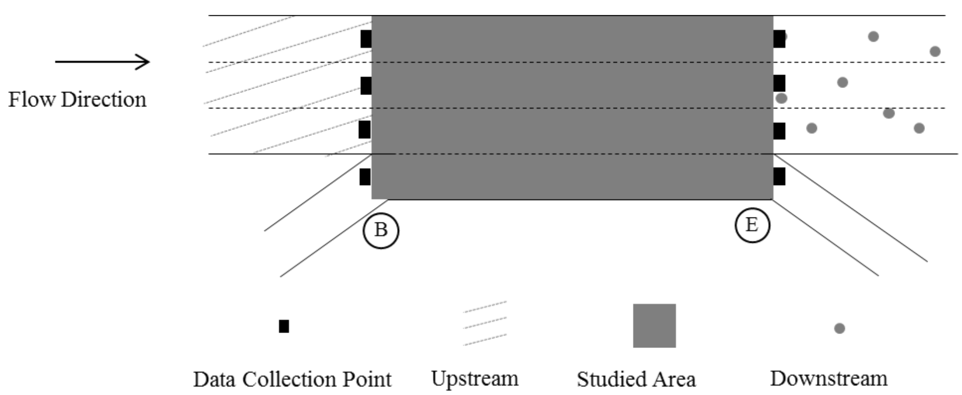

Figure 4-3 Traffic data extraction

The data extraction of the real-time conflict study is different from that of a crash precursor study. First, crash disruptive condition is usually 5-10 minutes before a crash (Abdel-Aty and Pemmanaboina 2006, Xu et al. 2013). The crash time in crash reports is actually the estimated crash time, which migh be after actual crash time. Thus, the traffic data which are 0-5 minutes before crash reporting time might already been impacted by a crash, so the trafific data 5-10 minutes before the time in crash report are usually chosen. However, for the conflict precursor study, the accurate conflict time can be obtained from SSAM. Hence, the traffic data, which are 0-5 minutes before a conflict, were chosen as conflict disruptive events. As for the non-disruptive events, they were 5-minute interval traffic data and were defined as the conditions, which neither resulted in a conflict nor were under influence of conflicts. In this study, it was assumed that traffic conditions were not impacted by conflicts if they were more than 60 seconds after conflicts, because conflicts are cleared quickly in simulation and the influence of conflicts on traffic vanish soon. Furthermore, in order to explore conflict mechanisms more closely, the study also adopted the traffic data that were 0-1 minutes before conflicts as disruptive condition, and the non-disruptive traffic data were also at 1-minute intervals. Hence, two datasets were prepared: one was based on 5-minute interval; the other one was based on 1-minute interval.

Second, in crash prediction studies, the number of non-disruptive conditions is much more than that of disruptive conditions. In order to balance the sample size of disruptive and non-disruptive conditions, non-disruptive condition observations are randomly selected from the full samples (Abdel-Aty et al. 2004, Hossain and Muromachi 2010, Xu et al. 2013). Nevertheless, conflict number is much more than crash number. Gettman et al. (2008) found that the probability of being involved in a crash given a traffic conflict is 0.005% at intersections. This indicates that the conflict number was 20,000 times of the crash number in their study. In real-time conflict study, the sample size of disruptive conflict condition is largely enriched, and the sample size of non-disruptive conflict condition is significantly decreased. There was no need to select randomly the non-disruptive conflict condition samples.

The variables obtained from data collection points of VISSIM network and from the geometric design of weaving segments are shown in Table 4-2.

Table 4-2 Variable definition

Variables*	Description
Bm_spd	Average speed at the beginning of weaving segments (mph)
Bm_vol	Vehicle count per lane at the beginning of weaving segments (vehicles)
Bm_occ	Average lane occupancy at the beginning of weaving segments (%)
Bm_std_spd	speed standard deviation at the beginning of weaving segments (mph)
Onr_spd	Average speed for on-ramp (mph)
Onr_vol	Total vehicle count for on-ramp (vehicles)
Onr_occ	Average lane occupancy for on-ramp (%)
Em_spd	Average speed at the end of weaving segments (mph)
Em_vol	Vehicle count per lane at the end of weaving segments (vehicles)
Em_occ	Average lane occupancy at the end of weaving segments (%)
Em_std_spd	speed standard deviation at the end of weaving segments (mph)
Offr_spd	Average speed for off-ramp (mph)
Offr_vol,	Total vehicle count for off-ramp (vehicles)
Offr_occ	Average lane occupancy for off-ramp (%)
V_{FF}	Mainline-to- mainline vehicle count (vehicles)
Vehcnt	Total traffic count in the weaving segment (vehicles)
VR	Weaving volume ratio, weaving volume over total traffic count (%)
Spd_dif	Speed difference. Spddif =0 if Bm_spd is lower than Em_spd; otherwise Spddif = Bm_spd- Em_spd
Bm_acc	Average acceleration at the beginning of weaving segments (fts)
Em_acc	Average acceleration at the end of weaving segments (fts)
Bm_headway	Average headway at the beginning of weaving segments (s)
Em_ headway	Average headway at the end of weaving segments (s)
Ls	Short length, distance between the end points of any barrier markings (solid white lines) that prohibit or discourage lane changing (feet)
Lb	Base length, distance between points in the respective gore areas where the left edge of the ramp-traveled way and the right edge of the freeway-traveled way meet (feet)
N_{WL}	Number of lanes from which a weaving maneuver may be made with one or no lane changes (lane)
N	Number of lanes within the weaving segment (lane)
LC_{RF}	Minimum number of lane changes that must be made by a single weaving vehicle moving from the on-ramp to the expressway (lane)
LC_{FR}	Minimum number of lane changes that must be made by a single weaving vehicle moving from expressway to off-ramp (lane)
LC	Weaving configuration, 0 when LC_{RF} =LC_{FR}=1, 1 otherwise
LC_{min}	Minimum rate of lane change that must exist for all weaving vehicles to complete their weaving maneuvers successfully (lane/hour)
L_{max}#	Maximum weaving influence length (1000 feet)

* All traffic data are separately measured in 5-minute interval and 1-minute interval

\# $L_{max} = [5728(1+VR)^{1.6} - 1566N_{WL}]/1000$ (in HCM 2010)

4.3 VISSIM Network Calibration and Validation

Based on the previous literatures (Koppula, 2002; Wu et al., 2005; Woody, 2006; Jolovic and Stevanovic, 2013), four parameters were chosen for VISSIM calibration and validation. They were desired lane change distance (DLCD), stand still distance (CC0), following headway time (CC1), and following variation (CC2). DLCD defines the distance at which vehicles begin to attempt to change lanes in order to arrive at their desinations. CC0 is desired distance between stopped vehicles. CC1 is following headway time, which means the time (in seconds) a driver wants to keep. The higher the CC1, the more cautious the driver is. CC2 is following variation, which restricts the longitudinal oscillation or how much more distance than the desired safety distance a driver allows before he/she intentionally moves closer to the car in front (PTV group, 2013).

The study first used the recommended parameters' value from previous studies to validate the VISSIM network (Koppula, 2002; Wu et al., 2005; Woody, 2006; Jolovic and Stevanovic, 2013). The results showed the previous studies' conclusions were valid only when traffic was compared. However, when comparing the simulated conflict counts with the field crash frequencies, the correlation coefficients were not significant. This is because the parameters' values were gained without considering the safety in previous studies.

There was a need to revalidate the weaving segment VISSIM network with respect to both traffic and safety. Twenty-three sets of parameters were tried and each set was run three times with different random seeds. After excluding 30 minutes VISSIM warm up time and 30 minutes cool down time, 60 minutes VISSIM data were put into use. For the 16 weaving segments network, the results showed that VISSIM could provide good traffic and safety results when the DLCD was 300 meters, CC0 was 1.5 meters, CC1 was 1.5 seconds, and CC2 was 4 meters. 15 more runs using the parameters above were carried out. For the 15 simulation runs, the average GEH value of the validated VISSIM network was 1.82, and 96.0% of GEH were less than 5 for a 15 minutes interval. As for the speed, the average absolute of speed difference was 2.00 mph, and 92.2% of speed differences were less than 5 mph for a 5 minutes interval. The good results also implied that implementing big traffic data can help in build microscopic simulation networks with good quality. The results approved that the traffic calibration and validation satisfy the requirements, and indicate the traffic on the weaving segment network was consistent with that of the field (Nezamuddin et al., 2011; Yu and Abdel-Aty, 2014).

After the traffic calibration and validation, the trajectory files of the simulation runs were processed in SSAM. Several conflict measurements can be obtained from SSAM, such as time-to-collision (TTC) and post-encroachment-time (PET). TTC is defined as the expected time for two vehicles to collide if they remain at their present speed and continue on their respective trajectories; PET is time difference between the arrivals of two vehicles at the potential point of collision (Gettman and Head, 2003). In this study, a conflict was identified when TTC was less than 1.5 seconds and PET was less than 5.0 seconds. The same thresholds were also widely adopted by other studies (Stevanovic et al., 2013; Saleem et al., 2014; Saulino et al., 2015). Meanwhile, when TTC was 0, the observation was deleted (Gettman et al., 2008).

The average simulated conflict count for each weaving segment was then compared with the corresponding crash frequency. The information can be found in Table 4-3. Then, SAS procedure 'Corr' was used to conduct a Spearman rank correlation test. The range of

Spearman's rank correlation coefficient is 0 to 1; a coefficient of 0 indicates no correlation and 1.0 represents a perfect agreement (Gettman et al., 2008). The result showed that the correlation coefficient between simulated conflict counts and field crash frequencies was 0.506 (p-value= 0.0457), which indicates that there was a significant positive relationship between field crash count and conflicts.

Table 4-3 Simulated conflict count and field crash count

ID	Run															Avg*	Crash
	1	2	3	4	5	6	7	8	9	10	11	12	13	14	15		
1	2	3	2	3	1	0	3	3	1	0	2	0	0	3	0	1.5	4
2	6	4	2	5	6	3	3	7	10	6	7	4	6	5	8	5.5	3
3	0	1	0	1	1	1	2	0	0	0	1	1	0	3	2	0.9	4
4	1	1	3	2	1	1	2	1	1	0	1	2	2	0	2	1.3	1
5	16	5	5	15	12	15	14	4	7	5	8	10	13	16	13	10.5	8
6	17	17	13	20	12	24	16	22	20	11	24	27	14	17	34	19.2	8
7	2	1	2	2	0	0	0	0	0	0	1	1	1	4	3	1.1	4
8	0	1	0	0	0	1	0	0	1	0	0	0	0	0	1	0.3	6
9	4	6	5	1	8	4	9	7	1	1	10	11	4	6	9	5.7	4
10	7	12	8	9	6	16	9	10	3	7	7	18	8	7	8	9.0	9
11	19	13	4	11	8	5	12	13	9	11	6	16	6	11	10	10.3	15
12	1	6	3	1	1	0	2	1	1	4	3	0	0	1	2	1.7	4
13	5	2	4	1	5	5	3	1	1	5	3	4	5	0	3	3.1	1
14	0	0	0	0	1	2	0	0	1	1	0	1	0	6	0	0.8	3
15	4	1	2	0	1	0	0	0	0	1	0	2	1	2	1	1.0	3
16	1	1	0	2	3	2	3	4	2	2	1	3	3	3	2	2.1	6

* Average conflict number

4.4 Model Estimation

In order to find significant conflict precursors and to quantify their impacts on conflict risk, two logistic regression models were built: one was based on 5-minute intervals; the other one was based on 1-minute intervals. K-folder cross validation method was used to validate models' performance. The *k*-fold cross-validation method is able to minimize the bias caused by the random sampling of the training and validation data samples (Olson and Delen, 2008). In k-fold cross-validation, the complete dataset is randomly divided into *k* mutually exclusive subsamples, each subsample having proximately equal sample size. The model is trained and tested *k* times. For each attempt, a subsample acts as the validation data for testing the model, and the remaining *k*-1 subsamples are training data. Each of the *k* subsamples is used exactly once as the validation data, so the cross-validation process is repeated *k* times in total. Then the *k* results from the *k* validation folds are combined to provide a single estimation of model performance. In this study, a 10-folder cross validation was adopted. The model results are shown in Table 4-4.

Table 4-4 Real-time conflict prediction model for weaving segment

Variables	Mean	Std.	p-value
Based on 5-minute interval			
Intercept	-17.99	1.42	<0.01
Log(Vehcnt)	2.40	0.21	<0.01
L_{max}	0.36	0.09	<0.01
Bm_acc	-2.85	0.54	<0.01
Training AUC		0.727	
Validation AUC		0.721	
Based on 1-minute interval			
Intercept	-19.24	0.69	<0.01
Log(Vehcnt)	3.82	0.16	<0.01
L_{max}	0.21	0.03	<0.01
Bm_acc	-1.73	0.22	<0.01
Training AUC		0.827	
Validation AUC		0.827	

Area Under the Curve (AUC) is a good inex of classification accuracy for logistic regression models (Hosmer Jr et al., 2013). It plots true positive rate against false positive rate for all possible thresholds. The range of AUC is 0.5 to 1.0, a higher value indicating a better ability in discriminating conflict and non-conflict events. When the AUC of a model is higher than 0.80, it indicates the model has a good discrimination between case and control (Hosmer Jr et al., 2013).

Both the 5-minute interval and 1-minute interval models showed that the Logarithm of vehicle count, maximum influence length, and average acceleration at the beginning of weaving segments were conflict precursors that were significant at the 5% confidence interval. The 1-minute interval model performed better than the 5-minute interval model by providing higher training and validation AUCs. Compared to the model using traffic aggregated at a 5-minute interval, the model using 1-minute interval traffic was able to capture information that is more detailed.

The coefficients of significant variables in the two models vary. The main reason might be the way through which traffic was aggregated. From the standard deviations of the coefficients, it could be found that the 1-minute interval model provided lower standard deviations than the 5-minute interval model, which indicates that the 1-minute interval model is more reliable than the 5-minute interval model. It is not hard to understand, the disruptive traffic 0-1 minutes before a conflict can better present the traffic condition contributing to the conflict than the disruptive traffic 0-5 minutes before the conflict.

The Logarithm of vehicle count was positively related to conflict risk. When vehicle count increases, the exposure increases and then the conflict likelihood increases. The maximum influence length was with a positive sign. A longer influence distance is because of a higher percentage of weaving volume. High weaving volume indicates high on-ramp or off-ramp volume or both. For on-ramp vehicles, they need to accelerate to merge into mainline traffic; for off-ramp vehicles, they have to diverge from mainline and decelerate to adjust to low speed limits on off-ramps; meanwhile, high on- and off-ramp traffic volume also rises weaving opportunity. The acceleration, deceleration, weaving, merging, and diverging actions definitely worsen traffic safety. Additionally, the average acceleration at the beginning of weaving segment was proven to have a significantly negative impact on conflict risk, which means an increase of average acceleration decreases conflict risks.

4.5 Summary

There has been plenty of traffic safety research based on surrogate safety measures. One of the most commonly used surrogate safety measures is traffic conflicts. The majority of previous conflict studies focused on conflict frequencies but did not explore conflict mechanisms from a microscopic aspect. This chapter built a real-time conflict prediction model for weaving segments based on the traffic and conflict information captured from microscopic VISSIM network. The simulation network was well calibrated and validated because of high-resolution big traffic data input.

Driving behavior parameters in simulation were adjusted to validate the simulation network. When DLCD was 300 meters, CC0 was 1.5 meters, CC1 was 1.5 seconds, and CC2 was 4 meters, not only the traffic condition but also the safety condition of simulated network were consistent with the field weaving segment network. The validated VISSIM network had an overall average GEH value of 1.82 and the average speed difference was 2.00 mph. The

Spearman rank correlation test was carried out to compare the simulated and filed safety, the coefficient was 0.506 and was significant at the 5% confidence interval.

Two conflict prediction models were estimated, one was based on a 5-minute interval and the other was based on a 1-minute interval. In both models, Logarithm of vehicle count, maximum influence length, and average acceleration at the beginning of weaving segment were significant variables. The model performance of the 1-minute interval model was better than that of the 5-minute interval model by providing higher AUCs and lower standard deviation of variable coefficients.

This study is the first one which use the simulated conflict to study the traffic parameters' impacts on safety in real-time. Before this study, if researchers intended to build the real-time safety prediction model, several months' crash and traffic data for several locations should be prepared to obtain enough sample size. The traffic data had to be collected continuously and be with high resolution. If the funding is limited, it is hard to equip road facilities with enough traffic detectors. Hence, implementing simulation to study the real-time safety analysis might be an economic, time saving, and reliable method.

CHAPTER 5: TRAVEL TIME RELIABILITY AND TRAFFIC SAFETY

5.1 Introduction

With a steady growth of traffic demands in urban areas, toll expressways have become an important alternative for transportation agencies to provide motorists with safe, efficient, and reliable trips. Three major focus of traffic operators are reducing crash occurrence, decreasing congestion, and improving travel time reliability on the highway systems. These three aspects might be interrelated. In other words, an aspect might have an effect on the others. For instance, crashes could lead to decreased efficiency and unreliable travel time; reduced efficiency could increase crash likelihood and lower travel time reliability; unreliable travel time could cause unstable traffic flow thus affecting efficiency and safety.

During the past few decades, there have been substantial efforts dedicated to exploring the crash mechanisms and the relationship between traffic efficiency (e.g., level of service, congestion) and traffic safety. Nevertheless, no research studies have been done to investigate how travel time reliability could affect traffic safety on urban expressways. The objective of this chapter is thus to identify whether travel time reliability has impacts on crash frequency and crash risk for expressways.

5.2 Background

Travel time reliability indicates the level of consistency in transportation service experienced by travelers compared with their normal experience. Given travel time data, various approaches have been proposed to measure the travel time reliability. Three types of measures could be generalized, namely statistical range measures, buffer measures, and tardy trip indicators (Martchouk, 2009). One of the statistical range measures is the Percent Variation as shown in Eq. 5-1 (Lomax and Margiotta, 2003).

$$Percent\ Variation = \frac{Standard\ Deviation\ of\ Travel\ Time}{Average\ Travel\ Time} \times 100\% \tag{5-1}$$

The Buffer Index in Eq. 5-2 is a buffer measure to assess how much extra time is needed for uncertainty in the travel conditions (Martchouk, 2009).

$$Buffer\ Index = \frac{95th\ Percentile\ Travel\ Time - Average\ Travel\ Time}{Average\ Travel\ Time} \times 100\% \tag{5-2}$$

Tardy trip indicators imply the amount of late trips. The Misery Index as displayed in Eq. 5-3 is a tardy trip indicator that compares the worst 20% of the trips against the average condition to show the impact of late traffic on reliability (Lomax and Margiotta, 2003).

$$Misery\ Index = \frac{Average\ of\ the\ Travel\ Time\ for\ the\ Longest\ 20\%\ of\ Trips - Average\ Travel\ Time\ for\ All\ Trips}{Average\ Travel\ Time\ for\ All\ Trips} \times 100\% \tag{5-3}$$

The indicator Percent Variation is easy for calculation and interpretation; meanwhile, it can be used in real-time analysis. However, it has a drawback since it treats early and late arrivals equally whereas in reality the public is more concerned about late arrivals. On the other hand, the Buffer Index and Misery Index focus on the impact of late arrivals on travel time reliability, but they are hard to be implemented in real-time analysis, since the calculation of Buffer Index and Misery Index requires large samples to reduce the possibility that individual observations have significant impacts on calculation results. Hence, the crash frequency study implemented the three indicators; whereas, the real-time safety analysis only adopted Percent Variation.

In some existing studies (Geedipally and Lord, 2010; Yu and Abdel-Aty, 2013a), there have already been discussions about different mechanisms between SV and MV crashes. For the purpose of this chapter, whether travel time reliability would have impact on SV and MV crashes in the same manner is worth investigation. Additionally, real-time crash analysis was utilized to estimate MV crash risk given a crash occurrence.

5.3 Data Preparation

SR 408, a 22-mile urban expressway, was selected as a study area. The expressway of interest is traveled by a large number of commuters and experiences heavy congestions during morning and evening peak hours. Hence, travel time reliability varies across time of day and across segments of the expressway. Three types of data were collected for SR 408: traffic, crash, and geometry.

Part of traffic data are from AVI system, which is used as ETC for toll expressways. For SR 408, most of the travelers (about 85%) have installed AVI tags in their vehicles for ETC. By collecting the travel time stamps of the encrypted individual vehicles at different locations, vehicles' travel time and speed information on a segment are readily available. The calculations of travel time and speed are as follows,

$$Traval\ Time = Timestamp_{downstream} - Timestamp_{upstream} \tag{5-4}$$

$$Speed = \frac{\left| Milepost_{downstream} - Milepost_{upstream} \right|}{Travel\ Time} \tag{5-5}$$

The AVI data have been collected since September 2012. At the time of study, data of two years and seven months until March 2015 were prepared. On the 22-mile expressway, there were 42 activate AVI segments with 22 on the eastbound and 20 on the westbound in the study period. Based on the AVI data, average speed, standard deviation of speed, and the three indicators, i.e., Percent Variation, Buffer Index, and Misery Index, were calculated.

Since the AVI system only detects vehicles equipped with tags but cannot detect all vehicles, the traffic volumes on each AVI segment cannot be obtained from AVI but were derived from the MVDS detectors, which are capable of detecting all vehicles. There were about 55 MVDS detectors on each direction of SR 408. When there were one or more MVDS detectors within an AVI segment, the average volume per lane from multiple locations would be calculated. If there were no MVDS detectors exists within an AVI segment, the average volume per lane from the nearest upstream and downstream MVDS detectors was used.

Meanwhile, crash data were prepared from S4A database. The crash data provide crash time, location, passenger numbers, and roadway surface condition (i.e., wet or dry), etc. For SR 408, 1,342 crashes occurred on the expressway mainline during the study period, among which 1,112 were MV crashes and 230 crashes were SV crashes. According to the crash counts, it can be found that the majority of crashes on this urban expressway were MV crashes, which might imply distinct mechanisms for these two types of crashes.

In addition to traffic data, roadway geometric characteristics are also significant crash contributing factors (Shankar et al., 1995; Ahmed et al., 2011; Yu et al., 2013). In this task, geometric data for the expressway were downloaded from FDOT RCI database. Homogeneous segments of the roadway were generated according to their geometric characteristics. Short distance segments (less than 0.1 mile) were combined with adjacent segment, which is with higher similarity. The chosen geometric characteristics included number of lanes, existence of auxiliary lanes, speed limit, horizontal degree of curvature, median width, and shoulder width. In total, there are 99 RCI segments generated on the eastbound and 99 RCI segments on the westbound.

5.4 Descriptive Analysis

For crash frequency analysis, after collecting AVI and MVDS traffic data, crash data, and geometric characteristics data, the three data were merged together. The Table 5-1 gives a descriptive analysis for the three datasets.

Table 5-1 Descriptive analysis for crash frequency analysis

Variables	Description	Mean	Std.	Minimum	Maximum
Y_{MV}	MV crashes per segment	5.62	9.60	0	83
Y_{SV}	SV crashes per segment	1.16	1.49	0	7
Lanevol	Traffic volume by lane	12198.77	3687.61	5612.55	20600.05
Speed	Average speed (mph)	63.55	4.93	51.82	74.09
Std_speed	Standard deviation of speed	7.65	2.05	4.76	13.58
Length	Segment length (mi)	0.22	0.13	0.07	0.76
Lanes	Number of lanes	--	--	2	5
Auxiliary	0=no auxiliary lanes; 1= auxiliary lanes	--	--	0	1
Spd_lmt	Speed limit	--	--	55	65
Hrzdgcrv	Horizontal degree of curvature	0.48	0.89	0	5.25
Mdwidth	Median width (feet)	35.37	18.64	20	64
Sldwidth	Shoulder width (feet)	10.03	0.25	10	12
Per_var	Percent Variation	36.34	17.44	14.43	87.02
Buffer_index	Buffer Index	19.47	15.08	11.34	102.61
Misery_index	Misery Index	0.22	0.09	0.13	0.56

For real-time safety analysis, the data from the three sources were merged together and created 973 complete real-time SV and MV crash observations. The descriptive analysis of the observations is shown in Table 5-2.

Table 5-2 Descriptive analysis for real-time safety analysis

Variables	Description	Mean	Std.	Minimum	Maximum
Y	0=crash is a SV crash; 1=MV crash	--	--	0	1
Speed	Average speed in 5 minutes (mph)	58.10	11.15	6.96	108.59
Std_speed	Standard deviation of speed in 5 minutes (mph)	4.99	2.45	0	38.69
Lanes	Number of lanes (lane)	3.12	0.97	2	5
Lane345	0=two lanes; 1=more than 2 lanes	--	--	0	1
Auxiliary	0=no auxiliary lanes; 1= auxiliary lanes	--	--	0	1
Spd_lmt	Speed limit	--	--	55	65
Hrzdgcrv	Horizontal degree of curvature	0.50	0.85	0	5.25
Mdwidth	Median width (feet)	28.12	15.82	20	64
Sldwidth	Shoulder width (feet)	10.00	0.09	12	10
Passenger	0=no passengers in the car; 1=otherwise	--	--	0	1
Wet	0=dry roadway surface condition; 1=otherwise	--	--	0	1
Per_var	Percent Variation in 5 minutes (%)	10.50	11.99	0	149.56

5.5 Methodology

5.5.1 Bayesian Hierarchical Poisson-lognormal Model

As crash counts are non-negative integers, generalized linear models are adopted in crash frequency analysis. Lord and Mannering summarized the statistical methods for crash-frequency data, their strength and disadvantages (Lord and Mannering, 2010). Among these methods, Bayesian inference is widely used for its capability to deal with sophisticated data structure that cannot be handled by Maximum Likelihood Estimation (Huang and Abdel-Aty, 2010).

The data used in crash frequency analysis might exhibit hierarchical structure. On each direction, there were 99 RCI segments but only about 20 AVI segments, multiple RCI segments shared the same traffic information. Given the structure of the data, the traditional assumption about the independent sample in regression models does not hold. To properly evaluate the effects of traffic variables, the hierarchical data structure needs to be addressed.

In this study, a Bayesian hierarchical Poisson-lognormal model framework was adopted. The introduction of lognormal random effects was to solve the issue of over-dispersion. The model specification is set up as:

$$Y_{ij} \sim Poisson(\lambda_{ij}) \tag{5-6}$$

$$\log(\lambda_{ij}) = \alpha_0 + \alpha_{j[i]} + X_{ij}\beta + \varepsilon_i \tag{5-7}$$

$$\alpha_j = U_j\gamma \tag{5-8}$$

where Y_{ij} is the observed crash frequency on RCI segment *i* (*i*=1,2,…,198) nested within AVI segment *j* (*j*=1,2,…,42) that follows Poisson distribution with parameter λ_{ij}. α_0 stands for intercept. X_{ij} are geometric characteristics variables and β are the corresponding coefficients. The random effects follows normal distribution $\varepsilon_i \sim N(0,1/\tau_i)$. α_j represents the effects of AVI traffic variables U_j. γ is coefficients for U_j. The models were calibrated with non-informative prior distributions in WinBUGS software (Lunn et al., 2000). β and γ are assigned with $N(0,10^6)$ and $\tau_i \sim gamma(10^{-3},10^{-3})$.

5.5.2 Logistic Regression Model

Logistic regression models have been widely used in real-time crash studies (Abdel-Aty and Pande 2005, Hourdos et al. 2006). They are capable to distinguish and quantify crash contributing parameters. For any given crash event *i*, it has two exclusive states: MV crash or

SV crash. In this task, the binary responses, MV crash (y_i=1) and SV crash (y_i=0), were converted into probabilities p_i (y_i=1) and 1-p_i (y_i=0), respectively. The model is as follows,

$$y_i \sim Bernoulli(p_i) \tag{5-9}$$

$$\log(\frac{p_i}{1-p_i}) = \beta_0 + \sum_{r=1}^{R} \beta_r x_{ri} \tag{5-10}$$

where β_0 is the intercept, β_r the coefficient of r^{th} predictors, x_{ri} the value of r^{th} explanatory variable for i^{th} observation. The logistic regression model was calibrated in SAS software using PROC LOGISTIC.

5.6 Model Results

5.6.1 Crash Frequency Analysis

In Bayesian inference, Deviance Information Criterion (DIC) was adopted for model performance evaluation. DIC is the summation of model fitting and the number of effective variables. Smaller DIC is better. Percent Variation, Buffer Index, and Misery Index were individually included in the crash frequency models for MV and SV crashes in Table 5-3 and Table 5-4.

Table 5-3 Parameter estimation for MV crash frequency

Variables	Percent Variation		Buffer Index		Misery Index	
	Estimate	Std.	Estimate	Std.	Estimate	Std.
Intercept	-0.746#	5.326	-0.2882#	3.07	-3.579#	3.38
Log_Lanevol	0.354**	0.052	0.342**	0.041	0.294**	0.052
Log_Length	1.302**	0.165	1.338**	0.171	1.289**	0.168
Auxiliary	0.433**	0.166	0.45**	0.169	0.426**	0.159
Mdwidth	-0.017**	0.007	-0.017**	0.006	-0.016**	0.006
Per_var	0.007#	0.007	--	--	--	--
Buffer_index	--	--	0.022**	0.008	--	--
Misery_index	--	--	--	--	3.716**	1.423
$\overline{D}$	731.997		731.642		730.989	
p_D	124.558		123.232		123.492	
DIC	856.555		854.874		854.481	

** Significant at the 5% Bayesian Credible Interval
# Not significant at the 10% Bayesian Credible Interval
All other variables are significant only at the 10% Bayesian Credible Interval

Table 5-4 Parameter estimation for SV crash frequency

Variables	Percent Variation		Buffer Index		Misery Index	
	Mean	Std.	Mean	Std.	Mean	Std.
Intercept	2.157#	2.496	2.31#	2.674	3.827#	2.674
Log_Lanevol	0.215**	0.049	0.213**	0.036	0.215**	0.044
Log_Length	1.148**	0.167	1.168**	0.165	1.162**	0.16
Auxiliary	0.143#	0.185	0.148#	0.173	0.136#	0.177
Mdwidth	-0.011	0.006	-0.01**	0.005	-0.011**	0.005
Per_var	0.001#	0.007	--	--	--	--
Buffer_index	--	--	0.003#	0.007	--	--
Misery_index	--	--	--	--	0.312#	1.215
$\overline{D}$	495.982		498.96		498.349	
p_D	51.167		49.494		49.083	
DIC	547.149		548.454		547.432	

** Significant at the 5% Bayesian Credible Interval
# Not significant at the 10% Bayesian Credible Interval
All other variables are significant only at the 10% Bayesian Credible Interval

In the MV crash frequency model, logarithmic volume per lane positively affects the crash frequency. Meanwhile, the logarithmic segment length, median width, and existence of auxiliary lanes are significant geometric characteristics. Traffic volume and segment length are the most common exposure variables in previous traffic safety analysis, of which many suggested that crash count is not linearly proportional to volume and segment length thus the logarithmic transformation was applied (Ahmed et al., 2011). The effects of median width and existence of auxiliary lanes are consistent with existing studies (Shi and Abdel-Aty, 2015). The median width has negative effect on crash frequency since it provides more space for vehicle leeway to avoid a crash. The auxiliary lanes provide turning movements near expressway ramps where speed changes and lane changes are required. The speed change actions might result in rear-end crashes, and lane change maneuvers might cause sideswipe crashes.

The modeling results of MV crash frequency study also confirmed that travel time reliability has an impact on MV crash count. Comparing the performances of Percent Variation, Buffer Index, and Misery Index in the models, both Buffer Index and Misery Index were found to be significant at the 5% Bayesian Credible Interval while Percent Variation was not. The different performances of indicators in the models might originate from their definitions. Both Buffer Index and Misery Index emphasize the effects of late arrivals on travel time reliability. In contrast, Percent Variation treats early and late arrivals equally. For most motorists, the risk and cost of early and late arrivals could be distinct. Late arrivals are more likely to cause anxiety and risky behaviors than early arrivals. In summary, as reflected in the significance of the three variables, lower travel time reliability caused by delayed trips would pose more challenges to traffic safety. Consequently, to better capture how travel time reliability affects crash frequency, the use of Buffer Index and Misery Index are recommended.

The parameter estimation for SV crashes is different from that for MV crashes. As exposure variables, higher values of logarithmic segment length and traffic volume per lane are related with more SV crashes. The effects of median width remain the same for both SV and MV crashes. The differences between these two types of crashes are mainly reflected by auxiliary lanes and travel time reliability. For SV crashes, existence of auxiliary lanes is no longer significant. Such result is expected as merging and diverging on the segments with auxiliary lanes would be more likely to cause MV crashes rather than SV crashes. Travel time reliability, unlike their effects on MV crashes, does not have significant impact on SV crashes. SV crashes are more likely to occur under free flow conditions, under which travel time might be more stable. Given the estimation results of SV and MV crashes, it is obvious that travel time reliability has greater effects on MV crashes than SV crashes.

5.6.2 Real-Time Crash Analysis

For the logistic regression model, in order to prevent high correlation between variables, the Pearson Correlation test was done before the modelling process. If the absolute of the correlation coefficient value of two continuous parameters was higher than 0.3, or when the chi-square test showed two categorical variables were significantly related, only the variable which resulted in a higher AUC was kept in the model. The range of AUC is 0.5 to 1.0, a higher value indicating a better ability in discriminating MV and SV crashes in this study. The model estimation is in Table 5-5.

Table 5-5 Parameter estimation for real-time MV and SV crash risk

Variables	Estimate	Standard Error	Wald Chi-Square	Pr > ChiSq
Intercept	-5.659	0.739	58.612	<.001
Speed	0.042	0.010	17.068	<.001
Lane345	0.841	0.299	7.887	<.001
Mdwidth	0.027	0.008	12.468	<.001
Passenger	-1.147	0.238	23.271	<.001
Wet	0.798	0.198	16.314	<.001
Per_var	0.015	0.007	4.611	0.03
AUC		0.725		

Speed was found to be significant with a positive sign. This indicates that a high speed will increase MV crash potential given a crash happens. When lane number is more than two, MV crash risk is increased. It is not hard to understand. Larger lane number indicates higher volume on a segment. Volume has more impact on MV crash frequency. This may be because a higher volume increases the exposure and possibility of MV crash, but decreases SV crash possibility. When volume increases, the possibility that a vehicle encounters another vehicles increases, and the possibility, that it is involved in a crash with other vehicles, also increases, so MV crash likelihood increases. However, under high volume conditions, a vehicle is less likely to have an SV crash without involving other vehicles. So higher volume indicates low SV crash probability (Hauer, 2015). To sum up, when volume increases, the combination of crash exposure and crash probability result in a higher MV crash potential than SV crashes.

Additionally, the median width has a positive sign, indicates that a segment with a narrow median width increase the SV crash risk. One of main reason for the occurrence of SV crashes is vehicle out of control. A wider median width could decrease SV crash risk by providing drivers with more leeway to regained control of vehicles. On the other hand, median width might not have as much impact on MV crashes as on SV crashes, because MV crashes are mainly because of danger interactions between vehicles, such as too close car following.

Furthermore, it was revealed that the presence of passenger was found to increase SV crash risk by having a significant negative coefficient. Drivers might be distracted by passenger(s) and out of control vehicle. Wet roadway surface condition might increase MV crash risks. Wet roadway surface has smaller friction and may result in longer braking distance than on dry surface. However, under wet roadway surface condition, drivers might keep the same following distances as under dry condition, and vehicles run into a heading vehicle because of long braking distance. Hence, wet roadway surface condition significantly increases MV crash risk.

The Percent Variation was statistically positive related to MV crash risk. A higher Percent Variation indicates that behaviors of motorists could vary substantially. On the other hand, SV crashes are more likely to occur under free flow conditions, under which condition travel time might be more stable. This result further confirms the conclusion from the crash frequency prediction models: travel time reliability has different impact on MV and SV crashes.

5.7 Summary

The reduced travel time reliability could cause unstable traffic flow thus affects efficiency and safety. In this task, MV and SV crash data on SR 408 have been collected. The different MV and SV crash frequencies indicated that the crashes mechanisms for MV and SV crashes might not be the same. Hence, the project has worked on crash frequency and real-time crash analysis for MV and SV crash using travel time reliability indicators: Percent Variation, Buffer Index, and Misery Index. The three indicators were used in crash frequency study, but only Percent Variation was used in real-time safety analysis because the other two indicators are not suitable to be used in real-time analysis.

Two Bayesian Hierarchical Poisson-lognormal models were developed to predict SV and MV crash frequencies separately. The results showed that Buffer Index and Misery Index had significant positive impact on MV crash frequency; however, Percent Variation was not significant. On the other hand, all the indicators were not significantly related to SV crash frequency. Then, a logistic regression model was built to evaluate the quantitative impact of Percent Variation on MV crash risk give a crash occurrence. The results showed that high Percent Variation, indicating low travel time reliability, would increase MV crash risk.

At present, many toll expressway agencies provide travelers with estimated real-time travel time and congestion warning using dynamic message signs. This is beneficial to help road users prepare for current traffic conditions and adjust their driving accordingly. Thus, the study has found that improving travel time reliability would decrease MV crash potential. Given the high proportion of MV crashes on expressways, it is expected that reduction of MV crashes will remarkably improve safety.

CHAPTER 6: REAL-TIME EVALUATION FOR RAMP CRASHES

6.1 Introduction

There have been numerous studies on real-time crash prediction models with the intention to link real-time crash likelihood with various predictors. The underlying assumption of these studies is that some predictors, called crash precursors, are relatively more 'crash prone' than other parameters. Among the studied traffic predictors, the standard deviation of speed, traffic volume, and traffic density were common significant crash precursors (Lee et al., 2002; Abdel-Aty and Pande, 2005). Additonally, geometric parameters play important roles in the occurrence of crashes (Wang et al., 2015a).

However, the human factors' impact has not been widely examined in real-time safety studies. There are two types of events in real-time safety analyses: crash and non-crash events. For crash events, crash reports can provide information for drivers who are involved in a traffic crash. On the other hand, for non-crash events, driver information cannot be obtained from available data sources. Hence, real-time crash risk analysis is unable to consider driver characteristics as explanatory variables. Trip generation and land-use factors can reflect driver behavior and further reflect their effect on traffic safety. From a macroscopic perspective of view, trip generation and land-use have already been proven significant crash frequency contributing factors (Abdel-Aty et al., 2013; Lee et al., 2015a; Lee et al., 2015b). However, there has been no study, which adopted trip generation and land-use factors in microscopic traffic safety analyses.

For crashes that happen on ramps, the origins or destinations of the vehicles involved in the crash are likely to be ramp nearby zones. Hence, if the trip generation and land-use information of the zone in which a ramp lies can be captured, these points of data might act as surrogates of driver characteristics for ramps.

The logistic regression model has been widely used in the analysis of data whose target variable is binary (Washington et al., 2010). It measures the relationship between the target variable and explanatory variables based on a logistic function. The model is easy for interpretation since the model results provide the coefficient value for each significant variable. However, the logistic regression assumes that the error term has a standard logistic distribution. In reality, this assumption may not be true. On the other hand, the data mining method might not be able to provide the impact of each independent variable on the target variable, but it does not have a restriction on the distribution of parameters. Among numerous data mining methods, Support Vector Machine (SVM) models have been applied in several transportation studies, because they can provide high accuracy (Qu et al., 2012). Hence, this chapter integrated data mining and traditional statistical model (logistic regression model) to conduct real-time crash analysis for ramps.

6.2 Methodology

6.2.1 Logistic Regression Model

For any given event *i*, it has two exclusive states: crash or non-crash. In this task, the binary responses, crash (y_i=1) and non-crash (y_i=0), are converted into probabilities p_i (y_i =1) and 1- p_i (y_i=0), respectively. The model is as follows,

$$y_i \sim Bernoulli(p_i) \tag{6-11}$$

$$\log(\frac{p_i}{1-p_i}) = \beta_0 + \sum_{r=1}^{R} \beta_r x_{ri} \tag{6-12}$$

where β_0 is the intercept, β_r the coefficient of r^{th} predictors, x_{ri} the value of r^{th} explanatory variable for i^{th} observation.

6.2.2 Support Vector Machine

SVM is used for classification analysis by constructing a hyperplane or set of hyperplanes in a high- or infinite-dimensional space (Suykens and Vandewalle, 1999). The hyperplane with the largest distance to the nearest training-data point is chosen, indicating that it provides the largest separation between two types of events. There are two sorts of SVM: linear and nonlinear. The choice of SVM sort is based on the data type, e.g., a linear SVM is better if data is linearly separated. A nonlinear SVM is achieved by applying a kernel. By introducing a kernel, SVM is flexible in the choice of the separation form and can handle nonlinear data (Deng et al., 2012). In this task, a nonlinear SVM is applied.

The crash occurrence outcome y is either 1 (crash) or -1 (non-crash). Training data D is a set of n points of the form,

$$D = \left\{ \left(x_i, y_i \right) \mid x_i \in R^P, y_i \in \left\{ -1, 1 \right\} \right\}_{i=1}^{n} \tag{6-13}$$

where x is the matrix of independent variables and P is the number of significant variables. The decision function is as follows,

$$f(x) = sign(w^T x + b) \tag{6-14}$$

$$\omega = [\omega_1 \ \omega_2 \ \dots \ \omega_p]^T \tag{6-15}$$

A hyperplane can be written as the set of points x satisfying

$$w^T x + b = 0 \tag{6-16}$$

$(w^T x_i + b)$ should be positive when y_i=1, and it should be negative when y_i=-1. To summarize, $y_i(w^T x_i + b) > 0$. The decision function is using a sign-function. This results in an uncertainty of distance or margin (Campbell and Ying, 2011). Hence, two parallel hyperplanes is constructed (Campbell and Ying, 2011):

$$w^T x + b = 1 \tag{6-17}$$

and

$$w^T x + b = -1 \tag{6-18}$$

The distance between these two hyperplanes is $\frac{2}{\|w\|}$. The target of SVM is to maximize the distance between the two hyperplanes by minimizing $\frac{1}{2}\|w\|^2$. In order to prevent data points from falling into the margin between two hyperplanes, the following constraint is added:

for each observation *i* either

$$w^T x_i + b \geq 1, if \;\; y_i = 1 \tag{6-19}$$

or

$$w^T x_i + b \leq -1, if \;\; y_i = -1 \tag{6-20}$$

Combing Eq. 6-9 and 6-10, produce the following new constrain:

$$y_i(w^T x_i + b) \geq 1, for \;\; all \;\; i \tag{6-21}$$

This is a constrained optimization problem in which $\frac{1}{2}\|w\|^2$ is minimized subject to constrain Eq. 6-11. The optimization problem can be reduced to the minimization of the following Lagrange function,

$$L(w,b)=\frac{1}{2}(w.w)-\sum_{i=1}^{n}\alpha_i[y_i(w.x_i+b)-1] \tag{6-22}$$

where α_i are Lagrange multipliers, and α_i>0. The Eq. 6-12 is taken the derivatives with respect to b and w, and set these derivatives to zero:

$$\frac{\partial L(w,b)}{\partial b}=\sum_{i=1}^{n}\alpha_i y_i=0 \tag{6-23}$$

$$\frac{\partial L(w,b)}{\partial w}=w-\sum_{i=1}^{n}\alpha_i y_i x_i=0 \tag{6-24}$$

Substituting Eq. 6-13 and 6-14 back into Eq. 6-12, the formulation is obtained,

$$\begin{aligned}W(\alpha)&=\frac{1}{2}\sum_{i=1}^{n}\sum_{j=1}^{n}\alpha_i\alpha_j y_i y_j(x_i.x_j)-\sum_{i=1}^{n}\alpha_i[y_i(\sum_{j=1}^{n}\alpha_j y_j x_j.x_i+b)-1]\\&=\frac{1}{2}\sum_{i=1}^{n}\sum_{j=1}^{n}\alpha_i\alpha_j y_i y_j(x_i.x_j)-\sum_{i=1}^{n}\sum_{j=1}^{n}\alpha_i\alpha_j y_i y_j(x_i.x_j)-\sum_{i=1}^{n}\alpha_i y_i b+\sum_{i=1}^{n}\alpha_i\\&=\sum_{i=1}^{n}\alpha_i-\frac{1}{2}\sum_{i=1}^{n}\sum_{j=1}^{n}\alpha_i\alpha_j y_i y_j K(x_i.x_j)\end{aligned} \tag{6-25}$$

Subject to

$$\alpha_i\geq 0 \quad and \quad \sum_{i=1}^{n}\alpha_i y_i=0 \tag{6-26}$$

Eq. 6-15 shows the linear kernel $K(x_i.x_j)=(x_i.x_j)$, but when the points are not linearly classified, there is a need to conduct another kernel. In this task, the Gaussian radial basis kernel was used,

$$K(x_i.x_j)=\exp(-\gamma\|x_i-x_j\|^2), \quad for \ \gamma>0 \tag{6-27}$$

where γ was set as 0.5. Compared to a linear kernel, the Gaussian radial basis kernel has been proven better in a real-time safety study by Yu and Abdel-Aty (2013b).

6.3 Data Preparation

This chapter chose 141 ramps from three expressways in Central Florida: SR 408, SR 417, and SR 528. The study period was from July 2013 to March 2014. Five dataset were collected: crash, traffic, geometry, trip generation, and land-use data.

The crash data were from S4A. For each crash observation, crash report provided crash time, coordinate, type and severity, etc. The traffic data were supplied by MVDS detectors from CFX. The MVDS detectors record aggregated vehicle counts, time mean speed, and lane occupancy every minute for each lane.

In addition to crash and traffic data, ramp geometric characteristics data were collected. The shoulder width information was obtained from the FDOT RCI database; ramp type (on- and off-ramp), ramp configuration (diamond and non-diamond ramp), and presence of a tollbooth were gathered manually using ArcGIS. The studied ramps exist in 69 SWTAZs. Both trip generation and land-use data of these SWTAZs were from the Florida Statewide Model from the FDOT Central Office. The trip generation data were estimated using observed socio-demographic data.

There were 122 crashes documented and matched with traffic, geometry, land-use and trip generation information. The traffic conditions, which were present 5-10 minutes before the reported crash time, were used as crash events. For example, if a crash occurs at 8:00 A.M., traffic data extracted are from 7:50 to 7:55 A.M. of the same day. The non-crash dataset was made up of normal traffic conditions which did not result in a crash or were not impacted by a crash. In this task, non-crash events were the traffic conditions that were more than 2 hours before or after a crash observation at the same ramp. Both crash and non-crash events were aggregated into 5-minute intervals to mitigate data noise.

The non-crash dataset consisted of more than 10 million observations. It was not practical to use the entire non-crash dataset. Hence, this task adopted an unmatched case-control design. A total of 1,220 controls (non-crash events) were randomly sampled from the non-crash dataset. Thus, the total number of observations was 122 crash and 1,220 non-crash events. The descriptive analysis of variables of the final dataset is shown in Table 6-1.

Table 6-1 Descriptive analysis for real-time ramp analysis

Variables	Description	Mean	Std.	Min	Max
Traffic Parameters					
Vehcnt	Vehicle count in 5-min intervals (veh/5minutes)	18.1	20.7	1	170
Speed	Average speed in 5-min intervals (mph)	52.7	9.0	3.8	103.6
Std_spd	Standard deviation of speed in 5-min intervals (mph)	4.1	3.2	0	34.0
Occ	Average lane occupancy in 5-min intervals (%)	2.5	3.7	0	47.0
Geometric Parameters					
Sldwth_R	Right shoulder width (in ft)	1.9	1.9	1.0	6.0
Sldwth_L	Left shoulder width (in ft)	4.3	2.9	1.0	12.0
Type	1=if the ramp is an off-ramp; 0=otherwise	0.46	0.50	0	1
Configuration	1=if the ramp is a diamond-ramp; 0=otherwise	0.58	0.49	0	1
Toll	1=if there is a toll booth on the ramp; 0=otherwise	0.29	0.46	0	1
Trip Generation Parameters					
Production	Total productions (trips/day)	5,601	5,910	84	25,010
Attraction	Total attractions (trips/day)	5,666	7,663	20	33,742
P_HBWA	Home-based-work attractions divided by total attraction (%)	16.4	9.3	0	74.8
P_HBWP	Home-based-work productions divided by total production (%)	14.8	7.1	0	27.6
P_HBSRA	Home-based-social recreational attractions divided by total attraction (%)	8.4	3.2	3.2	19.1
P_HBSRP	Home-based-social recreational productions divided by total production (%)	7.1	4.2	1.4	31.0
P_HBSHA	Home-based-shopping attractions divided by total attraction (%)	9.3	7.4	0	27.2
P_HBSHP	Home-based- shopping productions divided by total production (%)	15.8	5.8	3.9	25.0
Land-use Parameters					
Area	In square mile	1.25	1.62	0.02	10.62
Pop_density	Population density (people/square mile)	2,215	2,038	0	10,312
Emp_density	Employment density (people/ square mile)	1,577	2,633	0	13,295
Enr_density	Enrollment density (people/ square mile)	902	2,607	0	14,945
P_agri	Agriculture employment divided by total employment (%)	1.3	0.3	0	2.2
P_service	Service employment divided by total employment (%)	50.0	9.5	25.0	66.7
P_constr	Construction employment divided by total employment (%)	3.0	2.2	0	10.0
P_manu	Manufacturing employment divided by total employment (%)	2.7	2.1	0	8.3
P_whole	Wholesale employment divided by total employment (%)	3.1	2.3	0	10.0
P_retail	Retail employment divided by total employment (%)	19.3	10.4	0	48.8
P_financ	Financial employment divided by total employment (%)	6.7	1.3	3.3	9.5
P_public	Public administration employment divided by total employment (%)	8.5	1.5	5.0	11.1
P_transport	Transportation employment divided by total employment (%)	5.3	1.0	2.5	7.0

6.4 Model results

This section first estimates a logistic regression to identify the significant variables and then applies SVM in crash prediction. The whole dataset was randomly split into training and validation datasets with a ratio of 70:30, respectively.

For the logistic regression model, in order to prevent high correlation between variables, the Pearson correlation test was done before the modelling process. If the absolute of the correlation coefficient value of two parameters was higher than 0.3, only the variable which resulted in a lower Akaike information criterion (AIC) was kept in the model. The training and validation AUCs of the logistic regression model were 0.835 and 0.797, respectively. It indicated the model had a good ability to distinguish crash and non-crash events. The logistic regression model results are shown in Table 6-2.

Table 6-2 Logistic regression model result for ramp

Variables	Estimate	Std.	Z value	P value
Intercept	-3.25	1.31	-2.48	0.01
Log(Vehcnt)	0.80	0.16	5.10	0.00
Speed*	0.03	0.02	1.90	0.06
Type	0.66	0.28	2.36	0.02
Configuration	-1.12	0.27	-4.15	0.00
P_HBWP	0.05	0.02	2.60	0.01
P_Transport	-0.72	0.13	-5.41	0.00
Model Performance				
AIC			456.51	
Training AUC			0.835	
Validation AUC			0.797	

* Variable significant at a 90% confidence interval

The Logarithm of vehicle count in 5-minute intervals is positive, indicating that high traffic volume result in high crash risk on a ramp. Traffic volume is the most common exposure variables in previous traffic safety analysis, a significant positive relationship between traffic volume and crash count or crash risj has been widely found by researchers (Abdel-Aty and Pande, 2005). Speed was also found to be significant at the 10% confidence interval with a positive sign. Higher speed definitely increases both braking and reaction distance. Hence, a vehicle travelling at a higher speed would more likely have a collision with other objects.

Two geometric factors were found to be significant in the model. The results indicate that the crash ratio on off-ramps is about 1.93 times higher that of on-ramps. The reason is that vehicles on the off-ramps need to decelerate to adjust to lower speed limits on ramps; meanwhile, they have to decrease speed in order to prepare to brake or even stop at the cross-street intersection. If a following vehicle does not react or decelerate in time, it will collide with the vehicle ahead. Ramp configuration is significant and proven to be negatively related to crash likelihood. The odds of a crash on a diamond ramp are 0.33 times of that on non-diamond ramp. Non-diamond ramps have smaller turning radii, and can lead to a loss of vehicle control and result in crashes.

The percentage of Home-based-work production is positively related to crash risk. The Home-based-work production includes two trips, one is from home to work, and the other is from work to home. First, drivers who travel from home to work have to arrive at destinations on time. They may want to avoid being late and may rush to get to work. Thus, they might drive at a higher speed than usual. Second, drivers may be tired after whole day of work, so the crash potential of work-to-home trip may be higher than other trips.

The most significant land-use parameter is the percentage of transportation employment. It is interpreted that a higher percentage of transportation employees will produce better traffic safety conditions. Transportation employees are those who work in the trucking, mass transit, delivery, etc. Compared to other drivers, transportation employees need to strictly follow regulations such as drug and alcohol testing, resulting in safer driving (U.S. DOT, 2010). Meanwhile, they are more experienced in driving.

In addition to the logistic regression, SVM models with Gaussian radial basis kernel were tested using the same training and validation datasets as the logistic regression model. One SVM was based on the selected variables, which have been identified to be significant crash contributing factors by logistic regression model; and the other SVM used all variables. The model results are in Table 6-3.

Table 6-3 Performance of SVM models

	SVM with the selected variables	SVM with all variables
Training AUC	0.895	0.949
Validation AUC	0.900	0.739

The SVM model with the selected variables performed better than the logistic regression model by providing higher training and validation AUCs. It indicates that the SVM model was better in discriminating between crash and non-crash conditions. In addition, the training and validation AUCs of the SVM are almost the same and are more stable than that of the logistic regression. However, when all variables were used to estimate the crash occurrence by SVM, the validation AUC was as low as 0.739 though the training AUC was very high. It indicates that the SVM model using all variables had an overfitting issue. Too many independent variables migth cause the SVM model to "memorize" training data instead of finding the underlying the relationship between dependent and independent variables. The similar phenomenon was also found by other researchers (Yu and Abdel-Aty, 2013b).

Random Forests were then used to rank the importance of significant variables. Random forests build multiple trees in randomly selected subsets. Trees in different subsets generate their classification (Ho, 1995). Random Forests are also used as a frequent tool used in estimating variable importance (Breiman, 2001). In this task, the mean decrease in accuracy calculated by Random Forests was used to evaluate the significant variables' importance. A variable with a larger mean decrease in accuracy is more important for model estimation. The importance of significant variables are shown in Figure 6-1.

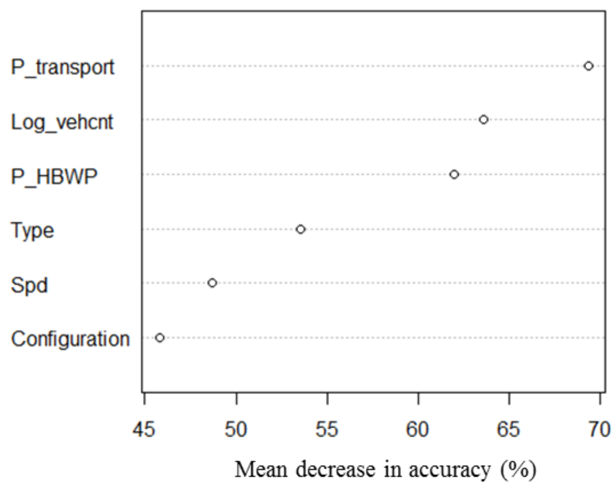

Figure 6-1 Variable importance

The variable importance analysis showed land-use and trip generation parameters (P_transport and P_HBWP) are significantly important in crash occurrence. Traffic parameters (Log_vehcnt and Speed) are more important than geometry parameters (Type and Configuration). The result indicates that land-use and trip generation parameters had made great contribution to improving the real-time crash prediction for ramp crashes. In future, more land-use and trip generation factors can be explored in other real-time safety analyses.

6.5 Summary

Previous studies found that several real-time traffic and environmental factors are significant crash precursors. However, no study has been conducted to analyze the impact of land-use and trip generation parameters on crash risk. This chapter explored real-time crash risk for expressway ramps using traffic, geometric, land-use, and trip generation predictors.

A logistic regression model was utilized to find the significant variables. The model identified that volume and speed have a positive impact on crash risk. It also indicated that off-ramps and non-diamond ramps also significantly increase the crash risk. As for the trip generation parameters, the percentage of home-based-work production compared to other trip-generation parameters was found to have a positive impact on crash risk. The percentage of transportation employment was negatively related to crash risk.

Subsequently, two SVM models were applied to predict crash occurrence: one with all variables and the other only with significant variables identified by the logistic regression model. It was found that the SVM model with identified significant variables outperformed the logistic regression model by providing higher and more stable AUCs. However, the SVM model with all variables might have an overfitting issue as it provided high training AUC but lower validation AUC. Therefore, instead of using all collected variables, it would be better to build SVM models based on significant variables identified by other models such as the logistic regression models. Meanwhile, Random Forests were used to rank the significant variables' importance, the result showed that land-use and trip generation parameters were parameters with high importance.

CHAPTER 7: INTERSECTION SAFETY PERFORMANCE FUNCTIONS

7.1 Introduction

A series of safety performance functions (SPFs) have been developed for different facilities for various crash types. Highway Safety Manual (HSM) (AASHTO, 2010) provides a range of segment- and intersection-based SPFs for many facility types including but not limited to rural two-lane two-way roads, rural multilane highways, and urban and suburban arterials. According to the HSM (AASHTO, 2010), the SPFs play a key role in identifying crash hotspots (i.e., screening), and evaluating safety countermeasures using the empirical Bayes method. A majority of the SPFs have been built at the micro-level, such as intersection, segment, or corridor level. On the other hand, some researchers have estimated SPFs at the macro-level (e.g., traffic analysis zones) to incorporate highway safety in the long-term transportation planning process.

A need of incorporating roadway safety considerations in long-term transportation planning process has been emphasized in the last decades in accordance with Moving Ahead for Progress in the 21st Century Act (MAP-21 Act) and Fixing America's Surface Transportation Act (FAST Act). This integration planning process is called transportation safety planning or macroscopic traffic safety analysis. Incorporating safety in the long-term transportation plans has been a vital issue. Safety is being used as one of the performance measures in transportation improvement program and in more advanced planning efforts, such as scenario planning at the Metropolitan Planning Organization (MPO) level. Therefore, transportation engineers need to place more efforts to improve traffic safety problems along with the long-term transportation planning and this is the main reason that the macroscopic safety studies have emerged since the last decade.

Although numerous macro-level studies have found that a variety of demographic and socioeconomic zonal characteristics have substantial effects on traffic safety, few studies have attempted to coalesce micro-level with macro-level data for estimating SPFs. Abdel-Aty et al. (2016) and Lee (2014) proposed a methodology to integrate macro-level and micro-level data to provide a comprehensive perspective by balancing the two-levels. Still, their methodology is based on the macro-level SPFs. Park et al. (2015) estimated segment-level SPFs to evaluate the effectiveness of bicycle facilities. The authors included block-group based macro-level data including population density and income and found that the macro-level parameters were statistically significant in the segment-level SPFs. Recently, Huang et al. (2016) estimated SPFs separately at micro-level and macro-level and compared the model performance. The results indicated that the micro-level model had a better fit and performance. The authors claimed that the micro-level approach was able to provide better insights on microscopic factors that directly contributed to traffic crashes; while, the macro-level approach was beneficial when monitoring regional safety and relating it with socio-demographic factors.

Huang and Abdel-Aty (2010) discussed the multi-level data in traffic safety. The multi-level included occupant, driver/vehicle, crash, site, geographic region, and the extra temporal dimension. The authors suggested many ideas to explore crashes at the multi-level. For instance, analyzing traffic crash counts 1) at intersection and time-level; 2) at county and corridor-level; 3) at county level with spatial effect; and so on. Guo et al. (2010) developed several SPFs for signalized intersections with corridor-level spatial correlation. The authors found that the Poisson spatial model with the corridor-level spatial effects provided the best model fitting. This study is inspired by the studies by Huang and Abdel-Aty (2010) and Guo et al. (2010), but it is different as it applies macro-level variables and random-effects along with micro-level variables to developed micro-level SPFs.

Several researchers explored the effects of geographic units on crash modeling at the macro-level. Abdel-Aty et al. (2013) investigated the effect of different zonal systems. The authors compared crash models based on three different areal units block groups (BGs), census tracts (CTs) and traffic analysis zones (TAZs). The result showed that the BG based model had the larger number of significant variables for total and severe crashes compared to models based on other geographical units. Lee et al. (2014b) developed traffic safety analysis zones (TSAZs) by aggregating existing TAZs with comparable crash characteristics, and they compared TAZ-based and TSAZ-based models and then claimed that the TSAZ-based model outperforms the TAZ model in terms of goodness-of-fit. The authors argued that if a zone size is small, it is possible that the shared characteristics between intersections in the same zone may not be sufficiently aggregated; on the contrary, many local features might be lost if the zone is too large (Lee et al., 2014b). Similarly, it is necessary to find the data from the optimal sized spatial unit that can provide the best modeling results for intersection SPFs.

Although several studies suggested ideas to link macro-level and micro-level data, no studies have tried to analyze the effects of macro-level variables on micro-level SPFs. Meanwhile, it is worth to investigate which geographic units provides the optimal data for micro-level SPFs. Therefore, this chapter aims at answering the three research questions: (1) can intersection SPFs be improved by considering macro-level geographic units? (2) what would be the best spatial unit for the SPFs? and (3) which macro-level factors do have significant effects on intersection crashes?

7.2 Methodology

Random-effects count models have been popularly used in the traffic safety field (Johansson, 1996; Shankar et al., 1998). One of the basic assumptions of the most statistical models is that observations are independent from each other. Nevertheless, this assumption is often violated in traffic data, because there might be possible correlation among observations. For instance, some observations that are from the same spatial units may have common unobserved factors (Lord and Mannering, 2010). Since this study aims at developing intersection SPFs using micro- and macro-level data, it is expected that intersections located in the same geographic units may have shared unobserved factors. Therefore, mixed-effects negative binomial model was adopted in the study to account for the potential correlation among intersections from the same geographic units. The mixed effects negative binomial model for two levels (i.e., micro- and macro-levels) in this study is specified as follows :

$$Y_{ij} \sim Poisson(\lambda_{ij}) \tag{7-1}$$

$$\lambda_{ij} = \exp(\beta X_{ij} + v_j)\exp(\varepsilon_{ij}) \tag{7-2}$$

where Y_{ij} is the number of crashes at intersection *i* (*i*=1, 2, …, *n*) from macro-level zone *j* (*j*=1, 2, … *m*). λ_{ij} is the expected number of crashes for intersection *i* belonging to macro-level zone *j*. X_{ij} is a vector of micro-level explanatory variables for intersection *i* in zone *j*. β is a vector of estimable parameters for a vector of explanatory variables X_{ij},

$\exp(\varepsilon_{ij})$ follows a Gamma distribution with mean one and variance α, and v_j is the macro-level component as follows:

$$v_j = \gamma X_j + \mu_j \tag{7-3}$$

where X_j is a vector of macro-level explanatory variables for zone j, γ is a vector of estimable parameters for a vector of explanatory variables X_j, and μ_j is the random effects for j which follows N(0, σ^2). Figure 7-1 shows the hierarchical structure used in this study.

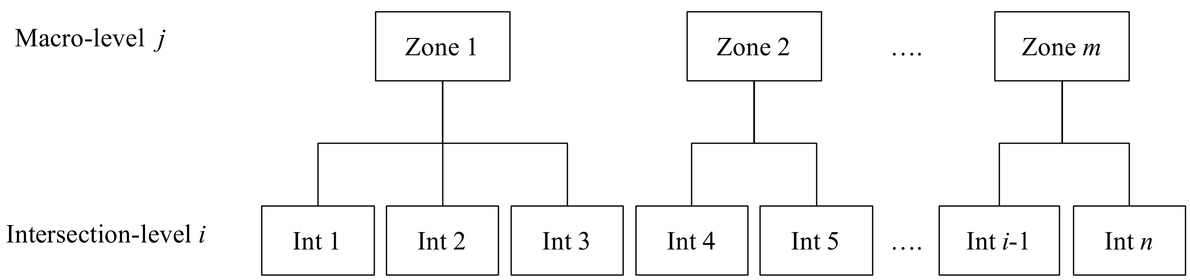

Figure 7-1 Hierarchical structure of intersection-level and macro-level data

The best SPF for each crash type was selected based on AIC, Bayesian information criterion (BIC), McFadden's ρ^2, and adjusted ρ^2. The formulae for these measures are as follows:

$$AIC = 2k - 2LL(Full) \tag{7-4}$$

$$BIC = k\ln(n) - 2LL(Full) \tag{7-5}$$

$$\rho^2 = 1 - \frac{LL(Full)}{LL(Intercept\ only)} \tag{7-6}$$

$$Adjusted\ \rho^2 = 1 - \frac{LL(Full) - k}{LL(Intercept\ only)} \tag{7-7}$$

where k is number of parameters, n is the number of observations, $LL(Full)$ is the log-likelihood for the full model, and $LL(Intercept\ only)$ is the log-likelihood for the intercept-only model.

In order to prevent the multicollinearity problem, the models formed in this study do not include highly correlated variables in the same model. The correlations between the variables were checked by Spearman's rank correlation method. If two variables were highly correlated, they were not used simultaneously in the same model.

7.3 Macro-level Spatial Units

Varieties of spatial units have been used in macro-level studies. The spatial units include census-based, traffic-based, or political boundaries. Figure 7-2 shows the examples of various spatial units in the Orlando metropolitan area, Florida.

Census Block

A census block is the smallest geographic units used by the U.S. Bureau for the collection and tabulation of decennial census data. However, detailed information of census block is not available due to confidentiality requirement. On average, there are only 85 people in one census block. Due to the lack of detailed information and extremely small sizes, census blocks have not been used in this traffic safety studies.

Census Block Group (BG)

A census block group (BG) is the next level above the census block. A BG is combinations of census blocks. Each BG contains about 39 census blocks on average. Population in a BG ranges between 600 and 3,000 people. Some macroscopic traffic safety studies adopted BGs as a base geographic unit (Levine et al., 1995, Abdel-Aty et al., 2013).

Traffic Analysis Zone (TAZ)

TAZs are special purpose geographic entities delineated by state and local transportation officials for tabulating traffic-related data, especially journey-to-work and place-of-work statistics (USCB, 2010). Since TAZs are the only traffic related zone system, TAZs have been most popularly used in the macroscopic safety literature (Ladron de Guevara et al., 2004; Lovegrove and Sayed, 2007; Hadayeghi et al., 2010; Naderan and Shahi, 2010; Abdel-Aty et al., 2011; Wang et al., 2012; Abdel-Aty et al., 2013; Lee et al., 2014b, 2015b).

Census Tract (CT)

A census tract (CT) is designed to maintain homogenous socioeconomic status in a zone. CTs are statistical sub-divisions of a county, and a CT may include 2,500 to 8,000 people. Several researchers have analyzed macroscopic traffic safety based on CTs (LaScala et al., 2000; Wier et al., 2009; Ukkusuri et al., 2011).

ZIP-Code Tabulation Area (ZCTA)

ZIP code is the system of postal codes, it was created and used by the United States Postal Service since 1963. In fact, ZIP codes are not a geographic unit but a collection of mail delivery routes. U.S. Census Bureau created ZIP-Code Tabulation Areas (ZCTAs), which are generalized areal representations of ZIP code service areas. ZCTA based data are also provided from the U.S. Census Bureau. Many traffic safety studies using ZIP code have been conducted (Stamatiadis and Puccini, 2000; Lee et al., 2014a; Lee et al., 2015a).

Traffic Analysis District (TAD)

Traffic analysis districts (TADs) are new; they are higher-level geographic entities for traffic analysis (USCB, 2010). TADs are created by aggregating existing traffic analysis zones. Traffic analysis districts may cross county boundaries, but they must nest within

MPOs. In recent, Abdel-Aty et al. (2016) developed macro-level safety models based on TADs.

Census County Division (CCD)

Census county divisions (CCDs) are the statistical spatial units established cooperatively by the U.S. Census Bureau and officials of state and local governments in 21 states. CCDs are designed to represent community areas, which focus on trading centers or major land-use areas (USCB, 1994). No safety studies have been done using CCDs until this point.

County

Counties are the primary administrative divisions for most states ((USCB, 1994). For higher level of the macroscopic analysis, a county is also used as a geographic unit for the macro-level study. Miaou et al. (2003), Noland and Oh (2004), Aguero-Valverde and Jovanis (2006), and Huang et al. (2010) aggregated data into county-levels and analyzed crashes.

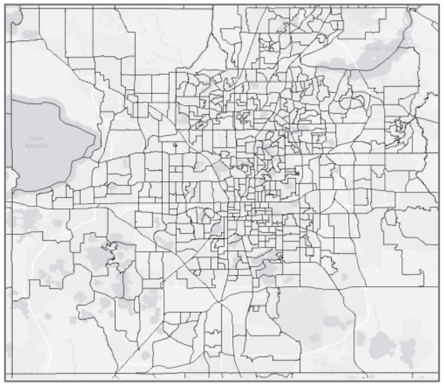

Census Block Group (BG)

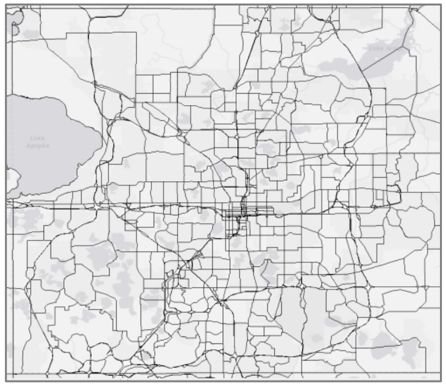

Traffic Analysis Zone (TAZ)

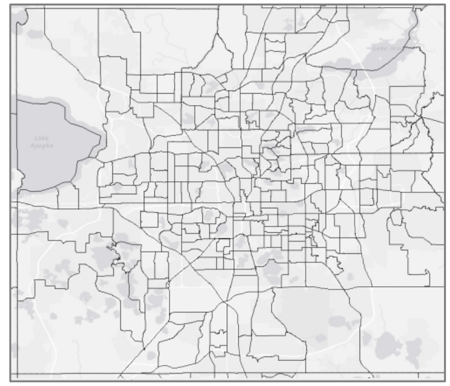

Census Tract (CT)

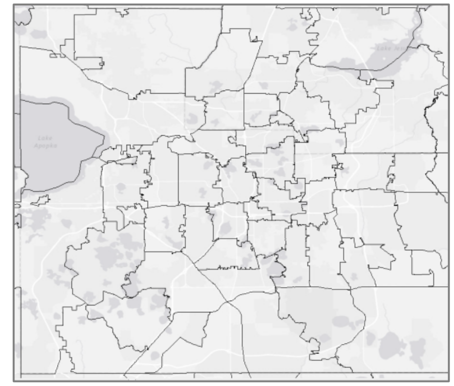

ZIP Code Tabulation Area (ZCTA)

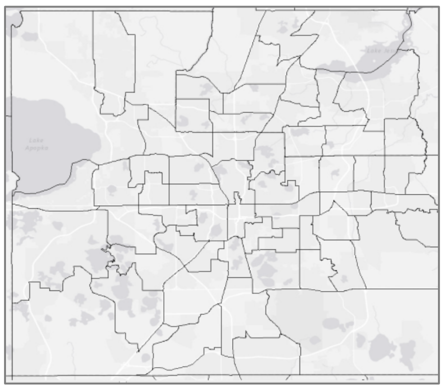

Traffic Analysis District (TAD)

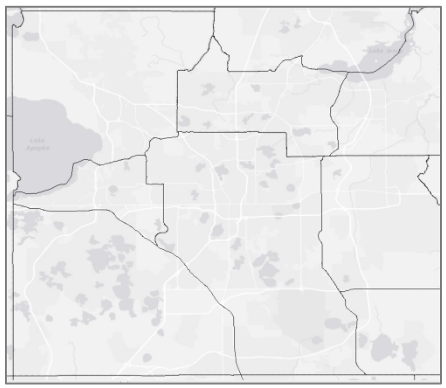

Census County Division (CCD)

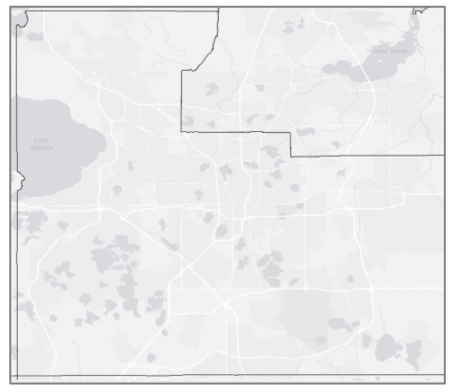

County

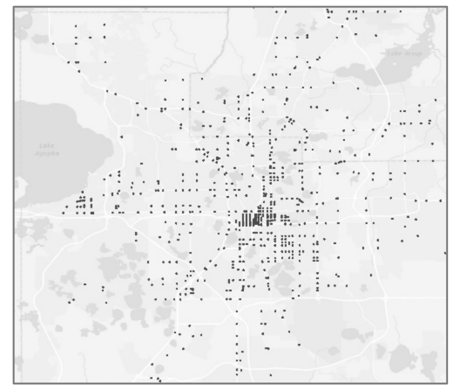

Intersection locations

Figure 7-2 Various geographic units in Orlando metropolitan area, Florida

7.4 Data Preparation

Florida's statewide data were collected from multiple sources. First, three years statewide crash data from 2010 to 2012 were obtained from the two sources: FDOT's CARS and S4A. Traffic and basic roadway geometric variables were collected from the FDOT RCI, and some other features (e.g., control type) were checked by Google Earth and Google Street View. Macro-level data in the whole Florida were acquired from ACS of the U.S. Census Bureau. The prepared data list is shown in Figure 7-3.

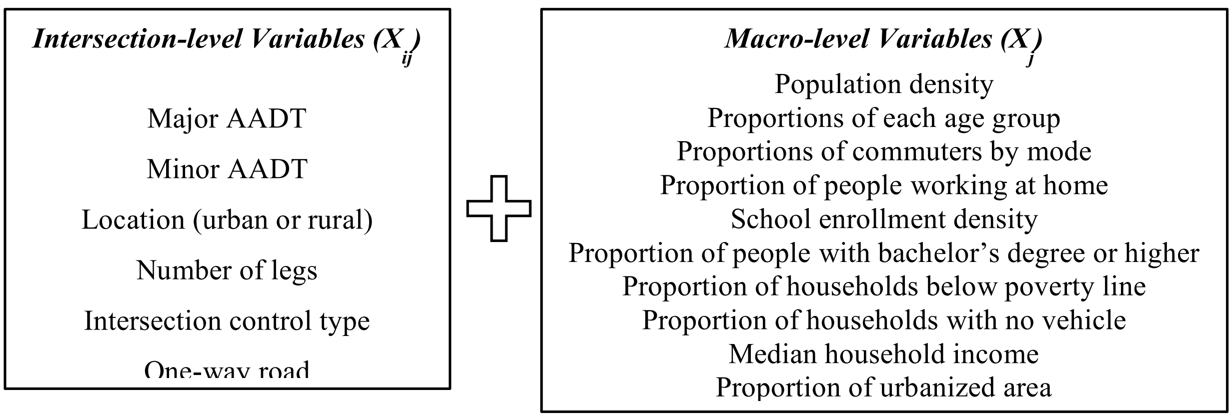

Figure 7-3 Intersection-level and macro-level variables

Table 7-1 displays the descriptive statistics of area and intersection counts by each geographic unit, and Table 7-2 summarizes the descriptive statistics of the prepared data from intersection-level (a) and macro-level (b).

Table 7-1 Area and intersection counts by spatial unit

Spatial unit	Count	Area (sqmi)				No of intersections			
		Mean	Stdev	Min	Max	Mean	Stdev	Min	Max
BG	11442	5.747	33.14	0.002	1583	0.730	1.441	0	45
TAZ	8518	6.472	24.80	9.085E-9	885.3	0.958	1.489	0	20
CT	4245	15.49	63.44	0.037	1583	1.967	2.915	0	46
ZCTA	983	50.45	88.12	0.007	1124	12.92	6.639	1	34
TAD	594	103.3	260.1	2.617	3096	13.05	12.09	0	87
CCD	316	208.1	208.1	5.753	1893	26.42	44.89	0	406
County	67	981.5	572.3	249.8	3737	124.6	155.9	1	639

Table 7-2 Descriptive statistics of the prepared data

(a) Intersection-level dependent and independent variables (Y_{ij} and X_{ij})

Dependent variables (N=8,347)				
Variable	**Mean**	**Stdev**	**Min**	**Max**
Number of total crashes	17.494	24.481	0	260
Number of severe crashes	1.004	1.700	0	26
Number of pedestrian crashes	0.353	0.871	0	13
Number of bicycle crashes	0.362	0.784	0	9

Independent variables (N=8,347)				
Variable	**Mean**	**Stdev**	**Min**	**Max**
Major AADT	6,774	7,159	20	56,000
Minor AADT	20,435	15,878	70	92,000
Location (urban=1, rural=0)	0.884	0.320	0	1
No of legs (4 legs or more=1, 3 legs=0)	0.726	0.446	0	1
Control type (signal=1, stop=0)	0.663	0.473	0	1
One-way road (yes=1, no=0)	0.036	0.186	0	1

(b) Macro-level independent variables (X_j)

Independent variable (N=8,347)	BG		TAZ		CT		ZCTA		TAD		CCD		County	
	Mean	**Std.**	**Mean**	**Std.**	**Mean**	**Std.**	**Mean**	**Std.**	**Mean**	**Std.**	**Mean**	**Std.**	**Mean**	**Std.**
Population density (per sqmi)	2559	2970	2067	2235	2442	2566	2031	2139	2159	2117	1482	1488	631.9	473.6
Proportion of infants and toddlers (<5 years)	0.053	0.041	0.055	0.022	0.055	0.027	0.055	0.018	0.056	0.014	0.056	0.013	0.056	0.008
Proportion of children (5-14 years)	0.107	0.061	0.109	0.037	0.109	0.043	0.110	0.032	0.113	0.026	0.114	0.022	0.115	0.014
Proportion of adolescent (15-24 years)	0.129	0.092	0.132	0.070	0.131	0.078	0.131	0.062	0.135	0.065	0.135	0.059	0.131	0.034
Proportion of middle-age (25-64 years)	0.523	0.107	0.524	0.070	0.523	0.084	0.520	0.065	0.516	0.054	0.514	0.046	0.515	0.031
Proportion of young elderly (65-74 years)	0.097	0.065	0.096	0.044	0.096	0.052	0.097	0.043	0.096	0.041	0.098	0.037	0.099	0.031
Proportion of elderly (75 years or older)	0.089	0.086	0.085	0.053	0.085	0.066	0.084	0.050	0.084	0.045	0.084	0.040	0.084	0.032
Proportion of commuters using car	0.875	0.124	0.883	0.078	0.880	0.093	0.886	0.073	0.890	0.054	0.893	0.040	0.898	0.024
Proportion of commuters using public transit	0.022	0.051	0.022	0.037	0.022	0.040	0.021	0.029	0.021	0.029	0.019	0.022	0.016	0.015
Proportion of commuters using taxi	0.001	0.010	0.001	0.004	0.001	0.005	0.001	0.002	0.001	0.002	0.001	0.001	0.001	0.001
Proportion of commuters using motorcycle	0.004	0.013	0.004	0.006	0.004	0.008	0.004	0.004	0.004	0.003	0.004	0.003	0.004	0.002
Proportion of commuters using bicycle	0.010	0.031	0.009	0.018	0.010	0.022	0.009	0.014	0.008	0.010	0.007	0.009	0.006	0.006
Proportion of commuters who walk	0.024	0.052	0.022	0.034	0.022	0.035	0.019	0.021	0.018	0.017	0.017	0.014	0.015	0.006
Proportion of commuters using other means	0.013	0.035	0.012	0.014	0.013	0.019	0.012	0.012	0.012	0.009	0.012	0.008	0.012	0.006
Proportion of people working at home	0.047	0.062	0.047	0.033	0.046	0.042	0.046	0.028	0.046	0.031	0.047	0.021	0.049	0.014
School enrollment density (per sqmi)	611.0	864.0	201.1	5.472	592.4	740.9	488.9	545.2	535.4	583.4	383.0	437.1	157.2	122.8
Proportion of people with bachelor's degree or higher	0.238	0.165	0.246	0.136	0.243	0.149	0.247	0.129	0.241	0.120	0.249	0.094	0.259	0.074
Proportion of households below poverty line	0.152	0.150	0.148	0.096	0.153	0.113	0.146	0.081	0.150	0.082	0.137	0.058	0.123	0.030
Proportion of households with no vehicle	0.100	0.114	0.093	0.080	0.094	0.087	0.087	0.065	0.085	0.057	0.076	0.035	0.068	0.016
Median household income (in 1,000 USD)	45.62	22.60	46.77	16.70	46.17	19.13	47.54	15.61	47.36	15.16	48.94	11.14	50.999	7.026
Proportion of urbanized area	0.816	0.355	0.725	0.386	0.785	0.364	0.667	0.362	0.710	0.395	0.578	0.346	0.301	0.177

7.5 Results and discussion

Three types of models were developed for each crash type as follows:

• Model Type (1): SPFs with micro-level variables only;

• Model Type (2): SPFs with micro-level variables and macro-level random-effects; and

• Model Type (3): SPFs with micro-level variables and macro-level variables with random-effects

Table 7-3 summarizes the goodness-of-fit measures of the developed models. There are several findings from the model performances. Firstly, it was found that the models with macro-level random-effects or variables outperform their counterpart without random-effects (i.e., models with micro-level variables only). It is noteworthy that significant improvements were observed by only adding macro-level random-effects. The AIC of the total crash SPF with micro-level variables only is 54,862 whereas those of the SPFs with macro-level random-effects only range between 53,336 and 54,554, which indicates a substantial enhancement. Also, severe, pedestrian, and bicycle SPFs were enhanced only by adding random-effects. Furthermore, the geographic units that provide the optimal data for intersection SPFs were uncovered, in terms of AIC, BIC, ρ2, and Adjusted ρ2. The models revealed that the total, severe, and bicycle crash SPF performs the best with ZCTA-based data, and the pedestrian crash SPF showed the greatest performance with CT-based data. Figure 7-4 compares adjusted ρ^2 values of the SPFs with macro-level random-effects and variables (Model Types (1) & (3)). From the results, it can be inferred that some geographic units may be too small to aggregate meaningful shared characteristics between intersections whereas other geographic units are too large. They are highly aggregated, so they may lose many local characteristics. Regardless of the crash type, the SPFs' performance is the worst with county-based data among the Model Type (3). Although the total crash SPF with ZCTA-based data has the best performance, TAD-based data also provide comparably good results. In contrast, the SPF with ZCTA-based data clearly outperforms other models. Regarding the pedestrian crash SPF, CT-based macro-level data can estimate the best pedestrian crash SPF but also TAZ, ZCTA, and TAD-based data offer equally good SPFs. Lastly, the bicycle crash SPF based on ZCTA performs significantly better than other bicycle models.

Table 7-3 Summary of model performances

SPFs	Category	Spatial	LL (full)	AIC	BIC	ρ^2	Adjusted ρ^2
Total crashes	(1) Model with micro-level variables only	None	-27424	54862	54912	0.1443	0.1441
	(2) Model with macro-level random-effects	BG	-26989	53994	54050	0.1579	0.1576
		TAZ	-26986	53988	54044	0.1580	0.1577
		CT	-26847	53710	53766	0.1623	0.1621
		ZCTA	**-26660**	**53336**	**53392**	**0.1681**	**0.1679**
		TAD	-26670	53357	53413	0.1678	0.1676
		CCD	-26998	54008	54050	0.1576	0.1574
		County	-27269	54554	54610	0.1491	0.1489
	(3) Model with macro-level random-effects and variables	BG	-26940	53899	53970	0.1594	0.1591
		TAZ	-26865	53752	53830	0.1617	0.1614
		CT	-26758	53539	53616	0.1651	0.1647
		ZCTA	**-26609**	**53240**	**53317**	**0.1697**	**0.1694**
		TAD	-26637	53293	53363	0.1689	0.1686
		CCD	-26968	53950	53999	0.1585	0.1583
		County	-27256	54529	54593	0.1496	0.1493
Severe crashes	(1) Model with micro-level variables only	None	-10205	20423	20473	0.1156	0.1150
	(2) Model with macro-level random-effects	BG	-10081	20177	20233	0.1264	0.1257
		TAZ	-10066	20147	20204	0.1277	0.1270
		CT	-10026	20068	20124	0.1311	0.1304
		ZCTA	-9903	19822	19878	0.1418	0.1411
		TAD	-9937	19887	19936	0.1389	0.1383
		CCD	-9929	19875	19931	0.1395	0.1388
		County	-10105	20227	20283	0.1242	0.1236
	(3) Model with macro-level random-effects and variables	BG	-10068	20156	20226	0.1275	0.1266
		TAZ	-10049	20118	20188	0.1291	0.1283
		CT	-10010	20043	20120	0.1325	0.1315
		ZCTA	**-9893**	**19806**	**19876**	**0.1427**	**0.1418**
		TAD	-9927	19873	19936	0.1397	0.1389
		CCD	-9925	19871	19941	0.1398	0.1390
		County	-10081	20181	20251	0.1264	0.1255
Pedestrian crashes	(1) Model with micro-level variables only	None	-5471	10957	11006	0.1313	0.1302
	(2) Model with macro-level random-effects	BG	-5434	10883	10939	0.1374	0.1361
		TAZ	-5431	10878	10935	0.1377	0.1365
		CT	-5406	10828	10884	0.1418	0.1405
		ZCTA	-5352	10720	10776	0.1503	0.1490
		TAD	-5333	10682	10738	0.1534	0.1521
		CCD	-5269	10564	10655	0.1635	0.1614
		County	-5402	10819	10875	0.1424	0.1412
	(3) Model with macro-level random-effects and variables	BG	-5236	10502	10607	0.1688	0.1664
		TAZ	-5228	10483	10581	0.1701	0.1679
		CT	**-5216**	**10456**	**10541**	**0.1719**	**0.1700**
		ZCTA	-5232	10488	10572	0.1694	0.1675
		TAD	-5224	10475	10566	0.1706	0.1685
		CCD	-5273	10567	10644	0.1629	0.1612
		County	-5370	10759	10829	0.1475	0.1459
Bicycle crashes	(1) Model with micro-level variables only	None	-5709	11430	11472	0.1264	0.1255
	(2) Model with macro-level random-effects	BG	-5673	11359	11409	0.1320	0.1309
		TAZ	-5671	11356	11405	0.1323	0.1312
		CT	-5651	11316	11365	0.1353	0.1343
		ZCTA	-5600	11214	11263	0.1431	0.1420
		TAD	-5587	11188	11237	0.1451	0.1441
		CCD	-5568	11150	11199	0.1480	0.1470
		County	-5611	11235	11284	0.1415	0.1404
	(3) Model with macro-level random-effects and variables	BG	-5561	11141	11472	0.1492	0.1476
		TAZ	-5536	11094	11172	0.1529	0.1512
		CT	-5529	11078	11149	0.1539	0.1524
		ZCTA	**-5516**	**11054**	**11132**	**0.1560**	**0.1543**
		TAD	-5531	11083	11160	0.1538	0.1521
		CCD	-5531	11079	11135	0.1536	0.1524
		County	-5582	11183	11246	0.1458	0.1444

*The best models for each crash type were bolded

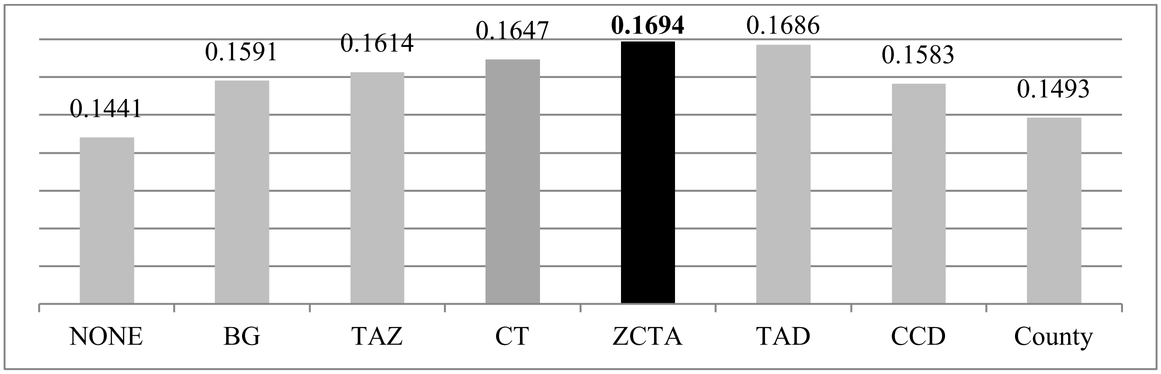

(a) Total Crashes

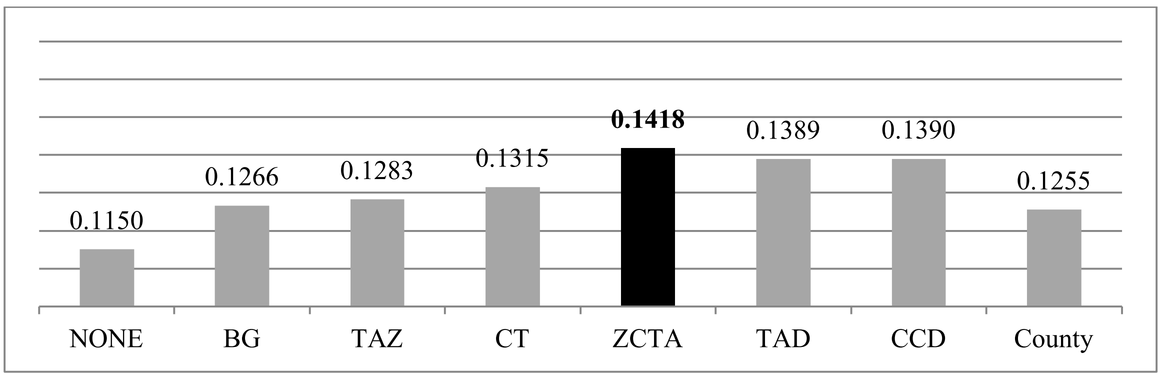

(b) Severe Crashes

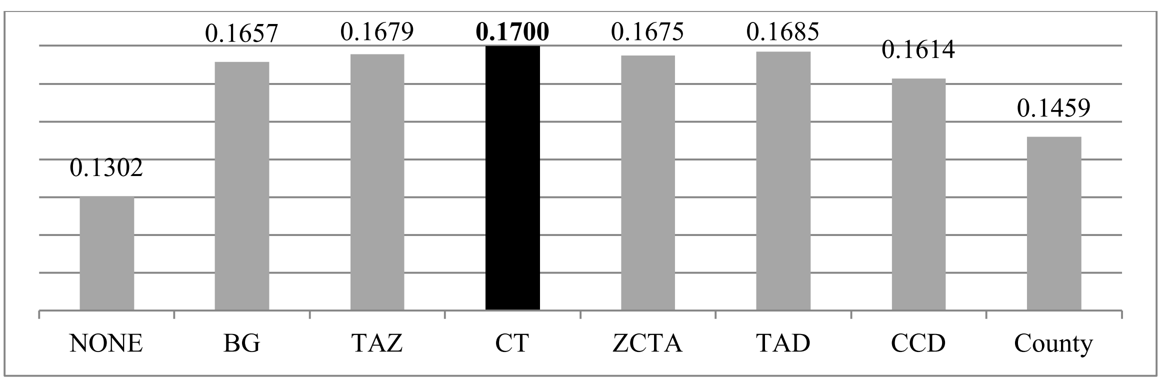

(c) Pedestrian Crashes

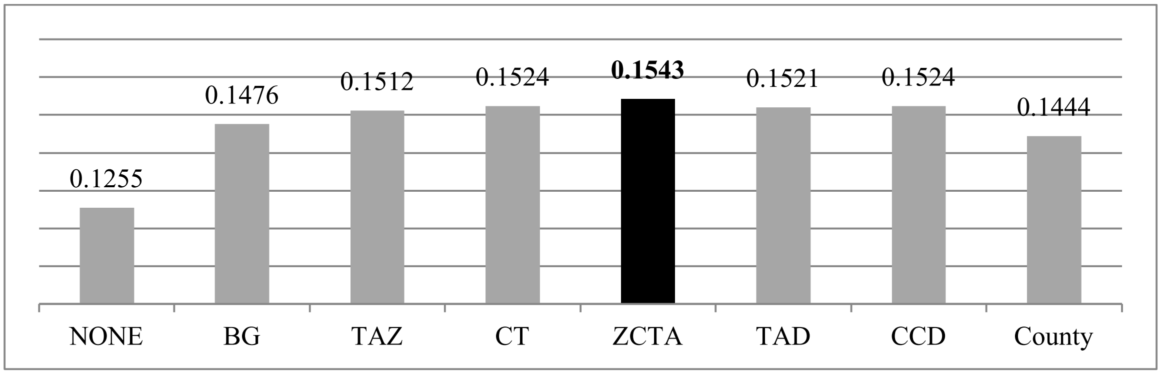

(d) Bicycle Crashes

Figure 7-4 Comparison of adjusted ρ^2 values of the SPFs with macro-level random-effects and variables

Tables 7-4 to 7-7 display the modeling results for total, severe, pedestrian, and bicycle crashes at intersections with macro-level variables. All the variables in the final model are significant at the 5% confidence interval, and the following explanations are based on the best model for each crash type.

7.5.1 Total Crash SPF

The best SPF of total crash was estimated with ZCTA-based data. Except for 'Location (urban=1, rural=0)' variable, all other intersection variables were statistically significant at 5% in the SPF with ZCTA-based data. The location dummy variable was highly correlated with 'Log (population density)' and thus these two variables could not be used at the same time. These variables were attempted one by one and the model with 'Log (population density)' outperforms the one with the location variable. Both 'Log (major AADT)' and 'Log (minor AADT)' were used as exposure variables and as expected they had positive and significant impacts on total crashes at intersections. The major AADT had a greater impact than the minor AADT as the major AADT had a larger coefficient. It was also confirmed by previous studies (AASHTO, 2010; Jonsson et al., 2009). This phenomenon is also observed in all other models (i.e., severe, pedestrian, and bicycle crash SPFs). Meanwhile, 'No of legs (4 legs or more=1, 3 legs=0)', 'Control type (signal=1, stop=0)', and 'One-way road (yes=1, no=0)' were positively related with total crashes. The intersections with more legs have more conflict points that result in more crashes. Regarding the signalization, it may reduce some types of crashes (i.e., angle); however, existing studies has proven that the signalization significantly increase other types of crashes (i.e., rear-end). Thus, the overall crash counts may increase due to the signalization. It was also shown the intersections with one-way road tend to have more crashes. It may be because one-way roads may confuse the drivers who are not familiar with the one-way road operation, especially at intersections.

'Log (population density)' was positively related to total crash counts (Ladron de Guevara et al., 2004, Lovegrove and Sayed, 2007; Lee et al., 2014b). Ladron de Guevara et al. (2004) explained that population density reflects the degree of interaction among people; therefore, the areas with larger population density may result in greater interactions and conflicts. 'Proportion of elderly (75 years or older)' has a negative effect on total crash counts, which is consistent with several prior studies (Lee et al., 2014a; Huang et al., 2010). It may be explained by the degree of exposure. Lee et al. (2014a) claimed that elderly drivers are less exposed to traffic crashes because they have much shorter trip lengths compared to other age groups. Furthermore, median household income (in $1,000) was negatively associated with total crash counts, which implies that the area with lower income households has a propensity to experience more crashes at intersections (Lee et al., 2014a; Huang et al., 2010). Lee et al. (2014a) and Martinez and Veloz (1996) explained that people from lower-income areas are not able to afford to purchase newer and safer vehicle or equipment, and have less chance to get traffic safety information. Therefore, they are more likely to be involved in traffic crashes. Lastly, 'Proportion of commuters using public transit' has a positive effect on total crashes. The zones with higher public transit use are often located in highly urbanized area with concentrated activities; and thus they are likely to experience more crashes (Abdel-Aty et al., 2013; Lee et al., 2013).

7.5.2 Severe Crash SPF

Again, the severe crash SPF performed the best with ZCTA-based data. Almost all intersection-level variables were significant in the SPF with ZCTA-based data. 'Location (urban=1, rural=0)' is significant and negatively associated with severe crashes. It infers that more severe crashes occur at rural intersections, compared to urban intersections. At this time, the SPF with the location dummy variable performs better than that with 'Log (population density)'. 'One-way road (yes=1, no=0)' was not significant for severe crashes. The other intersection-level variables are consistent with the total crash SPF. Three ZCTA-based variables were found significant. 'Proportion of commuters using motorcycle' had a positive coefficient whereas 'Proportion of commuters who walk' and 'Median household income (in $1,000)' had a negative coefficient in the severe crash SPF. The motorcycle variable showed that the intersections within the area with higher proportion of motorcycle using commuters had more severe crashes (WHO, 2013). On the other hand, the intersections with more walking commuters had a propensity to experience less severe crashes. It may be because the areas with higher proportion of walking commuters are in urbanized areas with possibly lower speed limit. The income variable is in line with that in the total crash SPF.

7.5.3 Pedestrian Crash SPF

The optimal macro-level data for the pedestrian crash SPF is CT-based data. The intersection-level variables including 'Log (major AADT)', 'Log (minor AADT)', 'No of legs (4 legs or more=1, 3 legs=0)', and 'Control type (signal=1, stop=0)' have a positive relationship with pedestrian crashes. Overall six CT-based variables were statistically significant. 'Log (population density)', 'Proportion of commuters using public transit', and 'Proportion of commuters who walk' are positively while 'Proportion of adolescent (15-24 years)', 'Proportion of elderly (75 years or older)', and 'Median household income (in $1,000)' are negatively related with pedestrian crash counts. The three CT-based variables with positive effects may be a good surrogate exposure variable for pedestrian crashes. In Model Type (1), there is no exposure variable for pedestrians but only traffic volume; therefore, the pedestrian crash model could be significantly improved by including the macro-level variables including the surrogate exposure variables explained above. Regarding to the public transit using and walking commuters, they are pedestrians when they access to public transportation facilities or to workplace (e.g., bus stop or rail station) by walking (Abdel-Aty et al., 2013). Lastly, the areas with both adolescent and elderly people have less pedestrian crashes, which hint at that these people are less exposed to pedestrian crashes compared to other age groups (e.g., middle age).

7.5.4 Bicycle Crash SPF

The preeminent bicycle SPF was developed with ZCTA-based data. The significance of the intersection-variables is the same as those in the pedestrian crash SPF. Five ZCTA-based variables were found significant for bicycle crashes. 'Log (population density)', ‘Proportion of motorcycle’, and ‘Proportion of commuters using bicycle’ have a positive while ‘Proportion of adolescent’ and ‘Median household income (in $1,000)’ have a negative relation with bicycle crashes. The population density and the bicycle commuter variables were as expected but it is interesting that the motorcycle commuter variable also has a positive effect. It is thought that there are common features in motorcycle and bicycle use. Both transportation modes are used for recreational and leisure activities. Therefore, the communities with the larger number of bicyclists also may have more motorcyclists. Similar to the pedestrian crash SPF, the model has been significantly improved by adding macro-level variables (i.e., population density, bicycle/motorcycle using commuter variables) compared to the model with intersection-level variables only.

Table 7-4 The estimated safety performance functions for total crashes at intersections with macro-level variables

Variables (N=8,347)	Model Type (1)		Model Type (3)															
	None		BG		TAZ		CT		ZCTA		TAD		CCD		County	
	Coef	S.E.	Coef	S.E.	Coef	S.E.	Coef	S.E.	**Coef**	**S.E.**	Coef	S.E.	Coef	S.E.	Coef	S.E.
Intercept	-7.62	0.11	-7.90	0.12	-7.70	0.12	-7.80	0.12	-7.53	0.13	-7.55	0.14	-7.66	0.13	-6.91	0.17
Log (major AADT)	0.74	0.01	0.73	0.01	0.72	0.01	0.73	0.01	0.71	0.01	0.70	0.01	0.70	0.01	0.69	0.01
Log (minor AADT)	0.27	0.01	0.30	0.01	0.28	0.01	0.29	0.01	0.27	0.01	0.27	0.01	0.27	0.01	0.25	0.01
Location (urban=1, rural=0)	-0.13	0.04														
No of legs (4 legs or more=1, 3 legs=0)	0.45	0.02	0.43	0.02	0.42	0.02	0.42	0.02	0.42	0.02	0.42	0.02				
Control type (signal=1, stop=0)	0.58	0.03	0.50	0.03	0.52	0.03	0.50	0.03	0.52	0.03	0.52	0.03	0.69	0.02	0.71	0.02
One-way road (yes=1, no=0)	0.36	0.05	0.12	0.05	0.12	0.05	0.11	0.05	0.09	0.05	0.09	0.04	0.28	0.04	0.23	0.04
Log (population density)			0.02	0.01	0.04	0.01	0.03	0.01	0.05	0.01	0.04	0.01	0.10	0.01	0.20	0.02
Proportion of children (5-14 years)																
Proportion of adolescent (15-24 years)																
Proportion of young elderly (65-74 years)																
Proportion of elderly (75 years or older)					-1.85	0.19	-1.17	0.16	-1.71	0.30	-1.94	0.36				
Proportion of commuters using public transit			1.45	0.21	1.73	0.30	1.95	0.32	3.07	0.67	3.28	0.70			10.02	0.99
Proportion of commuters using motorcycle																
Proportion of commuters using bicycle																
Proportion of commuters who walk																
Proportion of people working at home																
Proportion of households with no vehicle																
Median household income (in $1,000)			-0.002	0.000	-0.003	0.001	-0.003	0.001	-0.003	0.001					-0.025	0.002
Variance of random-effects			0.21	0.01	0.19	0.01	0.19	0.01	0.15	0.01	0.14	0.01	0.20	0.02	0.16	0.04
α	0.47	0.01	0.24	0.01	0.25	0.01	0.26	0.01	0.29	0.01	0.30	0.01	0.36	0.01	0.41	0.01
LL (full)	-27424		-26940		-26865		-26758		-26609		-26637		-26968		-27256	
AIC	54862		53899		53752		53539		53240		53293		53950		54529	
BIC	54912		53970		53830		53616		53317		53363		53999		54593	
McFadden's ρ^2	0.1443		0.1594		0.1617		0.1651		0.1697		0.1689		0.1585		0.1496	
Adjusted ρ^2	0.1441		0.1591		0.1614		0.1647		0.1694		0.1686		0.1583		0.1493	

*All variables are significant at 5%

Table 7-5 The safety performance functions for severe crashes at intersections with macro-level variables

Variables (N=8,347)	Model Type (1)		Model Type (3)													
	None		BG		TAZ		CT		ZCTA		TAD		CCD		County	
	Coef	S.E.	Coef	S.E.	Coef	S.E.	Coef	S.E.	**Coef**	**S.E.**	Coef	S.E.	Coef	S.E.	Coef	S.E.
Intercept	-8.87	0.22	-8.89	0.23	-9.05	0.23	-8.85	0.24	-8.60	0.23	-8.36	0.24	-8.44	0.27	-9.64	0.27
Log (major AADT)	0.76	0.03	0.74	0.03	0.75	0.03	0.75	0.03	0.74	0.03	0.73	0.03	0.74	0.03	0.74	0.03
Log (minor AADT)	0.19	0.02	0.20	0.02	0.20	0.02	0.19	0.02	0.18	0.02	0.19	0.02	0.20	0.02	0.20	0.02
Location (urban=1, rural=0)	-0.85	0.08	-0.81	0.08	-0.79	0.08	-0.80	0.09	-0.77	0.09	-0.81	0.09	-0.79	0.09	-0.89	0.09
No of legs (4 legs or more=1, 3 legs=0)	0.36	0.04	0.35	0.04	0.34	0.04	0.34	0.04	0.32	0.04	0.34	0.04	0.32	0.04	0.36	0.04
Control type (signal=1, stop=0)	0.34	0.05	0.34	0.05	0.35	0.05	0.35	0.05	0.36	0.05	0.36	0.05	0.35	0.05	0.34	0.05
One-way road (yes=1, no=0)	-0.21	0.09	-0.21	0.10			-0.20	0.10					-0.17	0.09	-0.22	0.09
Log (population density)																
Proportion of children (5-14 years)			0.61	0.27	2.14	0.45	1.12	0.42								
Proportion of adolescent (15-24 years)							-0.46	0.23					-1.44	0.64		
Proportion of young elderly (65-74 years)																
Proportion of elderly (75 years or older)																
Proportion of commuters using public transit					-1.19	0.50										
Proportion of commuters using motorcycle									14.65	5.52						
Proportion of commuters using bicycle															17.74	6.08
Proportion of commuters who walk									-3.87	1.20	-6.34	1.79				
Proportion of people working at home																
Proportion of households with no vehicle															11.03	2.16
Median household income (in $1,000)			-0.003	0.001	-0.005	0.001	-0.005	0.001	-0.004	0.001	-0.006	0.002	-0.006	0.003		
Variance of random-effects			0.32	0.03	0.30	0.02	0.29	0.02	0.23	0.02	0.21	0.02	0.19	0.03	0.19	0.05
α	0.58	0.03	0.18	0.03	0.20	0.03	0.20	0.02	0.25	0.02	0.28	0.02	0.35	0.02	0.47	0.03
LL (full)	-10205		-10068		-10049		-10010		-9893		-9927		-9925		-10081	
AIC	20423		20156		20118		20043		19806		19873		19871		20181	
BIC	20473		20226		20188		20120		19876		19936		19941		20251	
McFadden's ρ^2	0.1156		0.1275		0.1291		0.1325		0.1427		0.1397		0.1398		0.1264	
Adjusted ρ^2	0.1150		0.1266		0.1283		0.1315		0.1418		0.1389		0.1390		0.1255	

*All variables are significant at 5%

Table 7-6 The safety performance functions for pedestrian crashes at intersections with macro-level variables

Variables (N=8,347)	Model Type (1)		Model Type (3)													
	None		BG		TAZ		CT		ZCTA		TAD		CCD		County	
	Coef	S.E.	Coef	S.E.	Coef	S.E.	Coef	S.E.	Coef	S.E.	Coef	S.E.	Coef	S.E.	Coef	S.E.
Intercept	-13.42	0.47	-14.16	0.43	-13.61	0.42	-13.91	0.42	-13.04	0.43	-11.97	0.53	-12.57	0.44	-12.14	0.72
Log (major AADT)	0.85	0.04	0.82	0.04	0.82	0.04	0.81	0.04	0.83	0.04	0.80	0.04	0.79	0.04	0.78	0.04
Log (minor AADT)	0.19	0.03	0.20	0.03	0.18	0.03	0.18	0.03	0.18	0.03	0.19	0.03	0.17	0.03	0.14	0.03
Location (urban=1, rural=0)	1.11	0.32	0.60	0.08												
No of legs (4 legs or more=1, 3 legs=0)	0.71	0.08	0.44	0.10	0.61	0.08	0.59	0.08	0.65	0.07	0.63	0.07	0.67	0.08	0.68	0.08
Control type (signal=1, stop=0)	0.58	0.10			0.44	0.10	0.44	0.10	0.47	0.10	0.49	0.10	0.54	0.10	0.61	0.10
One-way road (yes=1, no=0)	0.77	0.11											0.28	0.11	0.47	0.11
Log (population density)			0.34	0.03	0.32	0.03	0.35	0.03	0.22	0.03	0.21	0.03	0.20	0.04	0.23	0.06
Proportion of children (5-14 years)			-1.40	0.45							-4.30	1.65				
Proportion of adolescent (15-24 years)			-0.91	0.28	-1.26	0.33	-1.40	0.34	-2.45	0.54	-3.19	0.64	-2.74	0.71	-4.13	1.76
Proportion of young elderly (65-74 years)															-6.65	2.14
Proportion of elderly (75 years or older)			-1.72	0.35	-1.56	0.53	-1.46	0.42	-2.31	0.67	-4.09	1.01				
Proportion of commuters using public transit			1.74	0.45	3.18	0.61	3.57	0.59	6.54	1.07	7.32	1.17	11.76	1.98	8.42	3.13
Proportion of commuters using motorcycle																
Proportion of commuters using bicycle			1.91	0.70	3.96	1.12							8.41	3.62		
Proportion of commuters who walk			1.40	0.47	2.50	0.68	3.77	0.75	8.30	1.49	8.95	2.59	7.04	3.33	30.24	8.46
Proportion of people working at home					1.70	0.80										
Proportion of households with no vehicle			0.91	0.28												
Median household income (in $1,000)			-0.005	0.001	-0.012	0.002	-0.008	0.002	-0.009	0.002	-0.008	0.002	-0.010	0.004		
Variance of random-effects			0.27	0.05	0.20	0.05	0.19	0.04	0.15	0.03	0.14	0.03	0.09	0.03	0.05	0.02
α	1.11	0.08	0.39	0.07	0.45	0.07	0.46	0.06	0.53	0.06	0.56	0.06	0.69	0.06	0.88	0.07
LL (full)	-5471		-5236		-5228		-5216		-5232		-5224		-5269		-5370	
AIC	10957		10502		10483		10456		10488		10475		10564		10759	
BIC	11006		10607		10581		10541		10572		10566		10655		10829	
McFadden's ρ^2	0.1313		0.1688		0.1701		0.1719		0.1694		0.1706		0.1635		0.1475	
Adjusted ρ^2	0.1302		0.1664		0.1679		0.1700		0.1675		0.1685		0.1614		0.1459	

*All variables are significant at 5%

STC

Table 7-7 The safety performance functions for bicycle crashes at intersections with macro-level variables

Variables (N=8,347)	Model Type (1)		Model Type (3)													
	None		BG		TAZ		CT		ZCTA		TAD		CCD		County	
	Coef	S.E.	Coef	S.E.	Coef	S.E.	Coef	S.E.	Coef	S.E.	Coef	S.E.	Coef	S.E.	Coef	S.E.
Intercept	-12.36	0.45	-12.75	0.38	-12.70	0.38	-12.81	0.39	-12.43	0.39	-11.74	0.42	-12.47	0.40	-12.67	0.44
Log (major AADT)	0.73	0.04	0.71	0.04	0.72	0.04	0.71	0.04	0.71	0.04	0.70	0.04	0.70	0.04	0.71	0.04
Log (minor AADT)	0.20	0.03	0.19	0.03	0.18	0.03	0.19	0.03	0.19	0.03	0.21	0.03	0.18	0.03	0.19	0.03
Location (Urban=1, Rural=0)	1.59	0.33														
No of legs (4 legs or more=1, 3 legs=0)	0.51	0.06	0.40	0.06	0.44	0.06	0.40	0.06	0.45	0.06	0.45	0.06	0.46	0.06	0.51	0.06
Control type (signal=1, stop=0)	0.43	0.08	0.40	0.08	0.32	0.08	0.37	0.08	0.36	0.08	0.37	0.08	0.39	0.08	0.43	0.08
One-way road (yes=1, no=0)																
Log (population density)			0.32	0.02	0.33	0.02	0.34	0.03	0.31	0.03	0.25	0.03	0.26	0.04	0.38	0.04
Proportion of children (5-14 years)											-2.63	1.20				
Proportion of adolescent (15-24 years)			-0.65	0.24	-1.28	0.31	-1.11	0.29	-2.19	0.46	-1.78	0.50			-3.83	1.24
Proportion of young elderly (65-74 years)																
Proportion of elderly (>=75 years)																
Proportion of commuters using public transit																
Proportion of commuters using motorcycle					11.31	3.55			16.35	7.35						
Proportion of commuters using bicycle			3.45	0.62	7.29	1.01	7.09	0.88	13.42	1.90	14.08	3.17	25.05	3.04	44.73	4.54
Proportion of commuters who walk																
Proportion of people working at home																
Proportion of households with no vehicle																
Median household income (in $1,000)			-0.004	0.001	-0.004	0.001	-0.004	0.001	-0.005	0.002	-0.005	0.002				
Variance of random-effects			0.29	0.05	0.23	0.04	0.23	0.04	0.13	0.02	0.19	0.03	0.14	0.03	0.05	0.02
α	0.67	0.06	0.19	0.07	0.25	0.06	0.25	0.05	0.33	0.05	0.33	0.05	0.40	0.05	0.50	0.05
LL (full)	-5709		-5561		-5536		-5529		-5516		-5531		-5531		-5582	
AIC	11430		11141		11094		11078		11054		11083		11079		11183	
BIC	11472		11211		11172		11149		11132		11160		11135		11246	
McFadden's ρ^2	0.1264		0.1492		0.1529		0.1539		0.156		0.1538		0.1536		0.1458	
Adjusted ρ^2	0.1255		0.1476		0.1512		0.1524		0.1543		0.1521		0.1524		0.1444	

*All variables are significant at 5%

7.6 Summary

The SPFs play an important role in traffic safety as they are used to identify hotspots and assess the effectiveness of safety treatments. Numerous SPFs have been developed but most of them are based on the micro-level (i.e., intersection, segment, and corridor). Some researchers have analyzed crashes at the macro-level, but few studies have attempted to combine micro-level with macro-level data for developing SPFs.

This chapter aimed at answering the three research questions: (1) can intersection SPFs be improved by considering macro-level geographic units? (2) what would be the best spatial unit for the SPFs? and (3) what macro-level factors do have significant effects on intersection crashes? In order to answer these questions, traffic, geometric, and crash data for Florida's major intersections (N=8,347) were collected from the FDOT and Google Earth. Demographic, socioeconomic, and commute data were obtained from the ACS of the U.S. Census Bureau. The intersection-level data were combined with macro-level data from seven spatial units (i.e., BG, TAZ, CT, ZCTA, TAD, CCD, and county). A series of mixed-effects negative binomial models were developed for total, severe, pedestrian, and bicycle crashes with the intersection-level data merged with the macro-level data from the various geographic units mentioned above. The modeling results revealed the following key findings:

- The SPFs with macro-level random-effects only and those with both macro-level random effects and variables outperform those only with intersection-level variables.
- The intersection SPFs can be considerably augmented by only including macro-level random-effects.

• The intersection SPFs for total, severe, and bicycle crash SPFs have the greatest performance with ZCTA-based data.

• The intersection SPF for pedestrian crashes performs the best with CT-based data.

The results imply that generally medium-sized geographic units (i.e., ZCTA and CT) work well for intersection-level SPFs. It is because some spatial units (e.g., BG and TAZ) may be too small to aggregate meaningful shared characteristics between intersections; whereas, other geographic units (e.g., county) are excessively highly aggregated and miss much local information.

Furthermore, the modeling results revealed that the following macro-level variables are significant:

• The population density has a positive relationship with total, pedestrian, and bicycle crashes;

• The proportion of young (15-24 years) group is negatively related to pedestrian and bicycle crashes;

• Elderly (75 years or older) age group are less exposed to total and pedestrian crashes;

• The proportion of public transit using commuters has a positive relationship with total and pedestrian crashes;

• The proportion of motorcycle using commuters is positively associated to severe and bicycle crashes;

• The proportion of bicycle using commuters has a positive effect on bicycle crashes;

• The proportion of walking commuters has a negative effect for severe crashes while it has a positive effect for pedestrian crashes;

• The median household income is negatively associated with four types of crashes.

Both pedestrian and bicycle crash SPFs have been significantly enhanced with macro-level variables compared to that with intersection-level variables only. This is because there is no exposure variable for pedestrians and bicyclists but only traffic volume. The significant improvements of the pedestrian and bicycle crash SPFs imply that some macro-level variables such as population density, walking and bicycling commuter variables function as a good surrogate exposure variable. It is concluded that the performance of micro-SPFs can be considerably augmented with the proposed hierarchical modeling methodology in this study.

There are several possible extensions to this study. First, segment-level SPFs with macro-level variables can be estimated. It is possible that the optimal geographic unit for segment traffic safety estimation differs from the intersection-level SPFs. Second, it will be necessary to apply the data from different regions and check if the results from this study are valid in other states.

CHAPTER 8: CONCLUSIONS

Now more than ever more information is collected, stored, and processed. The large amount of information, characterized by variety, volume, velocity, variability, complexity, and value, is defined as big data. In return, the big data have brought about enormous benefits and challenges to human life. As an important aspect of human life, the transportation field has also generated big data. In turn, implementing the transportation related big data to monitor, assess, and improve traffic safety is the focus of this study.

Four types of data were collected and integrated to explore crash contributing factors with the aim of improving traffic safety. They are crash, traffic, road geometric, and macroscopic data. Each type of data was from several sources, and different sources were combined to give information that is more complete. The crash data were from CARS and S4A. CARS provides more detailed crash information than S4A, and S4A records more crash. The traffic data were from AVI and MVDS. AVI sensors provide traffic information for roadway segments: travel time and space mean speed for each vehicle. On the other hand, MVDS detectors are point-based and provide vehicle count, time mean speed, lane occupancy for each lane at 1-minute intervals for each point. Road geometric data were from RCI, which is maintained by FDOT, or manually collected. RCI dataset offer 323 road geometric characteristics for each roadway segment in Florida. However, some geometric parameters are specific to a roadway type and cannot find in RCI, for example weaving segment length. Thus, these geometric data were manually collected from ArcGIS map. Microscopic data were from the FDOT Central Office and the ACS of the U.S. Census

Bureau. These data reflect the behaviors of traffic participants, such as pedestrian, bicyclist, and driver.

After processing and integrating the data above, preliminary safety evaluation has been conducted by data visualization. Hourly volume distribution was described by three-dimension spatio-temporal and contour plots. The expressway congestion was pictured and was measured using TTI, occupancy, and CI based on AVI and MVDS traffic data. Subsequently, the spatial patterns of traffic crashes by facility types were visualized from 2011 to 2014. The visualization of crashes enabled researchers to easily detect crash hotspots and suggest appropriate engineering countermeasures.

Then, the big traffic data were used to build a microscopic simulation network for expressway weaving segments, which have a higher crash potential than other expressway mainline segments. The input big traffic data made the simulation network well calibrated and validated, because the simulated volume, speed, and safety were highly consistent with those of the field. Furthermore, two conflict prediction models were estimated using the traffic data from VISSIM simulation and conflict information from SSAM. One model was based on a 5-minute intervals and the other was based on a 1-minute intervals. In both models, Logarithm of vehicle count, maximum influence length, and average acceleration at the beginning of weaving segment were significant variables. The model performance of the 1-minute interval model was better than that of the 5-minute interval model by providing higher AUCs and lower standard deviation of variable coefficients.

Reduced travel time reliability could cause unstable traffic flow thus affects traffic safety. This study separately estimated SV and MV crash frequencies using three travel time reliability indicators: Percent Variation, Buffer Index, and Misery Index. The results showed that Buffer Index and Misery Index had significant positive impact on MV crash frequency; however, Percent Variation was not significant in MV crash frequency model. On the other hand, all indicators were not significantly related to SV crash frequency. Additionally, Percent Variation was used in real-time safety analysis to estimate MV crash potential given a crash occurrence. The model indicates that high Percent Variation would significantly increase MV crash risk.

The safety of a roadway facility is not only determined by the facility's geometric design and traffic, but also it might be impacted by the macroscopic characteristics of the zone, which the facility lies in. Macroscopic parameters were implemented in real-time crash analysis for expressway ramps and crash frequency estimation for intersections. In the real-time crash analysis for ramps, land-use and trip generation parameters were important crash contributing factors. Two SVM models were applied to predict crash occurrence: one with all variables and the other only with significant variables identified by a logistic regression model. The SVM with all variables had an overfitting issue. It is recommended to integrate data mining method and traditional statistical model to alleviate overfitting issue and to improve model performance.

In the crash frequency prediction for intersections, both pedestrian and bicycle crash SPFs have been significantly enhanced with macro-level variables compared to that with intersection-level variables only. The significant improvements of the pedestrian and bicycle crash SPFs imply that some macro-level variables such as population density, walking and bicycling commuter variables function as a good surrogate exposure variable. Additionally, total and severe crash SPFs were also improved by adding macro-level random effects and variables. The results also indicated that medium-sized geographic units (i.e., ZCTA and CT) might work better for intersection-level SPFs than other macro-level spatial units. Since, macro-level data are easily accessible from the U.S. Census Bureau, it is strongly recommended to incorporate macro-level data in developing micro-level SPFs.

REFERENCES

AASHTO, 2010. Highway safety manual. American Association of State Highway and Transportation Officials, Washington D.C.

Abdel-Aty, M., Lee J., Eluru N., Cai Q., Al Amili S., Alarifi S., 2016. Enhancing and Generalizing the Two-Level Screening Approach Incorporating the Highway Safety Manual (HSM) Methods, Phase 2 report.

Abdel-Aty, M., Lee, J., Siddiqui, C., Choi, K., 2013. Geographical unit based analysis in the context of transportation safety planning. Transportation Research Part A: Policy and Practice 49, 62-75.

Abdel-Aty, M., Pande, A., 2005. Identifying crash propensity using specific traffic speed conditions. Journal of Safety Research 36 (1), 97-108.

Abdel-Aty, M., Pemmanaboina, R., 2006. Calibrating a real-time traffic crash-prediction model using archived weather and its traffic data. Intelligent Transportation Systems, IEEE Transactions on Intelligent Transportation System 7 (2), 167-174.

Abdel-Aty, M., Siddiqui, C., Huang, H., Wang, X., 2011. Integrating trip and roadway characteristics to manage safety in traffic analysis zones. Transportation Research Record: Journal of the Transportation Research Board (2213), 20-28.

Abdel-Aty, M., Uddin, N., Pande, A., Abdalla, F., Hsia, L., 2004. Predicting freeway crashes from loop detector data by matched case-control logistic regression. Transportation Research Record: Journal of the Transportation Research Board (1897), 88-95.

Aguero-Valverde, J., Jovanis, P.P., 2006. Spatial analysis of fatal and injury crashes in pennsylvania. Accident Analysis & Prevention 38 (3), 618-625.

Ahmed, M., Huang, H., Abdel-Aty, M., Guevara, B., 2011. Exploring a bayesian hierarchical approach for developing safety performance functions for a mountainous freeway. Accident Analysis & Prevention 43 (4), 1581-1589.

Autey, J., Sayed, T., Zaki, M.H., 2012. Safety evaluation of right-turn smart channels using automated traffic conflict analysis. Accident Analysis & Prevention 45, 120-130.

Breiman, L., 2001. Random forests. Machine learning 45 (1), 5-32.

Cafiso, S., Garcia, A., Cavarra, R., 2011. Before-and-after study of crosswalks using pedestrian risk index. In: Proceedings of the Transportation Research Board 90th Annual Meeting. Washington, D.C.

Cambridge Systematics, Inc., 2004. Traffic congestion and reliability: Trends and advanced strategies for congestion mitigation. Federal Highway Administration report

Campbell, C., Ying, Y., 2011. Learning with support vector machines. Synthesis lectures on artificial intelligence and machine learning 5 (1), 1-95.

Deng, N., Tian, Y., Zhang, C., 2012. Support vector machines: Optimization based theory, algorithms, and extensions CRC press.

Essa, M., Sayed, T., 2015. Transferability of calibrated microsimulation model parameters for safety assessment using simulated conflicts. Accident Analysis & Prevention 84, 41-53.

Florida Department of Transportation, 2014. The RCI feature & characteristic handbook.

Geedipally, S.R., Lord, D., 2010. Investigating the effect of modeling single-vehicle and multi-vehicle crashes separately on confidence intervals of Poisson–Gamma models. Accident Analysis & Prevention 42 (4), 1273-1282.

Gerlough, D.L., Huber, M.J., 1975. Traffic flow theory: A monograph. Transportation Research Board.

Gettman, D., Head, L., 2003. Surrogate safety measures from traffic simulation models. Transportation Research Record: Journal of the Transportation Research Board (1840), 104-115.

Gettman, D., Pu, L., Sayed, T., Shelby, S.G., 2008. Surrogate safety assessment model and validation: Final report.

Glennon, J., Thorson, B., 1975. Evaluation of the traffic conflicts technique. Report: FHWA-RD-76- 88.

Grant, M., Bowen, B., Day, M., Winick, R., Bauer, J., Chavis, A., Trainor, S., 2011. Congestion management process: A guidebook. Report: FHWA-HEP-11-011.

Griffin, L. A., 2011. Enhancing Expressway Operations Using Travel Time Performance Data. In Facilities Management and Maintenance Workshop, Nashville, TN.

Guo, F., Wang, X., Abdel-Aty, M.A., 2010. Modeling signalized intersection safety with corridor-level spatial correlations. Accident Analysis & Prevention 42 (1), 84-92.

Hadayeghi, A., Shalaby, A., Persaud, B., 2010. Development of planning-level transportation safety models using full Bayesian semiparametric additive techniques. Journal of Transportation Safety & Security 2 (1), 45-68.

Hall, F.L., 1996. Traffic stream characteristics. Federal Highway Administration.

Hamad, K., Kikuchi, S., 2002. Developing a measure of traffic congestion: Fuzzy inference approach. Transportation Research Record: Journal of the Transportation Research Board (1802), 77-85.

Hauer, E., 2015. The art of regression modeling in road safety. Springer.

Ho, T.K., 1995. Random decision forests. In: Proceedings of the 3nd International Conference on, pp. 278-282.

Hosmer Jr, D.W., Lemeshow, S., Sturdivant, R.X., 2013. Applied logistic regression. John Wiley & Sons.

Hossain, M., Muromachi, Y., 2010. Evaluating location of placement and spacing of detectors for real-time crash prediction on urban expressways. In: Proceedings of the Transportation Research Board 89th Annual Meeting. Washington, D.C.

Hossain, M., Muromachi, Y., 2012. A Bayesian network based framework for real-time crash prediction on the basic freeway segments of urban expressways. Accident Analysis & Prevention 45, 373-381.

Hourdos, J., Garg, V., Michalopoulos, P., Davis, G., 2006. Real-time detection of crash-prone conditions at freeway high-crash locations. Transportation Research Record: Journal of the Transportation Research Board (1968), 83-91.

Huang, H., Abdel-Aty, M., 2010. Multilevel data and Bayesian analysis in traffic safety. Accident Analysis & Prevention 42 (6), 1556-1565.

Huang, H., Abdel-Aty, M., Darwiche, A., 2010. County-level crash risk analysis in Florida: Bayesian spatial modeling. Transportation Research Record: Journal of the Transportation Research Board (2148), 27-37.

Huang, H., Song, B., Xu, P., Zeng, Q., Lee, J., Abdel-Aty, M., 2016. Macro and micro models for zonal crash prediction with application in hot zones identification. Journal of Transport Geography 54, 248-256.

Johansson, P., 1996. Speed limitation and motorway casualties: A time series count data regression approach. Accident Analysis & Prevention 28 (1), 73-87.

Johnson, S., Murray, D., 2010. Empirical analysis of truck and automobile speeds on rural interstates: Impact of posted speed limits. In: Proceedings of the Transportation Research Board 89th Annual Meeting, Washington, D.C.

Jolovic, D., Stevanovic, A., 2013. Evaluation of VISSIM and FREEVAL to assess an oversaturated freeway weaving segment. In: Proceedings of the Transportation Research Board 92nd Annual Meeting, Washington, D.C.

Jonsson, T., Lyon, C., Ivan, J., Washington, S., Van Schalkwyk, I., Lord, D., 2009. Differences in the performance of safety performance functions estimated for total crash count and for crash count by crash type. Transportation Research Record: Journal of the Transportation Research Board (2102), 115-123.

Katal, A., Wazid, M., Goudar, R. H., 2013. Big data: issues, challenges, tools and good practices. 2013 Sixth International Conference on Contemporary Computing (IC3), Noida

Koppula, N., 2002. A comparative analysis of weaving areas in HCM, TRANSIMS, CORSIM, VISSIM, and INTEGRATION. Thesis, Virginia Polytechnic Institute.

Ladron De Guevara, F., Washington, S., Oh, J., 2004. Forecasting crashes at the planning level: Simultaneous negative binomial crash model applied in Tucson, Arizona. Transportation Research Record: Journal of the Transportation Research Board (1897), 191-199.

Lascala, E.A., Gerber, D., Gruenewald, P.J., 2000. Demographic and environmental correlates of pedestrian injury collisions: A spatial analysis. Accident Analysis & Prevention 32 (5), 651-658.

Lee, C., Saccomanno, F., Hellinga, B., 2002. Analysis of crash precursors on instrumented freeways. Transportation Research Record: Journal of the Transportation Research Board (1784), 1-8.

Lee, J., 2014. Development of traffic safety zones and integrating macroscopic and microscopic safety data analytics for novel hot zone identification. Dissertation, University of Central Florida Orlando, Florida.

Lee, J., Abdel-Aty, M., Choi, K., 2014a. Analysis of residence characteristics of at-fault drivers in traffic crashes. Safety science 68, 6-13.

Lee, J., Abdel-Aty, M., Choi, K., Huang, H., 2015a. Multi-level hot zone identification for pedestrian safety. Accident Analysis & Prevention 76, 64-73.

Lee, J., Abdel-Aty, M., Choi, K., Siddiqui, C., 2013. Analysis of residence characteristics of drivers, pedestrians, and bicyclists involved in traffic crashes. In: Proceedings of the Transportation Research Board 92nd Annual Meeting, Washington, D.C.

Lee, J., Abdel-Aty, M., Jiang, X., 2014b. Development of zone system for macro-level traffic safety analysis. Journal of transport geography 38, 13-21.

Lee, J., Abdel-Aty, M., Jiang, X., 2015b. Multivariate crash modeling for motor vehicle and non-motorized modes at the macroscopic level. Accident Analysis & Prevention 78, 146-154.

Levine, N., Kim, K.E., Nitz, L.H., 1995. Spatial analysis of Honolulu motor vehicle crashes: Ii. Zonal generators. Accident Analysis & Prevention 27 (5), 675-685.

Lomax, T., Schrank D., Turner S., Margiotta R., 2003. Selecting travel reliability measures. Texas Transportation Institute monograph (May 2003).

Lord, D., Mannering, F., 2010. The statistical analysis of crash-frequency data: A review and assessment of methodological alternatives. Transportation Research Part A: Policy and Practice 44 (5), 291-305.

Lovegrove, G., Sayed, T., 2007. Macrolevel collision prediction models to enhance traditional reactive road safety improvement programs. Transportation Research Record: Journal of the Transportation Research Board (2019), 65-73.

Lunn, D. J., Thomas A., Best N., Spiegelhalter D., 2000. WinBUGS-a Bayesian modelling framework: concepts, structure, and extensibility. Statistics and computing, 10 (4), 325-337.

Martchouk, M., 2009. Travel time reliability. Dissertation, Purdue University.

Martinez, R., Veloz, R.A., 1996. A challenge in injury prevention ‑ the Hispanic population. Academic Emergency Medicine 3 (3), 194-197.

Meng, Q., Qu, X., 2012. Estimation of rear-end vehicle crash frequencies in urban road tunnels. Accident Analysis & Prevention 48, 254-263.

Miaou, S.-P., Song, J.J., Mallick, B.K., 2003. Roadway traffic crash mapping: A space-time modeling approach. Journal of Transportation and Statistics 6, 33-58.

Migletz, D., Glauz, W., Bauer, K., 1985. Relationships between traffic conflicts and accidents volume 2-Final Technical Report. Report: FHWA/RD-84/042.

Naderan, A., Shahi, J., 2010. Aggregate crash prediction models: Introducing crash generation concept. Accident Analysis & Prevention 42 (1), 339-346.

National Research Council, 2010. HCM 2010: Highway Capacity Manual. Washington, DC: Transportation Research Board.

Nezamuddin, N., Jiang, N., Zhang, T., Waller, S.T., Sun, D., 2011b. Traffic operations and safety benefits of active traffic strategies on TXDOT freeways. Report: FHWA/TX-12/0-6576-1.

Noland, R.B., Oh, L., 2004. The effect of infrastructure and demographic change on traffic-related fatalities and crashes: A case study of Illinois county-level data. Accident Analysis & Prevention 36 (4), 525-532.

Oh, C., Oh, J.-S., Ritchie, S., Chang, M., 2001. Real-time estimation of freeway accident likelihood. In: Proceedings of the 80th Annual Meeting of the Transportation Research Board, Washington, DC.

Olson, D.L., Delen, D., 2008. Advanced data mining techniques. Springer Science & Business Media.

Park, J., Abdel-Aty, M., Lee, J., Lee, C., 2015. Developing crash modification functions to assess safety effects of adding bike lanes for urban arterials with different roadway and socio-economic characteristics. Accident Analysis & Prevention 74, 179-191.

PTV Group, 2013. VISSIM 6.0 user manual. Karlsruhe, Germany

Qu, X., Wang, W., Wang, W., Liu, P., Noyce, D.A., 2012. Real-time prediction of freeway rear-end crash potential by support vector machine. In: Proceedings of the Transportation Research Board 91st Annual Meeting, Washington, D.C.

Sacchi, E., Sayed, T., 2016. Conflict-based safety performance functions to predict traffic collisions by type. In: Proceedings of the Transportation Research Board 95th Annual Meeting, Washington, D.C.

Saleem, T., Persaud, B., Shalaby, A., Ariza, A., 2014. Can microsimulation be used to estimate intersection safety? Case studies using VISSIM and PARAMICS. Transportation Research Record: Journal of the Transportation Research Board (2432), 142-148.

Saulino, G., Persaud, B., Bassani, M., 2015. Calibration and application of crash prediction models for safety assessment of roundabouts based on simulated conflicts. In: Proceedings of the Transportation Research Board 94th Annual Meeting, Washington, D.C.

Shankar, V., Albin, R., Milton, J., Mannering, F., 1998. Evaluating median crossover likelihoods with clustered accident counts: An empirical inquiry using the random effects negative binomial model. Transportation Research Record: Journal of the Transportation Research Board (1635), 44-48.

Shankar, V., Mannering, F., Barfield, W., 1995. Effect of roadway geometrics and environmental factors on rural freeway accident frequencies. Accident Analysis & Prevention 27 (3), 371-389.

Shi, Q., Abdel-Aty, M., 2015. Big data applications in real-time traffic operation and safety monitoring and improvement on urban expressways. Transportation Research Part C: Emerging Technologies 58, 380-394.

Shi, Q., 2014. Urban expressway safety and efficiency evaluation and improvement using big data. Dissertation, University of Central Florida Orlando, Florida.

Stamatiadis, N., Puccini, G., 2000. Socioeconomic descriptors of fatal crash rates in the southeast USA. Injury control and safety promotion 7 (3), 165-173.

Stevanovic, A., Stevanovic, J., Kergaye, C., 2013. Optimization of traffic signal timings based on surrogate measures of safety. Transportation research part C: Emerging Technologies 32, 159-178.

Suykens, J.A., Vandewalle, J., 1999. Least squares support vector machine classifiers. Neural processing letters 9 (3), 293-300.

Ukkusuri, S., Hasan, S., Aziz, H., 2011. Random parameter model used to explain effects of built-environment characteristics on pedestrian crash frequency. Transportation Research Record: Journal of the Transportation Research Board (2237), 98-106.

USCB, 1994. Geographic Areas Reference Manual. Commerce, Washington, DC.

USCB, 2011. 2010 Census Traffic Analysis Zone Program Maf/Tiger Partnership Software Participant Guidelines. Commerce, Washington, DC

U.S. Department of Transportation Office of the Secretary, 2010. What Employers Need To Know About DOT Drug and Alcohol Testing (Guidance and Best Practices). http://www.fta.dot.gov/documents/EmployerGuidelinesOctober012010.pdf. Accessed on Sep 28, 2015.

Van Der Horst, A.R.A., De Goede, M., De Hair-Buijssen, S., Methorst, R., 2014. Traffic conflicts on bicycle paths: A systematic observation of behaviour from video. Accident Analysis & Prevention 62, 358-368.

Wang, L., Abdel-Aty, M., Shi, Q., Park, J., 2015a. Real-time crash prediction for expressway weaving segments. Transportation Research Part C: Emerging Technologies 61, 1-10.

Wang, L., Shi, Q., Abdel-Aty, M., 2015b. Predicting crashes on expressway ramps with real-time traffic and weather data. Transportation Research Record: Journal of the Transportation Research Board 2514, 32-38.

Wang, X., Jin, Y., Abdel-Aty, M., Tremont, P., Chen, X., 2012. Macrolevel model development for safety assessment of road network structures. Transportation Research Record: Journal of the Transportation Research Board (2280), 100-109.

Washington, S.P., Karlaftis, M.G., Mannering, F.L., 2010. Statistical and econometric methods for transportation data analysis. CRC press.

Wier, M., Weintraub, J., Humphreys, E.H., Seto, E., Bhatia, R., 2009. An area-level model of vehicle-pedestrian injury collisions with implications for land use and transportation planning. Accident Analysis & Prevention 41 (1), 137-145.

Woody, T., 2006. Calibrating freeway simulation models in vissim. Thesis, University of Washington.

WHO, 2013. Global Status Report on Road Safety 2013: Supporting a Decade of Action.

Wu, Z., Sun, J., Yang, X., 2005. Calibration of vissim for shanghai expressway using genetic algorithm. In: Proceedings the 37th Conference on Winter Simulation. Orlando, FL.

Xu, C., Tarko, A.P., Wang, W., Liu, P., 2013. Predicting crash likelihood and severity on freeways with real-time loop detector data. Accident Analysis & Prevention 57, 30-39.

Yu, R., Abdel-Aty, M., 2013a. Multi-level Bayesian analyses for single-and multi-vehicle freeway crashes. Accident Analysis & Prevention 58, 97-105.

Yu, R., Abdel-Aty, M., 2013b. Utilizing support vector machine in real-time crash risk evaluation. Accident Analysis & Prevention 51, 252-259.

Yu, R., Abdel-Aty, M., 2014. An optimal variable speed limits system to ameliorate traffic safety risk. Transportation research part C: Emerging Technologies 46, 235-246.

Yu, R., Abdel-Aty, M., Ahmed, M., 2013. Bayesian random effect models incorporating real-time weather and traffic data to investigate mountainous freeway hazardous factors. Accident Analysis & Prevention 50, 371-376.

Zheng, Z., Ahn, S., Monsere, C.M., 2010. Impact of traffic oscillations on freeway crash occurrences. Accident Analysis & Prevention 42 (2), 626-636.

APPENDIX

Publications

Wang L., Abdel-Aty M., Shi Q., Park J., 2015. Real-time Crash Prediction for Expressway Weaving Segments. Transportation Research Part C: Emerging Technologies. 61, 1-10.

Shi, Q., & Abdel-Aty, M., 2016. Evaluation of the Impact of Travel Time Reliability on Urban Expressway Traffic Safety. Transportation Research Record: Journal of the Transportation Research Board, Accepted.

Wang, L., Abdel-Aty, M., Wang , X., Yu, R., 2016. Analysis and Comparison of Safety Models Using AADT, Hourly, and Microscopic Traffic. Submitted to Transportation Research Record: Journal of the Transportation Research Board.

Lee, J., Abdel-Aty, M., Huang, H., Cai, Q., 2016. Intersection Safety Performance Functions with Macro-Level Data from Various Geographic Units. Submitted to Transportation Research Record: Journal of the Transportation Research Board.

Oral Presentations

Wang L., Abdel-Aty M., Shi Q., 2015. Conflict Precursors for Expressway Weaving Segments based on Microscopic Simulation. 2015 Road Safety & Simulation International Conference. Orlando.

Wang, L., Abdel-Aty M., Lee J., Shi Q., 2016, Analysis of Real-time Crash Risk for Expressway Ramps Using Traffic, Geometric, Land-use, and Trip Generation Predictors, World Conference on Transport Research, Shanghai.

Abdel-Aty, M., Lee, J., 2015. State-of-the-art macroscopic safety analysis. 15th COTA International Conference of Transportation Professionals, Beijing.

Posters

Lee, J., Cai, Q., 2015. Statewide county-level traffic crash modeling using land-use data: a case study of the State of Florida in the United States. Presented at the 25th World Road Congress 2015, Republic of Korea.

Lee, J., Cai, Q., 2015. Forecasting of the future traffic safety risks using land-use, socio-demographic, and trip generation predictors. Presented at the 25th World Road Congress 2015, Republic of Korea.

Wang, L., Abdel-Aty, M., Shi, Q., & Park, J., 2016. Predicting Expressway Weaving Segments Crashes using Bayesian Multilevel Logistic Regression. Presented at 95th Transportation Research Board Annual Meeting, Washington, D.C.

Shi, Q., Abdel-Aty, M., 2016. Evaluation of the Impact of Travel Time Reliability on Urban Expressway Traffic Safety. Presented at 95th Transportation Research Board Annual Meeting, Washington, D.C.

Wang, L., Abdel-Aty, M., Wang , X., Yu, R., 2016. Analysis and Comparison of Safety Models Using AADT, Hourly, and Microscopic Traffic. Submitted to present at Transportation Research Board 96th Annual Meeting, Washington, D.C.

Lee, J., Abdel-Aty, M., Huang, H., Cai, Q., 2016. Intersection Safety Performance Functions with Macro-Level Data from Various Geographic Units. Submitted to present at the Transportation Research Board 96th Annual Meeting, Washington, D.C.